



UNIVERSITÀ DEGLI STUDI DI ROMA “LA SAPIENZA”

PhD in Chemical Sciences

25° cycle

Curriculum: Synthesis and reactivity

Synthesis of functional magnetic nanoparticles for catalytic applications

Supervisors

Dr. Giuliana Righi

Dr. Lorenza Suber

Candidate

Alessandra Mari

Table of contents

1 Introduction	2
1.1 Asymmetric catalysis	3
1.2 β -amino alcohols	4
1.3 Nanoparticles in catalysis	15
2 Magnetite nanoparticle-supported chiral amino alcohol catalysts	29
2.1 Organic-phase synthesis of Fe_3O_4 nanoparticles	30
2.2 Pericas-type amino alcohol ligands	31
2.3 Ephedrine-type ligands	38
2.4 Our approach to new amino alcohol ligands	41
2.5 Conclusion	66
2.6 Experimental section	66
3 Magnetic nanoparticle-supported N-heterocyclic carbene catalysts	88
3.1 Introduction	88
3.2 Results and discussion	91
3.3 Conclusion	101
3.4 Experimental section	102
4 Conclusions	108

1 Introduction

Molecular chirality plays a key role in science and technology and has a large impact on our daily life. Humans and all other living organisms have single enantiomer molecular components.¹ Our enzymes are constructed with only one enantiomer of each amino acid and the sugar residues in DNA all have the same configuration. Hence the bioactivity of the two enantiomers of a food ingredient or drug can be totally different. Carvone, for example, has either a cummin or spearmint odor, depending on the enantiomer. In the case of pharmaceuticals, the different bioactivity of two enantiomers can have more serious consequences. The anesthetic ketamine was originally administered as a racemate, until it was found that the *S*-enantiomer is the desired compound while the *R*-enantiomer is a hallucinogen. Considering these effects of molecular chirality, it is not surprising that routes which lead to a single enantiomer are of high interest and value for the production of chiral compounds used in drugs, perfumes, flavors and agrochemicals.

Asymmetric catalysis represents a powerful method for the synthesis of enantiopure molecules. Numerous highly efficient homogeneous asymmetric catalysts have been developed in the past three decades.² Since their practical applications in industrial processes are extremely limited by their high costs, the possibility of recovery and reuse of catalysts is a very important factor. Ideally, enantioselective catalysis needs to be efficient, facile and economic if it is to be used widely in industry. For this reason, many different approaches have been employed to generate heterogeneous asymmetric catalysts. The heterogenization facilitates the separation of the catalyst from reagents and products and potentially allows the recycling of the immobilized catalysts. Unfortunately, the immobilization of chiral catalysts often results in lower activities and enantioselectivities in comparison to those observed for their homogeneous counterparts.

Recently, the use of magnetic nanoparticles led to the development of new catalysts that combine advantages of both homogeneous and heterogeneous catalysis. Nanoparticles, owing to their very high surface area, can be used as novel supports for asymmetric catalysts, with activity close to the homogeneous one. In addition, nanoparticle magnetic decantation allows a simple recovery of the catalyst from the reaction mixture and its reuse, as in the case of heterogeneous catalysts.

¹ Eliel, E. L.; Wilen, S. H. *Stereochemistry of organic compounds*, Wiley, New York, 1994.

² Brunner, H.; Zettlmeier, W., Ed. *Handbook of Enantioselective Catalysis*; VCH: New York, 1993.

In this context, during my three years of PhD I have focused my attention on the synthesis of magnetic nanoparticles functionalized with optically active β -amino alcohols, a class of compounds largely employed in asymmetric catalysis; the results obtained are discussed in Chapter 2. This first chapter aims to briefly introduce β -amino alcohol compounds, mentioning in particular their applications as chiral ligands, and also present an overview of the examples of asymmetric magnetic nanoparticle-supported catalysts reported in the literature up to now. During my third year of PhD I spent six months in Professor Stephen Connon's research group (School of Chemistry, Trinity College Dublin), where I have focused my work on the functionalization of magnetic nanoparticles with N-heterocyclic carbenes, a very useful class of organocatalysts; this part of my research is described in Chapter 3. The general conclusions of my work are presented in Chapter 4.

1.1 Asymmetric catalysis

Traditionally enantiopure compounds were obtained by the classical resolution of a racemate. A drawback of this method is the maximum yield of 50% one can theoretically obtain if the other enantiomer is considered to be useless.³ Another popular method was the transformation of readily accessible naturally occurring chiral compounds (chiral pool) such as amino acids, carbohydrates, terpenes and alkaloids. The disadvantage in this approach is that commonly in nature only one enantiomer is available in large quantities.⁴ A better approach is the asymmetric synthesis, where only one desired enantiomer of the target compound is synthesized. There are two ways towards this: chiral auxiliary-directed synthesis and asymmetric catalysis. In the case of a chiral auxiliary, a stoichiometric amount of an enantiopure reagent is covalently attached to the achiral substrate, making the subsequent introduction of a chiral center diastereoselective.⁵ However, the attachment of the auxiliary and its removal after the reaction adds two extra steps to the synthesis. When a chiral catalyst is used to transform a prochiral substrate into an enantiopure product, one speaks of asymmetric catalysis.⁶ The advantage of a catalytic method is that only small amounts of chiral material are needed to produce large amounts of chiral product

³ Jacques, J.; Collet, A.; Wilen, S. H.; *Enantiomers, racemates, and resolutions*, Wiley, New York, **1981**.

⁴ Hanessian, S.; *Total synthesis of natural products: the "Chiron" approach*, Pergamon Press, Oxford, **1983**.

⁵ Seyden-Penne, J. *Chiral auxiliaries and ligands in asymmetric catalysis*, Wiley, New York, **1995**.

⁶ a) Jacobsen E. N.; Pfaltz A.; Yamamoto H.; *Comprehensive Asymmetric Catalysis, Vol.1-3*, Springer, Berlin, **1999**; b) Ojima I.; *Catalytic Asymmetric Synthesis*, II Ed. (Wiley-VCH, New York), **2000**; c) Trost B. M.; *Proc. Nat. Acad. Sci.*, **2004**, *101*, 5348.

without the introduction of additional steps. The catalyst can be an enzyme (biocatalyst), a metal bearing chiral ligands or a small, chiral, organic molecule (organocatalyst).

Asymmetric catalysis is definitively the most elegant approach to enantiopure compound synthesis and the chemistry community has been revolutionized over the past 30 years by its advent.⁷ To get an idea of asymmetric catalysis impact, one can recall that in 2001 Knowles, Noyori, and Sharpless received the Nobel prize in chemistry “for their work on chirally catalysed hydrogenation and oxidation reactions”. Therefore, the development of chiral ligands for catalytic asymmetric synthesis is an extremely important aspect in modern synthetic chemistry.

1.2 β -amino alcohols

Vicinal amino alcohol motif (Figure 1-1), in addition to being present in a wide range of biologically active compounds such as enzyme inhibitors and α -adrenergic blockers,⁸ is also typical of numerous chiral auxiliaries, ligands and catalysts used in asymmetric synthesis.⁹

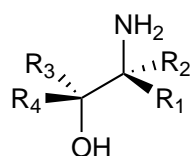


Figure 1-1 Vicinal amino alcohol framework.

In this regard, one famous example is represented by the chiral oxazolidinones known as *Evans auxiliaries* (Figure 1-2), which have been extensively applied as chiral auxiliaries in stereoselective aldol condensation,¹⁰ alkylation,¹¹ amination¹² and Diels-Alder reactions.¹³ Some examples of β -amino alcohols employed in asymmetric catalysis are reported in the next section.

⁷a) Sharpless, K.B.; *Angew. Chem. Int. Ed. Engl.* **2002**, *41*, 2024. b) Noyori, R.; *Angew. Chem. Int. Ed. Engl.* **2002**, *41*, 2008.

⁸ a) Connolly, M. E.; Kersting, F.; Bollery, C. T. *Prog. Cardio. Dis.* **1976**, *19*, 203. b) Bose, D. S.; Narsaiah, A. V. *Bioorg. Med. Chem.* **2005**, *3*, 627. c) Erhardt, P. W.; Woo, C. W.; Anderson, W. G.; Gorczynski, A. R. *J. Med. Chem.* **1982**, *25*, 1408. d) Zhu, S.; Meng, L.; Zhang, Q.; Wei, L. *Bioorg. Med. Chem. Lett.* **2006**, *16*, 1854.

⁹ Ager, D. J.; Prakash, I.; Schaad, D. R. *Chem. Rev.* **1996**, *96*, 835.

¹⁰ Evans, D. A.; Bartroli, J.; Shih, T. L. *J. Am. Chem. Soc.* **1981**, *103*, 2127

¹¹ Evans, D. A.; Weber, A. E. *J. Am. Chem. Soc.* **1986**, *108*, 6757.

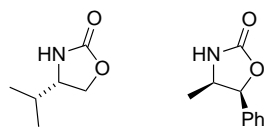
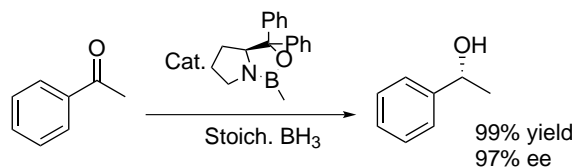


Figure 1-2 Evans auxiliaries.

1.2.1 β -amino alcohols in asymmetric catalysis

β -amino alcohols can be ligands, of both the acyclic and cyclic varieties, where the heteroatoms can be used to form a complex with the metal reaction center. They have been shown to be efficient chiral ligands for a variety of asymmetric reactions.

One successful example is the application of the Corey-Bakshi-Shibata (CBS) catalyst derived from the amino acid (*L*)-proline.¹⁴ This catalyst, an oxazaborolidine, was introduced by Corey and co-workers in the eighties for the preparation of enantiopure secondary alcohols from prochiral ketones (Scheme 1-1) and it is still one of the most efficient catalysts for this type of transformation.



Scheme 1-1 Reduction of acetophenone using the CBS catalyst.

β -amino alcohols are also one of the most effective classes of chiral ligands for asymmetric transfer hydrogenations.¹⁵ A variety of amino alcohols have been successfully used to generate catalysts *in situ* with $[\text{RuCl}_2(\text{p-cymene})]_2$, providing moderate to excellent catalytic activity in the asymmetric reduction of acetophenone (Scheme 1-2).

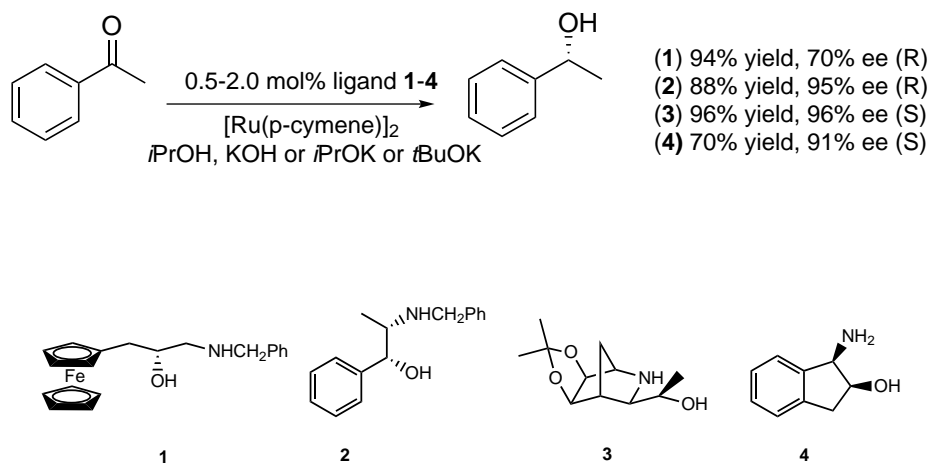
¹² Evans, D. A.; Britton, T. C.; Dorow, R. L.; Dellaria, J. F. *J. Am. Chem. Soc.* **1986**, *108*, 6395.

¹³ Ager, D. J.; Prakash, I.; Schaad, D. R. *Aldrichim. Acta* **1997**, *30*, 3.

¹⁴ Corey, E. J.; Bakshi, R. K.; Shibata, S. *J. Am. Chem. Soc.* **1987**, *109*, 555.

¹⁵ a) Yim, A. S. Y.; Wills, M.; *Tetrahedron* **2005**, *61*, 7994. b) Sun, X.; Manos, G.; Blacker, J.; Martin, J.; Gavriilidis, A. *Org. Process Res. Dev.* **2004**, *8*, 909. c) Hansen, K. B.; Chilenski, J. R.; Desmond, R.; Devine, P. N.; Grabowski, E. J. J.; Heid, R.; Kubryk, M.; Mathre, D. J.; Varsolona, R. *Tetrahedron: Asymmetry* **2003**, *14*, 3581. d) Patti, A.; Pedotti, S. *Tetrahedron: Asymmetry* **2003**, *14*, 597. e) Faller, J. W.; Lavoie, A. R. *Organometallics* **2002**, *21*, 2010. f) Yamakawa, M.; Yameda, I.; Noyori, R. *Angew. Chem., Int. Ed.* **2001**, *40*, 2818. g) Faller, J. W.; Lavoie, A. R. *Org. Lett.* **2001**, *3*, 3703. h) Frost, C. G.; Mendonca, P. *Tetrahedron: Asymmetry* **2000**, *11*, 1845. i) Petra, D. G. I.; Reek, J. N. H.; Handgraaf, J.-W.; Meijer, E. J.; Dierkes, P.; Kamer, P. C. J.; Brussee, J.; Schoemaker, H. E.; Van Leeuwen, P. W. N. M. *Chem. Eur. J.* **2000**, *6*, 2818. j) Yamakawa, M.; Ito, H.; Noyori, R.; *J. Am. Chem. Soc.* **2000**, *122*, 1466. k) Petra, D. G. I.; Kamer, P. C. J.; van Leeuwen, P. W. N. M.; Goubitz, K.; van Loon, A. M.; de Vries, J. G.; Schoemaker, H. E.; *Eur. J. Inorg. Chem.* **1999**, *12*, 233. l) Hashiguchi, S.; Noyori, R.; *Acc. Chem. Res.* **1997**, *30*, 97. m) Takehara, J.; Hashiguchi, S.; Fujii, A.; Inoue, S. I.; Ikariya, T.; Noyori, R.; *Chem. Commun.* **1996**, 233.

Patti *et al.* found that (R)-1-N-benzylamino-2-hydroxy-3-ferrocenylpropane **1** provided a 94% conversion and 70% ee (R) in 3 h at room temperature; through optimization of the ligand structure they were generally able to improve the reaction rate and asymmetric induction, by increasing the steric bulk around the amine moiety via N-alkylation.^{15d}



Scheme 1-2 Acetophenone transfer hydrogenation using amino alcohol ligands.

While examining the enantioselective effects of several substituted 2-amino ethanol and norephedrine-based ligands in transfer hydrogenation reactions, Van Leeuwen *et al.* reported that (1R,2S)-N-benzyl-norephedrine **2** provided the highest asymmetric induction.¹⁵ⁱ Andersson and co-workers¹⁶ were successful in developing highly active and selective catalysts from 2-azanorbonyl derivatives; reductions using amino alcohol **3** were fast, providing 96% conversion to the alcohol and 96% ee. Amino alcohol (1R,2S)-cis-1-aminoindan-2-ol **4** was developed by Wills *et al.*¹⁷ and has been evaluated for its effectiveness in the reduction of various substrates.

Singaram and co-workers have studied the Ru(II)-catalyzed asymmetric transfer hydrogenation of aromatic alkyl ketones using terpene-based β -amino alcohols. The limonene derived amino alcohol, (1S,2S,4R)-1-methyl-4-(1-methylethenyl)-2-(methylamino)cyclohexanol **5**, gave the best results (Figure 1-3); chiral secondary alcohols were obtained in good to excellent yields and moderate enantioselectivities (up to 71%).¹⁸

¹⁶ Brandt, P.; Roth, P.; Andersson, P. G.; *J. Org. Chem.* **2004**, 69, 4885.

¹⁷ Palmer, M. J.; Kenny, J. A.; Walsgrove, T.; Kawamoto, A.M.; Wills, M. J.; *Chem. Soc., Perkin Trans. 1* **2002**, 416.

¹⁸ Watts, C. C.; Thoniyot, P.; Cappuccio, F.; Verhagen, J.; Gallagher, B.; Singaram, B. *Tetrahedron: Asymmetry* **2006**, 17, 1301.

Recently new chiral β -amino alcohols have been synthesized from isosorbide, a by-product from the starch industry, and they have been used in asymmetric transfer hydrogenation reaction with Ru(II) complexes. The chiral amino alcohol **6** proved to be the most efficient ligand in the series examined for the reduction of acetophenone (85% yield, 74% ee).¹⁹

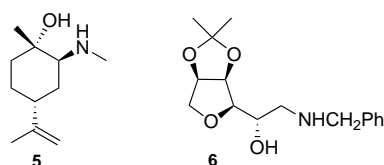
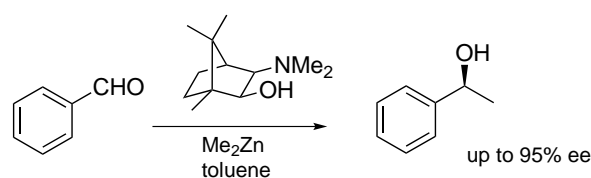


Figure 1-3 β -amino alcohols used as ligands in asymmetric transfer hydrogenation of ketones.

β -amino alcohols hold a prominent position also among the chiral catalysts for asymmetric organozinc additions to carbonyl compounds. In 1986, (-)-3-exo-dimethylaminoisobornenol [(-)-DAIB] was discovered by Noyori and co-workers²⁰ to be the first highly enantioselective ligand for the dialkylzinc addition to aldehydes (Scheme 1-3).



Scheme 1-3 Dimethylzinc addition to benzaldehyde catalyzed by (-)-DAIB.

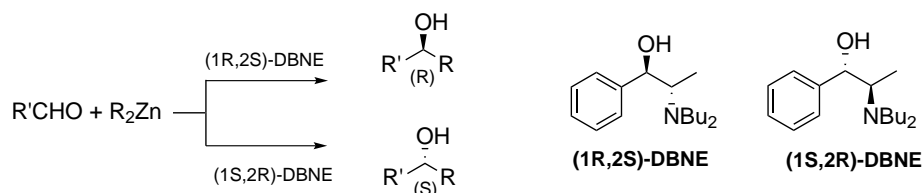
Numerous chiral amino alcohol ligands have since been developed for the asymmetric organozinc additions.²¹ These compounds react with dialkylzincs to generate a zinc-based chiral complex which can further coordinate with both the carbonyl substrate and the dialkylzinc reagents to conduct the catalytic addition. Thus, the *in situ* generated zinc complex is a multifunctional catalyst. It acts as a Lewis acid to activate the carbonyl substrates and also as a Lewis base to activate the organozinc reagents. The chiral environment of the ligand controls the stereoselectivity.

¹⁹ Guillaume S.; Nguyen T. X. M.; Saluzzo C.; *Tetrahedron: Asymmetry* **2008**, *19*, 1450.

²⁰ Kitamura, M.; Suga, S.; Kawai, K.; Noyori, R. J. *Am. Chem. Soc.* **1986**, *108*, 6071.

²¹ a) Pu, L.; Yu, H.-B. *Chem. Rev.* **2001**, *101*, 757. b) Soai, K.; Niwa, S. *Chem. Rev.* **1992**, *92*, 833. c) Wu Z.-L., Wu H.-L., Wu P.-Y., Uang B. J. *Tetrahedron Asymmetry*, **2009**, *20*, *13*, 1556.

N,N-di-*n*-butylnorephedrine (DBNE) was found by Soai and co-workers to be the most effective catalyst among ephedrine-based ligands (Scheme 1-4). It is able to catalyze the addition of dialkylzincs to a number of aliphatic and aromatic aldehydes affording secondary alcohols of high optical purity (up to >95% ee).²²



Scheme 1-4 The DBNE-catalyzed addition of dialkylzincs to various aldehydes.

Pericas and co-workers²³ reported that amino alcohol (1R,2R)-1-phenyl-1-piperidino-3-(triphenylmethoxy)-2-propanol **7** is capable to catalyze the asymmetric addition of diethylzinc to various benzaldehydes with ee in the range 91-95%.

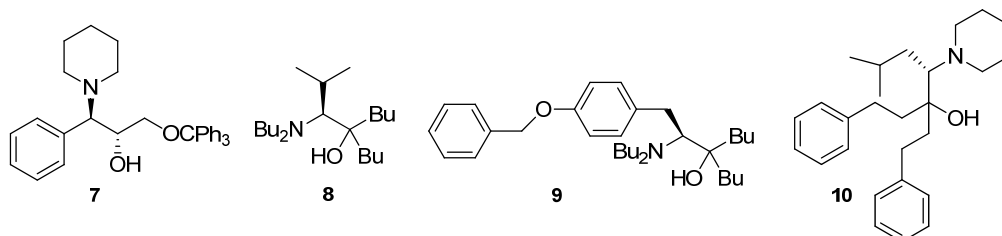


Figure 1-4 β -amino alcohols used as catalysts in asymmetric addition of dialkylzinc to aldehydes.

β -amino alcohols **8**, **9** e **10** derived respectively from (S)-valine,²⁴ (S)-tyrosine²⁵ and (S)-leucine²⁶ have been reported to show good enantioselectivity (85-97% ee) for the diethylzinc addition to both aromatic and aliphatic aldehydes.

²² Soai K.; Yokoyama S.; Hayasaka T.; *J. Org. Chem.*, **1991**, *56*, 4264.

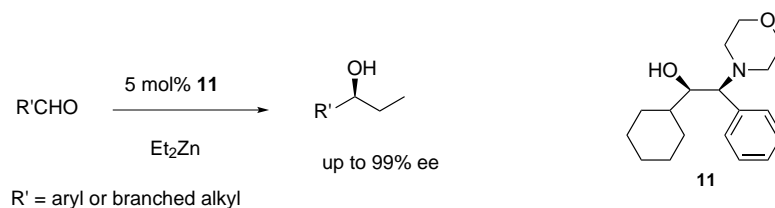
²³ Vidal-Ferran A.; Moyano A., Pericas M. A.; Riera A.; *J. Org. Chem.* **1997**, *62*, 4970.

²⁴ Delair, P.; Einhorn, C.; Einhorn, J.; Luche, J. L. *Tetrahedron* **1995**, *51*, 165.

²⁵ Beliczey, J.; Giffels, G.; Kragl, U.; Wandrey, C. *Tetrahedron: Asymmetry* **1997**, *8*, 1529.

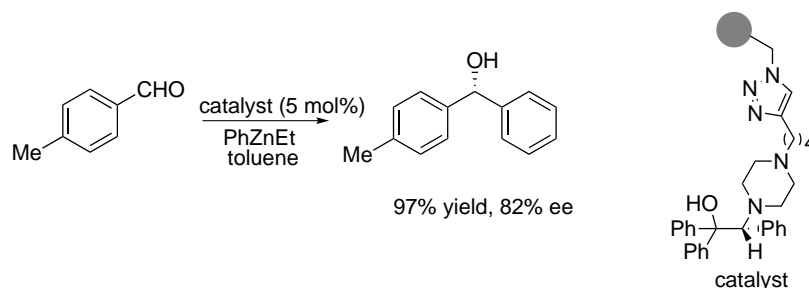
²⁶ Kawanami, Y.; Mitsue, T.; Miki, M.; Sakamoto, T.; Nishitani, K. *Tetrahedron* **2000**, *56*, 175.

Another notable example is ligand **11** which promotes the enantioselective addition of diethylzinc to aromatic and branched alkyl aldehydes at room temperature in up to 99% enantiomeric excess (Scheme 1-5).²⁷



Scheme 1-5 Asymmetric addition of diethylzinc to aldehydes.

Pericas and co-workers²⁸ have covalently linked alkynyl-functionalized amino alcohols to azidomethylpolystyrene resins through Cu(I)-catalyzed 1,3-dipolar cycloadditions. Such polymer-supported chiral amino alcohols have been used as catalysts in the asymmetric phenylation of aldehydes (Scheme 1-6) showing high catalytic activity and moderate or high enantioselectivity (up to 82%).



Scheme 1-6 Polymer-supported chiral amino alcohol used in the asymmetric phenylation of aldehydes.

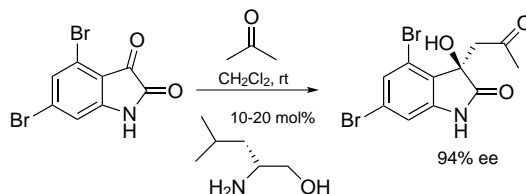
β -amino alcohols have also very often played successfully the role of chirality sources in the asymmetric aldol reaction.²⁹ For example leucinol and valinol, primary amino alcohols available from the corresponding natural α -amino acids in one step, have been shown to act as efficient, enantioselective organocatalyst for the aldol reaction of isatin and its derivatives with acetone; *D*-

²⁷ Nugent W. A.; *Org. Lett.* **2002**, *4*, 2133.

²⁸ Bastero A.; Font D.; Pericas M. A.; *J. Org. Chem.* **2007**, *72*, 2460.

²⁹ Vicario J. L.; Badia D.; Carrillo L.; Reyes E.; Extbarria J.; *Current Organic Chemistry*, **2005**, *9*, 219.

leucinol was successfully used in the asymmetric synthesis of natural convolutamydine A (Scheme 1-7), an anti-leukemia agent.³⁰



Scheme 1-7 Enantioselective synthesis of (R)-(+)-convolutamydine A catalyzed by D-leucinol.

1.2.2 Synthetic methods for β -amino alcohols

Due to the repeated occurrence of vicinal amino alcohol moiety in different compounds of interest, numerous methods have been developed for the stereocontrolled synthesis of 1,2-amino alcohols.³¹

Many existing routes to vicinal amino alcohols rely on the derivatization of naturally available enantiopure amino acids, which limits the number of accessible analogues.³² Alternative approaches include the well-known Sharpless asymmetric aminohydroxylation³³ and the stereoselective addition of several nucleophiles to α -aminocarbonyl compounds,³⁴ nitroalkenes,³⁵ α -hydroxy imines,³⁶ epoxides³⁷ and aziridines.³⁸ Recently, novel syntheses of vicinal amino alcohols by direct catalytic asymmetric Mannich-type reactions were developed by Shibasaki, Trost, List and Barbas.³⁹ With no intention to be fully comprehensive of the enormous literature on the subject, the reader is redirect to the articles and books cited and all references therein reported.

³⁰ Malkov, A. V.; Kabeshov, M. A.; Bella, M.; Kysilka, O.; Malyshev, D. A.; Pluhackova, K.; Kocovsky, P.; *Org. Lett.* **2007**, *9*, 5473.

³¹ Bergmeier S. C.; *Tetrahedron* **2000**, 2561.

³² Ager j. D.; Prakash I.; Schaad D. R.; *Chem. Rev.* **1996**, *96*, 835

³³ Li, G.; Chang, H.-T.; Sharpless, B. K. *Angew. Chem., Int. Ed. Engl.* **1996**, *35*, 451

³⁴ a) Reetz M. T.; *Angew. Chem. Int. Ed.* **1991**, *30*, 1531. b) Reetz M. T.; *Chem. Rev.* **1999**, *99*, 1121.

³⁵ Enders D.; Haertwig A.; G. Raabe G.; Runsink J.; *Eur. J. Org. Chem.* **1998**, 1771.

³⁶ Kobayashi S.; Ishitani H.; Ueno M.; *J. Am. Chem. Soc.* **1998**, *120*, 431. b) Hattori K., Yamamoto H.; *Tetrahedron* **1994**, *50*, 2785.

³⁷ For some recent examples, see: a) Castellnou D.; Solà L.; Jimeno C.; Fraile j. M.; Mayoral j. A.; Riera A.; Pericàs M. A.; *J. Org. Chem.* **2005**, *70*, 433. b) Samoshin V. V.; Chertkov V. A.; Gremyachinskiy D. E.; Dobretsova E. K.; Shestakova A. K.; Vatlina L. P. *Tetrahedron Lett.* **2004**, *45*, 7823. c) Bartoli G.; Bosco M.; Carlone A.; Locatelli M.; Melchiorre P.; Sambri L.; *Org. Lett.* **2004**, *6*, 3973.

³⁸ (a) Yun J. M.; Sim T. B.; Hahm H. S.; Lee W. K.; Ha H. J.; *J. Org. Chem.* **2003**, *68*, 7675. b) Ohno H.; Hamaguchi H.; Tanaka T.; *J. Org. Chem.* **2001**, *66*, 1867. c) Hwang G. I.; Chung J. H.; Lee W. K.; *J. Org. Chem.* **1996**, *61*, 6183. d) Ibuka T.; Nakai K.; Akaji M.; Tamamura H.; Fujii N.; Yamamoto Y.; *Tetrahedron* **1996**, *52*, 11739.

³⁹ (a) Sugita M.; Yamaguchi A.; Yamagiwa N.; Handa S.; Matsunaga S.; Shibasaki M.; *Org. Lett.* **2005**, *7*, 5339. b) Trost B. M.; Terrell L. R.; *J. Am. Chem. Soc.* **2003**, *125*, 338. c) List B.; Pojarliev P.; Biller W. T.; Martin H. J.; *J. Am. Chem. Soc.* **2002**, *124*, 827. d) Córdova A.; Notz W.; Zong G.; Betancort J. M.; Barbas C. F.; *J. Am. Chem. Soc.* **2002**, *124*, 1842.

The synthetic approach of our research group to achieve the 1,2-amino alcohol framework is based on the ring opening reactions of epoxides and aziridines. In particular, in recent years the attention has been focused on the use of metal halides to open these strained three-membered rings, mainly functionalised in the α position with hydroxyl, carbonyl and carboxyl group.⁴⁰ The obtained haloderivatives can be subsequently transformed in a variety of compounds, and in particular, through a substitution by a nitrogen nucleophile, to the 1,2-amino alcohol target structures. Through the latter and many other manipulations such as reductions, oxidations or different substitutions, this well established methodology has been largely applied to the synthesis of numerous biologically active products. In the present work the stereo- and regiocontrolled synthesis of different amino alcoholic structures was based on ring-opening of optically active epoxides.

Ring-opening reactions of epoxides

Ring-opening of epoxides is a widespread method for the synthesis of vicinal amino alcohols. Undoubtedly, this is due to the many available methods for the preparation of optically pure epoxides from olefins via stereo- and enantioselective routes.⁴¹

Amine and azides ions can readily open epoxides to form a vicinal amino alcohol or azido alcohol.⁴² Azido alcohols are readily converted to the amino alcohols.⁴³ Epoxide ring-opening is usually stereospecific. A potential problem is the regiochemical control because either of the carbon atoms of epoxide can react with the nucleophile to produce regioisomeric amino alcohols.

Crotti and co-workers have studied the regiocontrol in some ring-opening of epoxides bearing remote polar heterofunctionalities, through metal-assisted chelating or non chelating processes.⁴⁴ Chelating processes presume the presence of a metal salt in a polar aprotic solvent, while non chelating processes occur in acid-catalyzed conditions without any salt able to give chelation.

The reaction of the *cis*-epoxide derived from 4-(benzyloxy)cyclohexene **12** with diethylamine as nucleophile were carried out using acetonitrile as solvent and LiClO₄ as Lewis acid (Scheme 1-8),

⁴⁰ a) Righi, G.; Bonini, C. *Target in Heterocyclic Systems*, Attanasi, O. A.; Spinelli, D., Eds; Italian Society of Chemistry, **2000**, *4*, 139. b) Bonini, C.; Righi, G.; *Tetrahedron* **2002**, *58*, 4981.

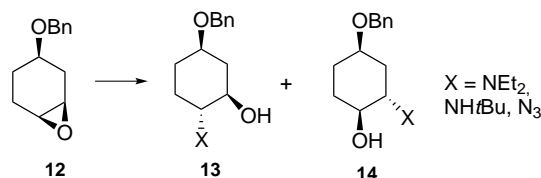
⁴¹ a) Erden, I. *Comprehensive Heterocyclic Chemistry II*, Katritzky, A. R.; Rees, C.; Scriven, E. F.; Padwa, A. Eds.; Elsevier: Oxford, UK, **1996**, Vol. 1A, 97.

⁴² a) Castejon, P.; Moyano, A.; Pericas, M. A.; Riera, A. *Tetrahedron* **1996**, *52*, 7063. b) Chng, B. L.; Ganesan, A. *Bioorg. Med. Chem. Lett.* **1997**, *7*, 1511. c) Van de Weghe, P.; Collin, J. *Tetrahedron Lett.* 1995, *36*, 1649. d) Hou, X.-L.; Wu, J.; Dai, L.-X.; Xia, L.-J.; Tang, M.-H. *Tetrahedron: Asymmetry* 1998, *9*, 1747. e) Lindstrom, U. M.; Franckowiak, R.; Pinault, N.; Somfai, P. *Tetrahedron Lett.* 1997, *38*, 2027.

⁴³ Scriven, E.; Turnbull, K. *Chem. Rev.* 1988, *88*, 297.

⁴⁴ (a) Chini, M.; Crotti, P.; Flippin, L. A.; Macchia, F. *J. Org. Chem.* **1990**, *55*, 4265; (b) Chini, M.; Crotti, P.; Flippin, L. A.; Macchia, F. *Tetrahedron Lett.* **1989**, *30*, 6563.

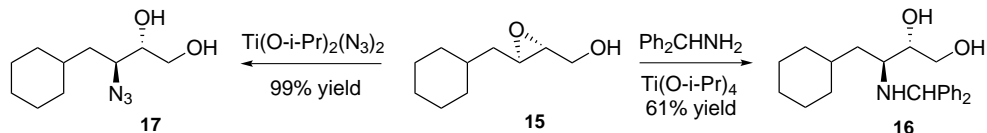
affording in good yield a mixture of the two amino alcohols in ratios that changed significantly with the amount of the lithium salt, always in favour of the regioisomers **13**.⁴⁵ Using *t*-butylamine and NaN₃ as nucleophiles similar results were obtained.



Scheme 1-8 Ring-opening of *cis*-epoxides.

As previously reported by Sharpless,⁴⁶ it was hypothesized that the role of the metal ion salt in these reactions is to coordinate the oxirane oxygen favoring the regioselective ring-opening process. The regioselectivity of the ring-opening of epoxide can be reversed in favour of **14** with sodium azide in a protic solvent under acidic and non chelating conditions.⁴⁷ The same azidolysis and aminolysis reactions were carried out on linear epoxy alcohols and epoxy benzyl ethers and analogous behaviours were observed.⁴⁸

Other examples of epoxide ring-opening are shown in Scheme 1-9.⁴⁹ The starting compound **15** was prepared from the corresponding allylic alcohol via a Sharpless asymmetric epoxidation.⁵⁰ Treatment of **15** with benzhydryl amine in the presence of Ti(O-*i*-Pr)₄ provides vicinal amino alcohol **16** in good yield. Likewise, treatment of the same epoxide with azide provides the azido alcohol **17** almost quantitatively.



Scheme 1-9 Regioselective opening of epoxides.

⁴⁵ a) Chini, M.; Crotti, P.; Macchia, F. *J. Org. Chem.* **1991**, *56*, 5939. b) Chini, M.; Crotti, P.; Flippin, L. A.; Macchia, F. *J. Org. Chem.* **1991**, *56*, 7043.

⁴⁶ Caron, M.; Sharpless, K. B. *J. Org. Chem.* **1985**, *50*, 1557.

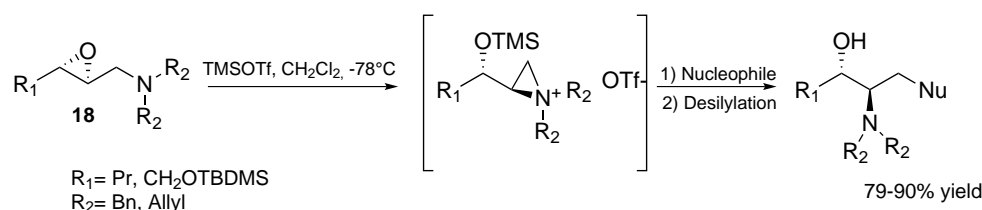
⁴⁷ Chini, M.; Crotti, P.; Uccello-Barretta, G.; Macchia, F. *J. Org. Chem.* **1989**, *54*, 4525.

⁴⁸ Chini, M.; Crotti, P.; Flippin, L. A.; Gardelli, C.; Giovani, E.; Macchia, F.; Pineschi, M. *J. Org. Chem.* **1993**, *58*, 1221.

⁴⁹ Pasto, M.; Castejon, P.; Moyano, A.; Pericas, M. A.; Riera, A. *J. Org. Chem.* **1996**, *61*, 6033.

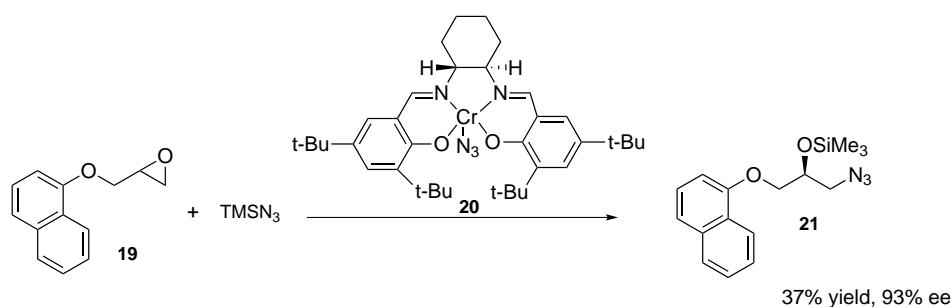
⁵⁰ Gao, Y.; Hanson, R. M.; Klunder, J. M.; Ko, S. Y.; Masamune, H.; Sharpless, K. B. *J. Am. Chem. Soc.* **1987**, *109*, 5765.

A regioselective intramolecular reaction to preparing vicinal amino alcohols involves 2,3-epoxy amines under Lewis acidic conditions.⁵¹ Treated with TMS-OTf (trimethylsilyltrifluoromethanesulfonate), epoxyamine **18** generates a reactive aziridinium ion which can be regiospecifically trapped with a nucleophile at C-1 (Scheme 1-10).



Scheme 1-10 Aziridinium ion generation and trapping.

If the enantiomerically pure epoxides are not easily available, the chemistry shown above becomes less interesting. There are several types of epoxides which are not readily prepared by the standard methods. Jacobsen overcame this limitation via a kinetic resolution (KR) of racemic terminal epoxides. The KR of the racemic epoxide **19**, using the chiral chromium catalyst **20**, provides the azido alcohol **21** with excellent enantiomeric purity (Scheme 1-11).⁵²



Scheme 1-11 Jacobsen KR.

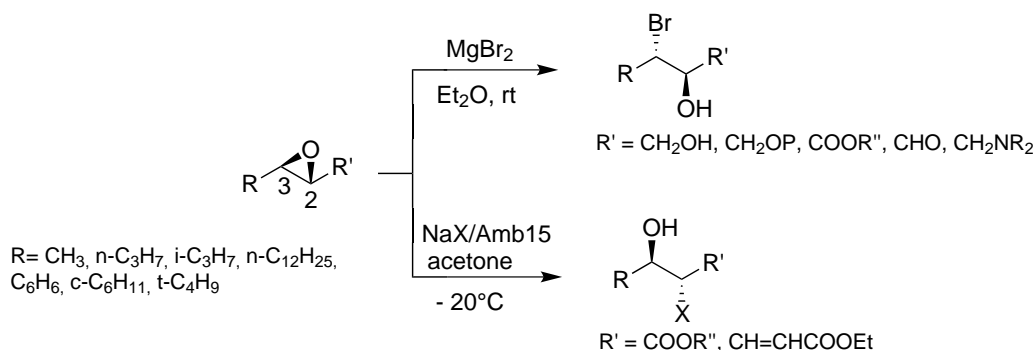
Useful nucleophiles for epoxide opening are also amides and carbamates.⁵³

⁵¹ Liu, Q.; Marchington, A. P.; Rayner, C. M. *Tetrahedron* **1997**, *53*, 15729.

⁵² Larrow, J. F.; Schaus, S. E.; Jacobsen, E. N. *J. Am. Chem. Soc.* **1996**, *118*, 7420.

⁵³ Albanese, D.; Landini, D.; Penso, M. *Tetrahedron* **1997**, *53*, 4787.

Our research group has developed two different methodologies to open regioselectively the epoxide ring at C-2 or C-3 position (Scheme 1-12), depending on the functionality present at C-2, by metal halides.⁵⁴



Scheme 1-12 Regioselectively opening of 2-functionalized epoxides by metal halides.

The use of MgBr_2 provided diastereomerically pure 3-bromo derivatives in excellent yields, with mild reaction conditions.⁵⁵ The high regio- and stereoselectivity can be attributed to the formation of a five-membered chelate complex among metal (Mg^{++}), epoxidic oxygen and the heteroatom present in R' group (Figure 1-5).⁵⁶

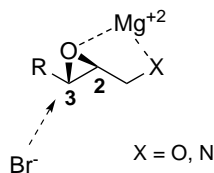


Figure 1-5 Hypothesized chelate complex among metal, epoxidic oxygen and the heteroatom in R' group.

In specific cases, using the $\text{NaX}/\text{Amberlyst 15}$ system in acetone the regioselectivity of the nucleophilic attack was reversed.⁵⁷ Probably in absence of any coordination between the metal and the epoxide substrate (Na is a poor Lewis acid), the C-2 position is preferred because of the electronic effect of the ester or olefinic group. The obtained haloderivatives can readily be transformed into 1,2-aminoalcohols through a substitution by a nitrogen nucleophile.

⁵⁴ See ref. 40.

⁵⁵ a) Bonini, C.; Righi, G.; Sotgiu, G. *J. Org. Chem.*, **1991**, *56*, 6206. b) Righi, G.; Franchini, T.; Bonini, C. *Tetrahedron Lett.*, **1998**, *39*, 2385. c) Righi, G.; Rumboldt, G. *J. Org. Chem.*, **1996**, *61*, 3557. d) Righi, G.; D'Achille, R. *Tetrahedron Lett.*, **1996**, *37*, 38, 6893.

⁵⁶ Righi, G.; Chionne, A.; Bonini, C. *Eur. J. Org. Chem.* **2000**, *18*, 3127.

⁵⁷ a) Righi, G.; Rumboldt, G. *Tetrahedron* **1995**, *51*, 48, 13401. b) Righi, G.; Chionne, A.; D'Achille, R.; Bonini, C. *Tetrahedron: Asymmetry* **1997**, *8*, 6, 903.

1.3 Nanoparticles in catalysis

In modern “green chemistry” approaches for catalysis of organic reactions, the possibility of recovery and reuse of catalysts become a fundamental factor because of the stringent ecological and economical demands for sustainability.⁵⁸ It is especially true for enantioselective transformations, in which the cost of sophisticated ligands often exceeds that of the noble metal employed.

Homogeneous catalysts have the advantage that they are well defined on a molecular level and readily soluble in the reaction medium. Such single-site catalysts are highly accessible to the substrates and often show high catalytic activity and selectivity, even under mild conditions. However, removing them from the reaction mixture requires expensive and tedious purification steps.⁵⁹ Thus, despite their intrinsic advantages, homogeneous catalysts are used in less than 20% of the industrially relevant processes.⁶⁰

Therefore, research into the development of heterogeneous/heterogenated catalyst systems that can be easily recovered and recycled has considerably increased.⁶¹ Commonly used techniques are based on the immobilization of catalytically active species on solid supports such as organic polymers/resins or inorganic oxides. However, the entrapment or immobilization of the homogeneous catalysts on the solid support normally results in a decrease in the reactivity of catalytic species. For example, amorphous resins often have the problem that catalytic sites are buried in the polymer backbone, thus limiting the access of reactants.⁶² In the case of solid particles suspended in a liquid, the rate of transfer of reactants within the liquid to the catalyst is inversely proportional to the particle diameter. Thus, the activity of the suspended catalyst will benefit from decreasing the particle size.⁶³ It is worth mentioning at this point that the dispersion of most conventional heterogeneous catalysts in liquid media is poor and in most cases distinct solid–liquid separation occurs, even after vigorous stirring. One way to overcome this drawback is to keep the size of the particles as small as possible.⁶⁴

⁵⁸ Gladysz, J.; *Chem. Rev.* **2002**, *102*, 3215.

⁵⁹ a) Bell, A. T.; *Science* **2003**, *299*, 1688. b) Schlogl R.; Abd Hamid S. B.; *Angew. Chem.* **2004**, *116*, 1656 .

⁶⁰ a) Sheldon, R. A.; *J. Environ. Monit.* **2008**, *10*, 406. b) Sheldon, R. A.; *Chem. Commun.* **2008**, 3352.

⁶¹ Cozzi, F.; *Adv. Synth. Catal.* **2006**, *348*, 1367.

⁶² Vaino, A. R.; Janda, K. D.; *J. Comb. Chem.* **2000**, *2*, 579.

⁶³ Teunissen, W.; Bol, A. A.; Geus, J. W. ; *Catal. Today* **1999**, *48*, 329.

⁶⁴ Narayanan, R.; El-Sayed, M. A.; *J. Phys. Chem. B* **2005**, *109*, 12663.

In this context, nanoparticles (NPs) have recently emerged as ideal supports for the immobilization of homogeneous catalysts.⁶⁵ Generally nanoparticles are defined as molecular or atomic aggregates in the size range between 1 and 100 nanometers.⁶⁶ Unlike conventional micrometer-sized particles, they can be easily dispersed in a liquid medium to form stable suspensions and their large specific surface area means that high loadings of catalytically active sites are guaranteed. For example, spherical nanoparticles with a diameter of about 10 nm have a calculated surface area of $600 \text{ m}^2/\text{cm}^3$, which is comparable to many porous supports used for the immobilization of homogeneous catalysts.⁶⁷ So nanoparticle-supported catalysts are well exposed on the particle surface, which makes them accessible to the reactants almost like their homogeneous counterparts, and then can exhibit catalytic activities approaching those of homogeneous, molecular systems.

Particles with diameters of less than 100 nm are often difficult to separate by filtration techniques. In such cases, expensive ultracentrifugation is sometimes the only way to separate the product and catalyst. This drawback can be overcome by using magnetic nanoparticles (MNPs), which can be easily removed from the reaction mixture by magnetic separation (**Figure 1-6**).

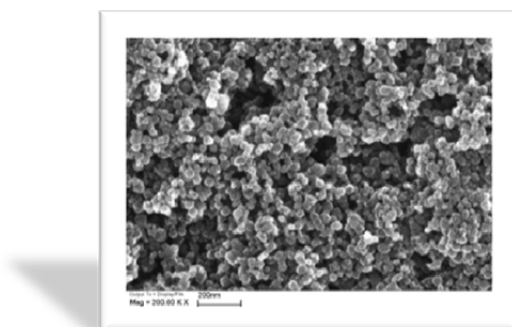


Figure 1-6 Scanning electron microscope (SEM) image of magnetic nanoparticles with size around 20 nm.

Therefore, the functionalization of the surfaces of magnetic nanoparticles is an elegant way to bridge the gap between heterogeneous and homogeneous catalysis. The resulting “nanocatalyst” is schematized in Figure 1-7: the nanoparticle acts as the structuring element for an assembly of ligands, which are bonded to the particle through an additional function, different from the chelating functional groups defining the catalytic center. A further advantage expected from this

⁶⁵ a) Schatz, A.; Reiser, O.; Stark, W. J.; *Chem. Eur. J.* **2010**, *16*, 8950. b) Roy, S.; Pericas, M. A.; *Org. Biomol. Chem.*, **2009**, *7*, 2669.

⁶⁶ Nogi, K.; Naito, M.; Yokoyama, T.; *Nanoparticle Technology Handbook*. **2012**, Elsevier.

⁶⁷ Hu, A.; Yee, G. T.; Lin, W.; *J. Am. Chem. Soc.* **2005**, *127*, 12486.

approach is the possibility to increase the catalytic activity due to the accumulation of active centers on the nanoparticle periphery.

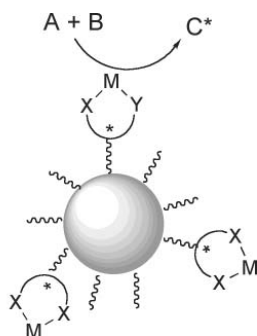


Figure 1-7 Functionalized nanoparticle for catalytic applications.

In this type of system the catalytic activity does not arise from the core material and the nanomaterial acts solely as a carrier for soluble catalysts. Another possible approach involves the use of systems where the nanoparticle constituent metal exerts a fundamental role for the planned catalytic activity.⁶⁸ Even more complex morphologies, capable of integrating multiple functionalities, are possible if bimetallic nanoparticles or multilayer shells are considered.⁶⁹

1.3.1 Magnetic nanoparticles

Decreasing the size of a particle results in a larger share of the atoms being located on the surface which can increase the influence of surface effects on the material properties. So nanoparticles are different from their bulk counterparts and exhibit unique properties. In particular, magnetic nanoparticles with size below 20 nm often exhibit a special form of magnetism called superparamagnetism.⁷⁰

Magnetic solids possess magnetic domains with well-defined magnetic sublattices which are separated by domain walls. The magnetic moments of these domains are oriented randomly if the solid has not been magnetized by the application of an external magnetic field. Below a critical size, which is dependent on the material, a nanoparticle becomes a single magnetic domain. In this condition, it is considered that the magnetization of the nanoparticles is a single

⁶⁸ See, for example: a) Tamura, M.; Fujihara, H.; *J. Am. Chem. Soc.*, **2003**, *125*, 15742. b) Jansat, S.; Picurelli, D.; Pelzer, K.; Philippot, K.; Gomez, M.; Muller, G.; Lecante P.; Chaudret, B.; *New J. Chem.*, **2006**, *30*, 115. c) Sawai, K.; Tatumi, R.; Nakahodo, T.; Fujihara, H.; *Angew. Chem. Int. Ed.*, **2008**, *47*, 6917. d) Kantam, M.L.; Laha, S.; Yadav, J.; Likhar, P.R.; Sreedhar, B.; Choudary, B. M.; *Adv. Synth. Catal.*, **2007**, *349*, 1797.

⁶⁹ Jun, C.-H.; Park, Y.J.; Yeon, Y.-R.; Choi, J.; Lee, W.; Ko, S.; Cheon, J.; *Chem. Comm.*, **2006**, 1619.

⁷⁰ Sorensen, C. M.; *Nanomaterials in Chemistry* (Ed. K. J. Klabunde), Wiley, New York, **2001**. b) Frey, N. A.; Peng, S.; Cheng, K.; Sun, S.; *Chem. Soc. Rev.* **2009**, *38*, 2532.

magnetic moment, sum of all the individual magnetic moments carried by the atoms of the nanoparticle. Such particles are named single-domain particles and are superparamagnetic above a certain temperature called blocking temperature. Superparamagnetic nanoparticles are intrinsically non magnetic but can be readily magnetized in the presence of an external magnetic field; they behave like a giant paramagnetic atom with a fast response to applied magnetic fields and negligible remanence (residual magnetism) and coercivity (the field required to bring the magnetization to zero).

These features make superparamagnetic nanoparticles very attractive for a broad range of applications because they can be manipulated by external magnetic field gradients, but the risk of forming agglomerates is negligible at room temperature (Figure 1-8). In very recent years, many novel uses of magnetic nanoparticles have been proposed and investigated in the fields of biolabeling and bioseparation, in catalysis, in magnetic resonance imaging as contrast agents, in drug delivery and in cancer treatments through hyperthermia.⁷¹



Figure 1-8 Magnetic separation of Fe_3O_4 nanoparticles.

Magnetic materials that can be prepared in the form of nanoparticles include metals (Fe, Co, Ni), alloys (FePt, CoPt, FePt₃), metal oxides (FeO, Fe₂O₃, Fe₃O₄), or ferrites (CoFe₂O₄, MnFe₂O₄). Among this wide variety of materials, iron oxides, either magnetite (Fe₃O₄) or maghemite (γ -Fe₂O₃), have certainly been and still are the most intensively studied. This is due to several factors, one being the approval by the Food and Drug Administration (FDA) of the use of superparamagnetic iron oxide nanoparticles as contrast agents in magnetic resonance imaging. FDA approval implies that iron oxides (in particular magnetite) seem to be quiet benign toward humans. Crystalline structure of magnetite is shown in Figure 1-9.

⁷¹ *Magnetic nanomaterials* (Ed. Challa S. S. R. Kumar), Wiley, New York, 2009.

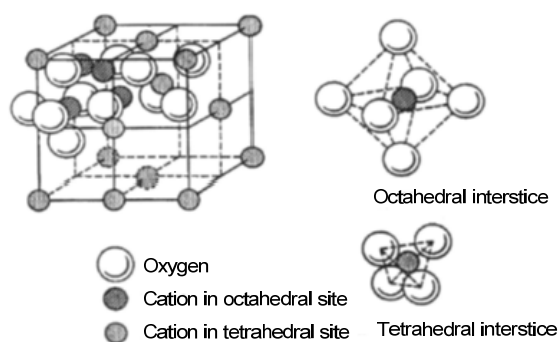


Figure 1-9 Crystalline structure of magnetite $[\text{Fe}^{3+}] [\text{Fe}^{2+}, \text{Fe}^{3+}] \text{O}_4$.

Synthesis of superparamagnetic nanoparticles

In the last decades, numerous methods including co-precipitation, thermal decomposition, synthesis in microemulsions or under hydrothermal conditions, and laser pyrolysis techniques were employed for the synthesis of nanostructured magnetic materials.⁷²

Iron chloride, acetate, acetylacetonate, and carbonyls are commonly used precursors for the synthesis of iron oxide nanoparticles.⁷³ In terms of simplicity of the synthesis, co-precipitation is the preferred way to prepare iron oxide nanoparticles. In terms of size and morphology control of the nanoparticles, thermal decomposition seems the best method developed to date. Stability and dispersibility of magnetic nanoparticles synthesized by these methods results either from steric or electrostatic repulsion, depending on the solvent and the surfactants or capping agents used to avoid agglomeration. Various physicochemical characterization techniques, such as X-ray diffraction (XRD) and transmission electron microscopy (TEM), can be employed to probe the crystalline nature, the phase purity and the morphology of magnetic nanoparticles.

Co-precipitation is typically carried out in aqueous $\text{Fe}^{2+}/\text{Fe}^{3+}$ salt solutions by the addition of a base under inert atmosphere at room temperature or at elevated temperature. The surfaces of the iron oxide nanocrystals formed are stabilized by surfactants or associated ions. The size, shape, and composition of the magnetic nanoparticles depend on the type of salts used (e.g. chlorides, sulfates, nitrates), the $\text{Fe}^{2+}/\text{Fe}^{3+}$ ratio, the reaction temperature and time, the pH value and ionic strength of the media. This method is very facile, use readily available metal precursors and

⁷² Lu, A.-H.; Salabas, E. L.; Schuth, F.; *Angew. Chem. Int. Ed.* **2007**, *46*, 1222.

⁷³ a) Wang, X.; Zhuang, J.; Peng, Q.; Li, Y. D.; *Nature* **2005**, *437*, 121. b) Redl, F. X.; Black, C. T.; Papaefthymiou, G. C.; Sandstrom, R. L.; Yin, M.; Zeng, H.; Murray, C. B.; O'Brien, S. P.; *J. Am. Chem. Soc.* **2004**, *126*, 14583.

provide high yields. Once the synthetic conditions are fixed, the quality of the magnetite nanoparticles is fully reproducible. Moreover, the as prepared nanoparticles are very versatile, *i.e.* well suited to bind molecules because of the free hydroxyl groups on their surface.

Despite all these advantages, the aqueous coprecipitation method has several drawbacks when it comes to the control of the average size and monodispersity (narrow particle size distribution) of the produced nanocrystals. Since the blocking temperature depends on particle size, a wide particle size distribution will result in a wide range of blocking temperatures and therefore non-ideal magnetic behavior for many applications. Particles prepared by co-precipitation unfortunately tend to be rather polydisperse.

When a better control over the size distribution and high nanoparticle stability are desired, organic phase thermal decomposition methods are generally used. In these methods, nanocrystals are synthesized essentially through the high-temperature decomposition of metal precursors in high-boiling organic solvents containing stabilizing surfactants. The metal precursors include metal acetylacetonates, metal cupferronates or carbonyls. Fatty acids and long chain amine are often used as surfactants. In principle, the ratios of the starting reagents, the reaction temperature, reaction time, as well as aging period, are the decisive parameters for the control of the size and morphology of magnetic nanoparticles. While the mechanism leading to particle nucleation under these conditions is not well-known, the method has proven to be effective in producing magnetite nanoparticles with good crystallinity and controlled monodisperse size distribution.

In particular, the strategy developed by Sun *et al.* allows to prepare monodisperse MFe_2O_4 ($M = Fe, Co, Mn$) nanoparticles with a particle size ranging from 4 to 20 nm.⁷⁴ The drawback of Sun's method is that the particles can only be prepared in the presence of oleic acid and oleyl amine as stabilizers and they are, therefore, soluble only in non-polar organic solvents.

However, the oleic acid moieties initially present on the nanoparticles surface can be replaced later with other ligands, by a ligand exchange reaction. The ligand exchange is a flexible route for attaching to particle molecules that have a high affinity for its surface.⁷⁵ Whiteside's group was the first to show that molecules carrying thiol groups can adsorb very efficiently onto gold, with the thiol moiety binding to the gold surface.⁷⁶ It has since been shown that it is relatively easy to replace one molecule with another by using an excess of the new molecule while providing

⁷⁴ Sun, S. H.; Zeng, H.; Robinson, D. B.; Raoux, S.; Rice, P. M.; Wang, S. X.; Li, G. X. *J. Am. Chem. Soc.* **2004**, *126*, 273.

⁷⁵ Lattuada, M.; Alan Hatton, T.; *Langmuir* **2007**, *23*, 2158.

⁷⁶ Bain, C. D.; Troughton, E. B.; Tao, Y. T.; Evall, J.; Whitesides, G. M.; Nuzzo, R. G. *J. Am. Chem. Soc.* **1989**, *111*, 321.

enough heat and/or sonication. The same principle applies to iron oxide surfaces and molecules containing functionalities like carboxyl acid group. Functionalized nanoparticles with good stability are very promising for applications in catalysis and in biotechnology/biomedicine applications.

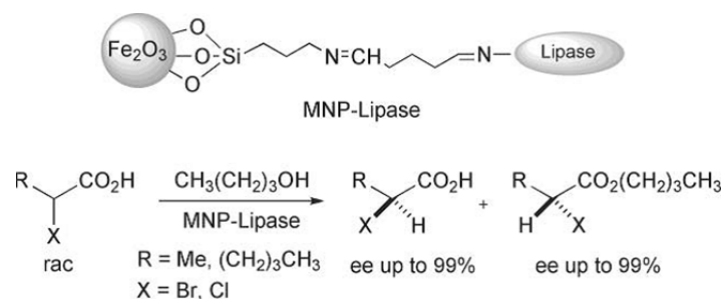
Functional magnetic nanoparticles in asymmetric catalysis

The specific advantages of magnetic nanomaterials in catalysis can be summarized as follows:

- * particles possess high external surfaces where the catalytically active sites can be distributed; thus pore diffusion constraints are avoided;
- * the small size of the particles (typically <50 nm) means that they are highly dispersible in solvents, thus the external active sites are readily accessible to the incoming reactants;
- * the application of an external magnetic field allows the particles to be removed in a simple and efficient way.

In particular, in the case of asymmetric catalysis, enantiocontrol is possible due to the close similarity with purely homogeneous processes. However, in spite of the huge progress experienced by asymmetric catalysis, up to now it has been reported a limited number of applications of functional magnetic nanoparticles in this field.

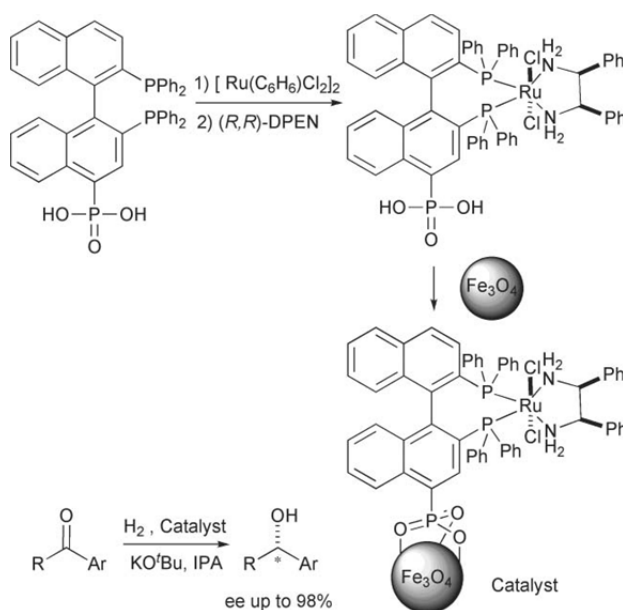
In a pioneer development, Gao and co-workers⁷⁷ reported the kinetic resolution of racemic carboxylates catalyzed by a maghemite nanoparticle-immobilized lipase from *Candida rugosa* (Scheme 1-13). This biocatalytic system exhibited high stereoselectivity and improved long-term stability over its parent free enzyme, allowing the supported enzyme to be magnetically separated and reused.



Scheme 1-13 Kinetic resolution of carboxylates using MNP-supported lipase.

⁷⁷ Gardimalla, H. M. R.; Mandal, D.; Stevens, P. D.; Yen, M.; Gao, Y.; *Chem. Comm.* **2005**, 4432.

In 2005, Lin *et al.*⁷⁸ have synthesized a magnetically recoverable chiral catalyst through immobilizing a ruthenium(II) complex, $[\text{Ru}(\text{BINAP-PO}_3\text{H}_2)\text{-(DPEN)Cl}_2]$ (BINAP=2,2'-bis(diphenylphosphino)-1,1'-binaphthyl; DPEN=1,2-diphenylethylenediamine), on Fe_3O_4 nanoparticles through the phosphonate group. This nanoparticle-supported chiral catalyst was used for asymmetric hydrogenation of aromatic ketones (Scheme 1-14) with very good enantiomeric excess values, even higher than those recorded with the homogeneous Noyori's catalyst, $\text{Ru}(\text{BINAP})(\text{DPEN})\text{Cl}_2$.



Scheme 1-14 Asymmetric reduction of ketones catalyzed by MNP-immobilized Ru-catalyst.

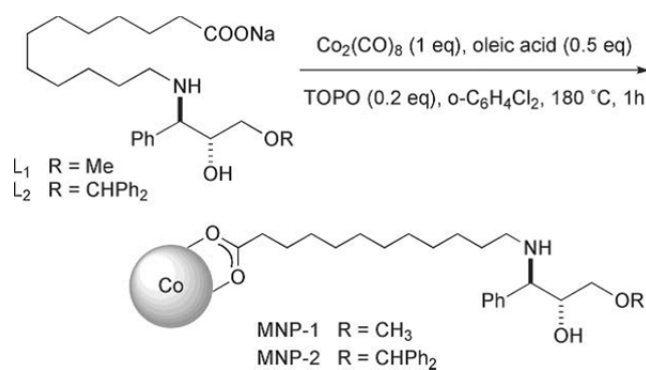
The immobilized catalysts were recycled by magnetic decantation and reused up to 14 times without loss of activity and enantioselectivity. Most likely, the three-point binding provided by the phosphonic acid group plays a fundamental role in preventing the leaching of the catalytic species into solution, thus contributing to the preservation of the catalytic activity.

In 2008, Pericas and co-workers have reported the unique example of magnetic nanoparticle-supported enantiopure β -amino alcohol ligand for asymmetric catalysis, known so far.⁷⁹ Cobalt nanoparticles are usually stabilized by long chain carboxylic acids (such as oleic acid); therefore, incorporating a long chain carboxylic acid into the structure of the amino alcohol allowed the immobilization of the ligand onto the surface of the nanoparticles (Scheme 1-15). These

⁷⁸ Hu, A.; Yee, G. T.; Lin, W.; *J. Am. Chem. Soc.*, **2005**, *127*, 12486.

⁷⁹ Michalek, F.; Lagunas, A.; Jimeno, C.; Pericas, M. A.; *J. Mater. Chem.*, **2008**, *18*, 4692.

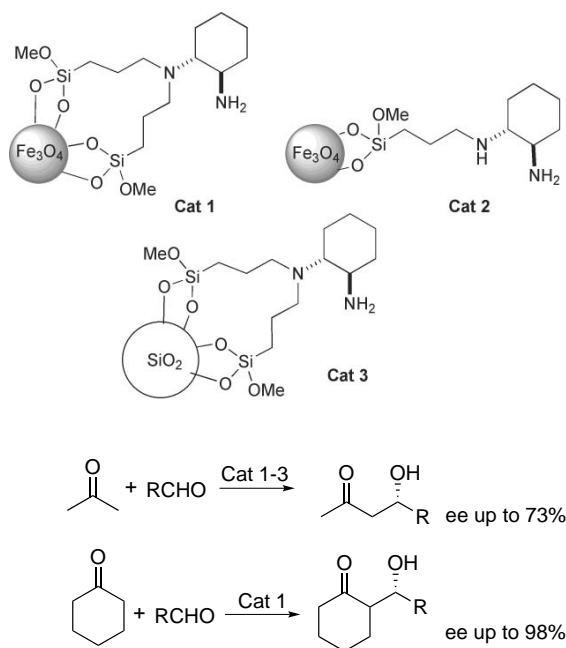
nanoparticles have been tested as magnetically decantable ligands in the Ru-catalyzed asymmetric transfer hydrogenation of alkyl aryl ketones with interesting results. In contrast with what was observed with the free ligands **L1** and **L2**, it was found that the Co NPs functionalized with the less bulky ligand (**MNP-1**) induced the highest enantioselectivity in the reactions. Even more importantly, it was found that the enantioselectivities recorded with the functional nanoparticles **MNP-1** are generally higher than those observed with structurally related, monomeric amino alcohols. This fact confirms the advantages derived from supporting the ligand on nanoparticles for asymmetric catalysis. The main drawback associated with this approach is the low reusability. In fact, a significant decrease in catalytic activity was detected upon magnetic recovery and the reuse appeared to be subject to leaching of the carboxylate ligands.



Scheme 1-15 Preparation of functional cobalt nanoparticles for asymmetric transfer hydrogenation of ketones. (TOPO= trioctylphosphine oxide).

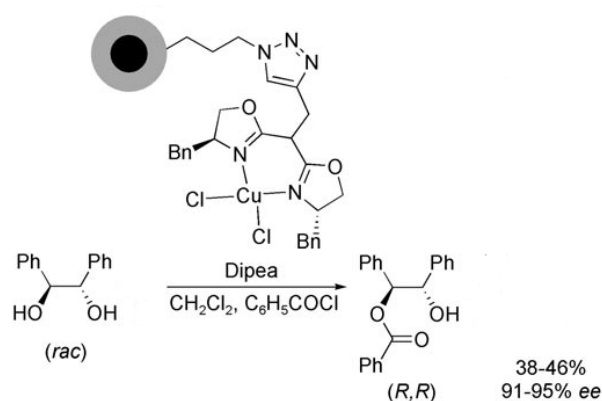
Late in 2008, Luo *et al.* reported an asymmetric aldol reaction catalyzed by magnetite nanoparticle-supported chiral amine catalysts (Scheme 1-16).⁸⁰ It was observed that the tertiary–primary amine catalyst supported on magnetic nanoparticles (**Cat 1**) was better than the secondary–primary amine catalyst on the same support (**Cat 2**). The same tertiary–primary diamine catalyst supported on chromatographic silica (**Cat 3**) showed less activity than **Cat 1**. The optimal catalyst (**Cat 1**) was recycled for 11 times with consistent activity and enantioselectivity.

⁸⁰ Luo, S.; Zheng, X.; Cheng, J. -P., *Chem. Comm.* **2008**, 5719.



Scheme 1-16 MNP-supported chiral amines for asymmetric amine-catalyzed aldol reactions.

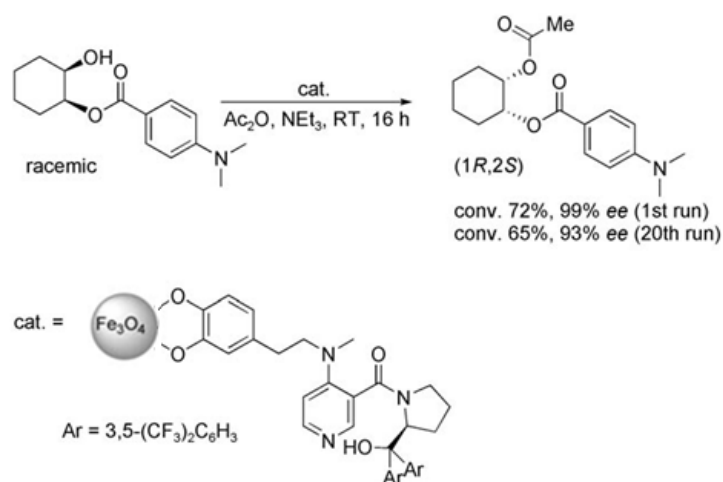
In 2009, Reiser and co-workers⁸¹ have reported silica-coated magnetic nanoparticles functionalized with azide groups for the immobilization of copper(II)-azabis(oxazoline) complexes via a copper(I) catalyzed azide-alkyne cycloaddition reaction. The potential of the immobilized complexes as catalysts was tested in the desymmetrization of racemic 1,2-diols through asymmetric benzylation (Scheme 1-17). Compared to azabis(oxazolines) “clicked” to common polymeric supports, this system has been shown to be more efficient, as exemplified by employing the catalysts in up to five runs with consistent high activity and selectivity.



Scheme 1-17 Asymmetric benzylation with azabis(oxazoline)copper(II) catalysts heterogenized on MNPs. (Dipea=diisopropylethylarginine).

⁸¹ Schatz, A.; Hager, M.; Reiser, O.; *Adv. Funct. Mater.* **2009**, *19*, 2109.

In the same year, Connon and co-workers have reported the first chiral 4-N,N-dimethylaminopyridine (DMAP) analogue supported on MNPs.⁸² The synthesis was carried out by anchoring N-methyldopamine hydrochloride onto magnetite nanoparticles, followed by a S_NAr reaction with a chiral chloropyridine in toluene. This system has been shown to be very efficient in promoting the acylative kinetic resolution of a range of *sec*-alcohols (Scheme 1-18). It is worth noting that the catalyst was reusable in a minimum of 32 consecutive cycles while retaining high activity and selectivity profiles.



Scheme 1-18 MNP-supported chiral DMAP derivative used as asymmetric acylation catalyst.

In 2010, Wang *et al.* have immobilized for the first time the Jørgensen–Hayashi catalyst ((*S*)- α,α -diphenylprolinol trimethylsilyl ether) onto silica-coated magnetic nanoparticles (Figure 1-10).⁸³

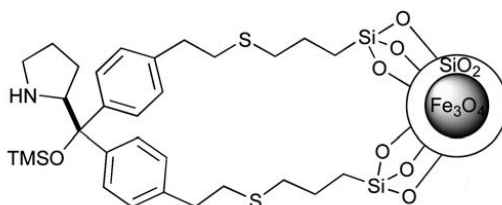


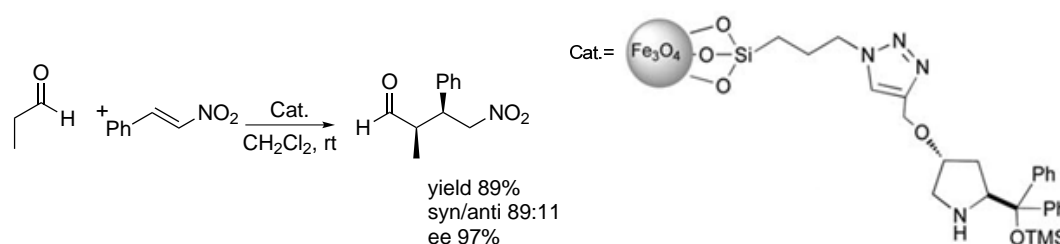
Figure 1-10 MNP-supported Jørgensen–Hayashi catalyst.

⁸² Gleeson, O.; Tekoriute, R.; Gun'ko, Y. K.; Connon, S. J.; *Chem. Eur. J.* **2009**, *15*, 5669

⁸³ Wang, B. G.; Ma, B. C.; Wang, Q.; Wang, W.; *Adv. Synth. Catal.*, **2010**, *352*, 2923.

The supported catalyst was used in the asymmetric Michael addition of aldehydes to nitroalkenes in water, providing moderate to good yields (up to 96%), good enantioselectivities (up to 90% ee) and diastereoselectivities (up to 99:1). The catalyst could be recycled for four times without significant loss of catalytic efficiency.

In 2011, Pericas and co-workers⁸⁴ have supported a C-4 substituted (S)- α,α -diphenylprolinol trimethylsilyl ether onto azide-functionalized Fe₃O₄ nanoparticles, via Cu(I) catalyzed alkyne–azide cycloaddition reaction.



Scheme 1-19 MNP-supported C-4 substituted (S)- α,α -diphenylprolinol trimethylsilyl ether used for asymmetric Michael addition.

The resulting functionalized magnetic nanoparticles were used for the asymmetric Michael addition of propanal to nitroolefins providing high enantioselectivities (Scheme 1-19). Also in this case, the catalyst could be used in 4 consecutive runs without significant deterioration of its stereochemical performance.

In 2012 Hu *et al.*⁸⁵ have reported the immobilization of a 4,4'-bisphosphonic acid-substituted BINAP-Ru-DPEN complex onto magnetite nanoparticles (Figure 1-11). The resulting catalyst **22** was used for the asymmetric hydrogenation of a wide range of aromatic ketones with remarkably high activity (99% conversion with 0.1 mol% catalyst) and enantioselectivity (up to 98.1% ee) as a result of the bulky 4,4'-substituents (*i.e.*, phosphonic acid groups) on BINAP.

⁸⁴ Riente, P.; Mendoza, C.; Pericas, M. A.; *J. Mater. Chem.*, **2011**, *21*, 7350

⁸⁵ Hu, H.; Liu, S.; Lin, W.; *RSC Advances*, **2012**, *2*, 2576.

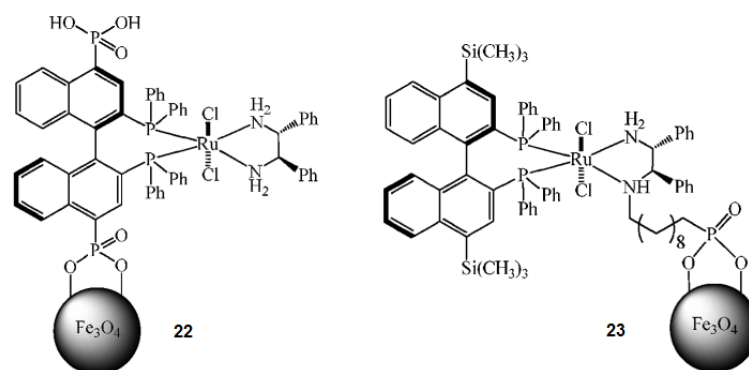


Figure 1-11 4,4'-substituted BINAP-Ru-DPEN complexes immobilized onto magnetite nanoparticles for asymmetric hydrogenation of aromatic ketones.

The catalyst could be readily recycled and reused 9 times with comparable activity and enantioselectivity. However, this catalyst tended to aggregate upon storage due to the ability of its second phosphonic acid substituent to bind other nanoparticles. Therefore, an alternative strategy to synthesize MNP-supported 4,4'-substituted BINAP-Ru-DPEN-based catalysts was investigated by coating MNPs with a DPEN derivative, then complexing the surface-bound DPEN with $[\text{Ru}(4,4'-(\text{TMS})_2\text{-BINAP})(\text{DMF})_2\text{Cl}_2]$. However, the as prepared catalyst **23** is not robust, presumably due to the oxidation of the Ru(II) intermediate by iron oxide nanoparticles.

Very recently, for the first time, Connon and co-workers have conducted a systematic study concerning the immobilization onto magnetic nanoparticles of chiral organocatalysts, which rely on a confluence of weak, easily perturbed van der Waals and hydrogen bonding interactions.⁸⁶ In particular, a cinchona alkaloid-derived urea-substituted catalyst has been demonstrated to be wholly incompatible with immobilization onto magnetite nanoparticles. The supported catalyst (Figure 1-12) was evaluated as a promoter of the asymmetric addition of dimethyl malonate to (*E*)- β -nitrostyrene. A marked drop in catalyst efficiency (from both activity and selectivity standpoints) was observed after immobilization and the catalyst was unstable over only a few iterative recycles. Most significantly, a short study, aimed at discovering the origin of the low stereoselectivity, has determined that background catalysis by the nanoparticles themselves is problematic in the examined reaction.

⁸⁶ Gleeson, O.; Davies, G. L.; Peschiulli, A.; Tekoriute, R.; Gun'ko, Y. K.; Connon, S. J.; *Org. Biomol. Chem.* **2011**, *9*, 7929.

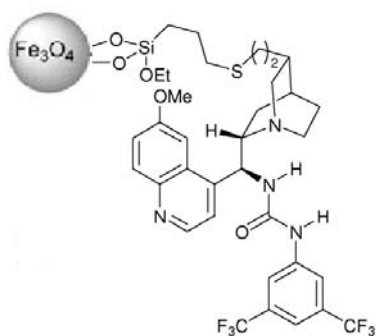


Figure 1-12 MNP-immobilized cinchona alkaloid-derived urea-substituted catalyst.

This study has revealed that magnetic nanoparticles cannot be automatically considered to be inert in catalytic processes: in some cases they can interact with both the loaded catalyst, and (on occasion) the substrate, compromising either activity/stability or selectivity. Therefore, the success of immobilization strategy is strongly correlated with the structure of the catalyst being immobilized and must be established on case- by- case basis.

In summary, the field of functional magnetic nanoparticles in asymmetric catalysis promises to provide the chemical community with a new generation of highly active and enantioselective, fully recyclable, catalytic systems for metal-catalyzed and organo-catalyzed reactions, although still presents many areas to be explored.

2 Magnetite nanoparticle-supported chiral amino alcohol catalysts

Due to our research experience on stereocontrolled synthesis of amino alcohols⁸⁷ and synthesis of metal and metal oxide nanoparticles,⁸⁸ we were attracted by the possibility of supporting optically active amino alcohol ligands onto magnetite nanoparticles. In fact, given the extensive use of chiral amino alcohols in asymmetric catalysis, we considered that we could obtain new very useful, magnetically recoverable and recyclable, chiral “nanocatalysts”. As mentioned in Chapter 1, only one example of an asymmetric magnetic (cobalt) nanoparticle-supported amino alcohol catalyst has been reported up to now.⁸⁹

Magnetite (Fe_3O_4) nanoparticles have been chosen because of their superparamagnetic behavior, convenient available preparation methods and low toxicity. Moreover, iron oxides particles present on their surface a large number of hydroxyl groups⁹⁰ that are suitable for the supporting of ligands and/or catalysts.

With respect to the strategy for the robust anchoring of the catalyst on the nanoparticle surface, it is known that either multipoint ionic binding or covalent anchoring are able to prevent catalyst leaching and, thus, decrease of activity. In particular, alkoxy silanes have been increasingly reported as important functionalization agents for iron oxide nanoparticles because they can form stable Si-O covalent bonds with -OH groups on nanoparticle surface.⁹¹

Importantly, enantioselectivity strongly depends on ligand design. It is necessary to modify the catalyst molecule for supporting in such a way that neither the linker nor the nanoparticle bulk perturbs the catalytically active site in order to obtain enantioselectivities comparable or even higher than those recorded in the homogeneous phase.

⁸⁷ a) See ref. 54-57. b) Righi, G.; Ferrara, A.; Mari, A.; Bovicelli, P.; *Synthetic Communications* **2010**, *40*, 1650.

⁸⁸ a) Mari, A.; Imperatori, P.; Marchegiani, G.; Piloni, L.; Mezzi, A.; Kaciulis, S.; Cannas, C.; Meneghini, C.; Mobilio, S.; Suber, L.; *Langmuir* **2010**, *26*, 15551. b) Suber, L.; Imperatori, P.; Ausanio, G.; Fabbri, F.; Hofmeister, H.; *J. Phys. Chem. B.* **2005**, *109*, 7103.

⁸⁹ See ref. 79.

⁹⁰ Mc Cafferty, E.; Wightman, J. P.; *Surf. Interface Anal.* **1998**, *26*, 549.

⁹¹ De Palma, R.; Peeters, S.; Van Bael, M. J.; Van den Rul, H.; Bonroy, K.; Laureyn, W.; Mullens, J.; Borghs, G.; Maes, G.; *Chem. Mater.*, **2007**, *19*, 1821.

Having regards to these factors, the system schematized in Figure 2-1 has been designed, where the anchoring to the nanoparticle surface is provided by an alkoxy silane group incorporated at one end of the chiral amino alcohol structure.

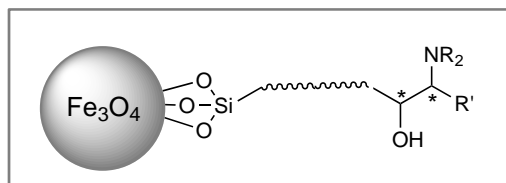
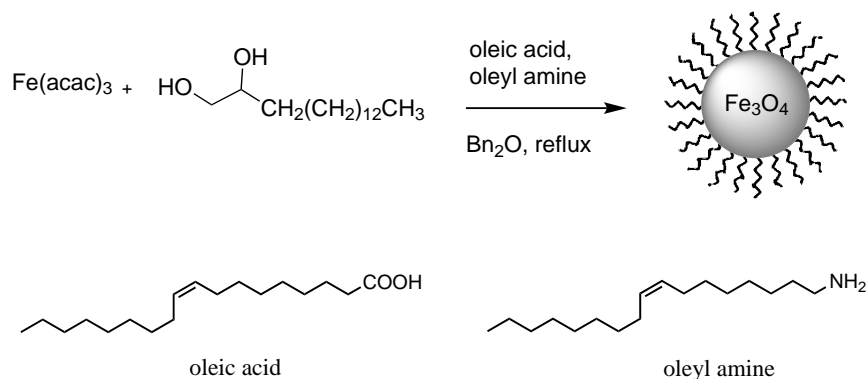


Figure 2-1 Magnetite NP-supported chiral β -amino alcohol.

Also the control of nanoparticle size and stability requires much attention. Smaller magnetic nanoparticles have a larger surface area and are consequently more active. The absence of growth and agglomeration of nanoparticles during the different steps (particle synthesis, their surface functionalization and catalytic use) is the key for the observation of high catalytic activity and for recyclability.

2.1 Organic-phase synthesis of Fe_3O_4 nanoparticles

Fe_3O_4 magnetic nanoparticles were generated by thermal decomposition of the iron (III) acetylacetonate in organic solvent with 1,2-hexadecandiol as the reducing agent, in the presence of oleic acid and oleylamine as the surfactants (Scheme 2-1).⁹²



Scheme 2-1 Synthesis of oleic acid-coated Fe_3O_4 nanoparticles.

⁹² Sun, S.; Zeng, H. *J. Am. Chem. Soc.* **2002**, *124*, 8204.

This method has been chosen because it is known to have a notably beneficial effect on the formation of well-defined superparamagnetic magnetite nanoparticles with a small diameter when compared with aqueous co-precipitation technique. High-resolution scanning electron microscopy (HR-SEM) analysis revealed the formation of spherical and rather monodisperse nanoparticles with size around 6 nm (Figure 2-2).

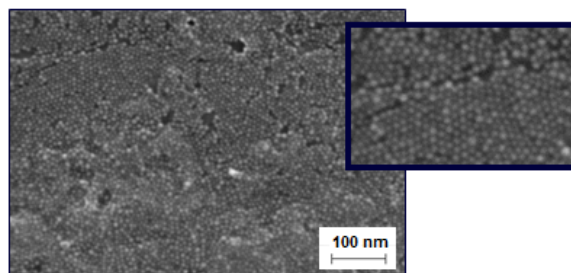


Figure 2-2 HR-SEM image of magnetite NPs.

As confirmed by elemental analysis and IR spectroscopic analysis, magnetite nanoparticles are coated with oleic acid. This hydrophobic ligand layer makes nanoparticles ready dispersible in non-polar organic solvents like hexane and toluene. In fact, it is known⁹³ that oleic acid is chemisorbed on the particle surface as a carboxylate with its alkyl chains sticking out into solution.

2.2 Pericas-type amino alcohol ligands

One possible route was to suitably modify some amino alcoholic structures well-known in literature for their asymmetric catalytic properties, in order to support them onto magnetite nanoparticles.

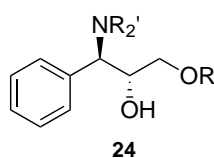
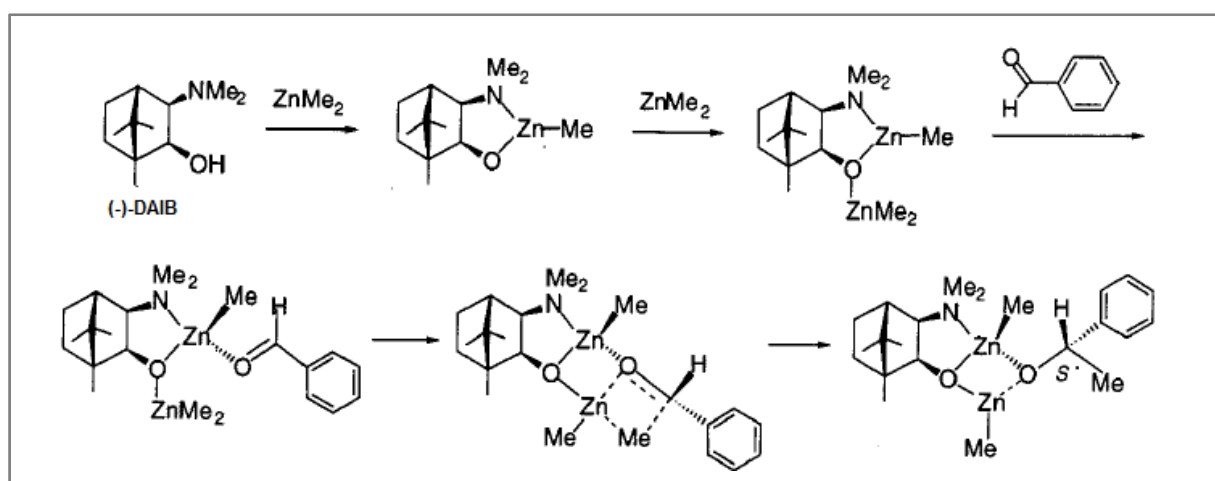


Figure 2-3 Pericas-type ligand.

⁹³ Wu, N.; Fu, L.; Su, M.; Aslam, M.; Wong, K.C.; Dravid, V.P. *NanoLett.* **2004**, *4*, 383.

Pericas and co-workers⁹⁴ have synthesized a family of optically active (1*R*,2*R*)-1-(dialkylamino)-1-phenyl-3-(*R*-oxy)-2-propanols **24** (Figure 2-3) and have tested these compounds as asymmetric catalysts in the addition of diethylzinc to aldehydes. In fact, the enantioselective addition of organo-zinc compounds to aldehydes, mediated by chiral non racemic amino alcohols, represents one of the most studied examples of ligand-accelerated catalysis⁹⁵ and it is placed among the most powerful methodologies for the production of the ubiquitous secondary alcohols in enantiomerically pure form.⁹⁶ This reaction has also become a classical test in the design of novel ligands for catalytic enantioselective synthesis. The mechanism of the process is well understood due to the careful mechanistic work initially carried out by Noyori⁹⁷ and more recent kinetic calculations.⁹⁸ Chiral amino alcohol ligands not only control the stereochemistry of the organo-zinc addition, but also activate the zinc reagents. Scheme 2-2 shows the mechanism proposed by Noyori for the reaction catalyzed by (-)-3-exo-dimethylaminoisobornenol [(-)-DAIB].



Scheme 2-2 Proposed mechanism for the dimethylzinc addition to benzaldehyde catalyzed by a chiral amino alcohol.

The ligand first reacts to form the zinc complex *in situ*; a second equivalent of zinc reagent coordinates to the ligand oxygen, while the aldehyde coordinates to the first zinc atom. In the transition state the alkyl migrates to one enantioface (*si* face) of the aldehyde. After the addition, the alkoxide product dissociates from the catalyst as its zinc complex; aqueous workup gives (*S*)-1-phenylethanol.

⁹⁴ See ref. 23.

⁹⁵ Berrisford, D. J.; Bolm, C.; Sharpless, K. B. *Angew. Chem., Int. Ed. Engl.* **1995**, *34*, 1050.

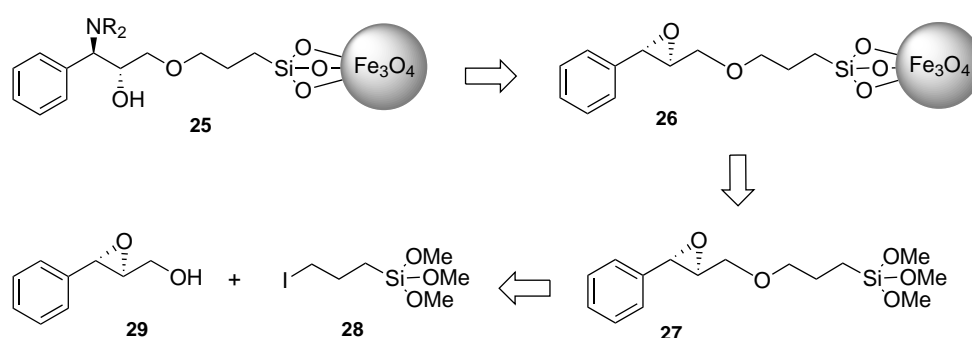
⁹⁶ Noyori, R.; Kitamura, M. *Angew. Chem., Int. Ed. Engl.* **1991**, *30*, 49.

⁹⁷ a) Yamakawa, M.; Noyori, R. *J. Am. Chem. Soc.* **1995**, *117*, 6327. 19. b) Yamakawa, M.; Noyori, R. *Organometallics* **1999**, *18*, 128.

⁹⁸ Micheau, J.-C.; Buhse, T.; Lavabre, D.; Islas, J. R. *Tetrahedron: Asymmetry* **2008**, *19*, 416.

As mentioned in Chapter 1, among Pericas amino alcohols the optimized ligand **24** with R-oxy = trityloxy and dialkylamino = piperidino exhibited the most convenient activity and selectivity profile in the enantioselective addition of Et_2Zn to various aldehydes (91-95% ee).

Our first objective was to achieve this type of amino alcoholic ligand supported on MNPs. For this purpose, we have planned to attach the precursor enantiopure epoxide **29** to the particles by an alkoxy silane group introduced at the end of the molecule (Scheme 2-3). Regio- and stereocontrolled opening of this epoxide could provide direct access to the desired MNP-supported amino alcohol **25** (Scheme 2-3).



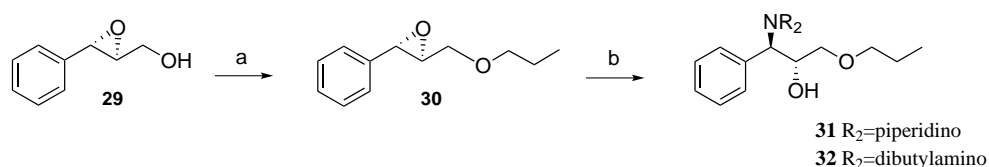
Scheme 2-3 Strategy to achieve a MNP-supported Pericas-type amino alcohol.

The reaction of (2*S*,3*S*)-2,3-epoxy-3-phenylpropanol **29**, arising from the Sharpless asymmetric epoxydation of cinnamyl alcohol,⁹⁹ with 3-iodopropyltrimethoxysilane **28**, commercially available, seemed to be a convenient route (Scheme 2-3).

Before preparing **25**, it was needed to synthesize the corresponding free (unsupported) ligand (1*R*,2*R*)-1-(dialkylamino)-1-phenyl-3-(R-oxy)-2-propanol **24** with R-oxy = propyloxy (to mimic our linker length) and different dialkylamino groups, to identify the structure with the best catalytic activity and enantioselectivity. For this purpose, propyl ether **30** was obtained in quite good yield by treating the epoxy alcohol **29** with NaH and iodopropane at low temperature (Scheme 2-4). For the regioselective and stereospecific ring opening of the epoxy ether **30** with secondary amines, the procedure developed by Crotti and co-workers,¹⁰⁰ which involves the use of LiClO_4 as Lewis acid, was used.

⁹⁹ Gao, Y.; Hanson, R. M.; Klunder, J. M.; Ko, S. Y.; Masamune, H.; Sharpless, K. B. *J. Am. Chem. Soc.* **1987**, *109*, 5765.

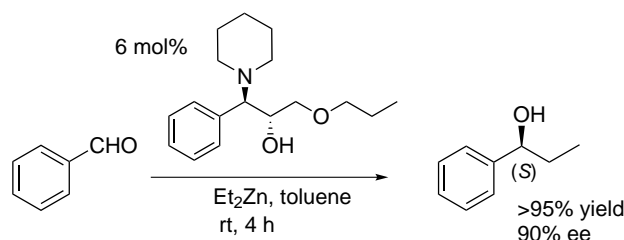
¹⁰⁰ See ref. 45, 48.



Scheme 2-4 Reagents and conditions:¹⁰¹ a) NaH, THF, *n*-PrI, -20 °C, 68% b) R₂NH, LiClO₄, CH₃CN, 55 °C, >95%.

Pericas and co-workers identified the steric bulk of the R-oxy group and the choice of the dialkylamino substituent as a nitrogen-containing six-membered ring as the key structural features for high catalytic activity and enantioselectivity. Taking into account this, at first we used piperidine as the nucleophile for the epoxide ring-opening, achieving the amino alcohol **31** in very high yield (Scheme 2-4).

Amino alcohol **31** was then evaluated as an enantioselective catalyst in the addition of Et₂Zn to benzaldehyde, in the same reaction conditions described by Pericas (Scheme 2-5). We were pleased to find that this ligand proved to be an efficient enantioselective catalyst (>95% yield, 90% ee). Therefore, the steric bulk of the R-oxy group is not an indispensable requirement.



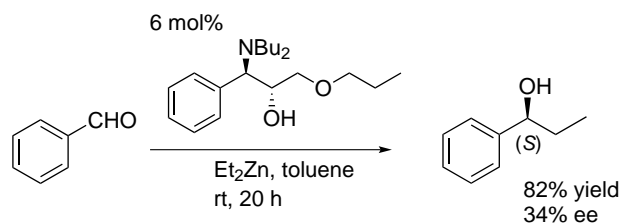
Scheme 2-5 Evaluation of **31**.

We also tried to use dibutylamine as the nucleophile for the epoxide ring-opening (Scheme 2-4), with the aim to insert the di-*n*-butylamino substituent, which has been successfully employed by Soai and co-workers in norephedrine-derived ligands for asymmetric catalysis.¹⁰² Using the amino alcohol **32** in our test reaction (Scheme 2-6), the yield was good (82%) but the enantioselectivity was far from satisfactory (34% ee).¹⁰³

¹⁰¹ All yields reported here and later are referred to the isolated compounds, unless otherwise specified.

¹⁰² See ref. 22.

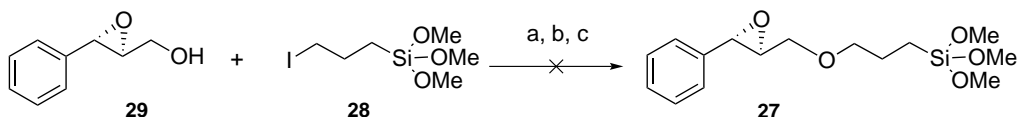
¹⁰³ In this and all the subsequent cases, ee values were based on the reported value of $[\alpha]_D = -40.74$ ($c=5.2$, CHCl₃) for 90% ee. See ref. 22.



Scheme 2-6 Evaluation of **32**.

With these preliminary results in hand, we were ready to follow our strategy to prepare the amino alcohol ligand, with dialkylamino = piperidino, supported on magnetite nanoparticles.

To our disappointment, all conditions we have tested to react the epoxy alcohol **29** with iodopropyltrimethoxysilane **28** gave negative results (Scheme 2-7). Using NaH in THF at low temperature the starting epoxy alcohol was recovered unchanged, while under reflux conditions a complex mixture of side products was obtained. Probably, epoxide ring-opening polymerization and hydrolysis and polymerization of the trimethoxysilane group occurred.¹⁰⁴ To prevent the occurrence of these secondary reactions, less basic reaction conditions were chosen and the reaction was carried out in pyridine solution, at 90 °C in the presence of a catalytic amount of 4-dimethylaminopyridine (DMAP),¹⁰⁵ but also in this case the desired product was not obtained.

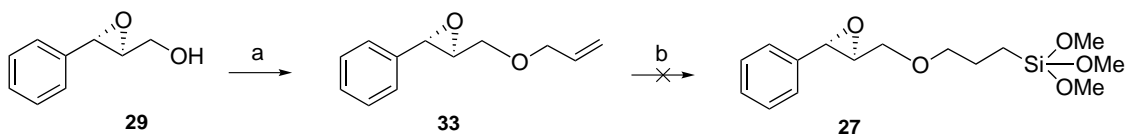


Scheme 2-7 Reagents and conditions: a) NaH, THF, -20 to 0 °C b) NaH, THF, reflux c) DMAP, Pyr, 90 °C.

These unsatisfactory results led us to attempt another route to obtain the compound **27**. For this purpose, the epoxy alcohol **29** was converted into the corresponding allyl ether **33**. The idea was to introduce a trimethoxysilane group in the molecule by means of Pt-catalyzed hydrosilylation (Scheme 2-8). Unfortunately also this attempt failed giving a complex mixture of side products.

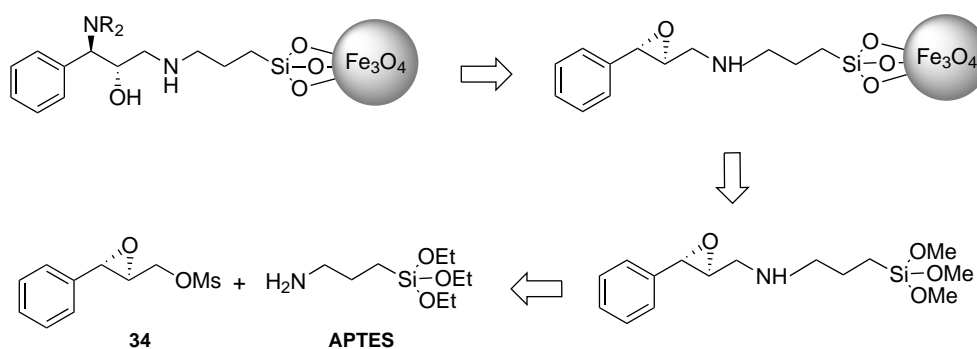
¹⁰⁴ Pena-Alonso, R.; Rubio, F.; Rubio, J.; Oteo, J. L.; *J. Mater. Sci.* **2007**, *42*, 595.

¹⁰⁵ Chaudhary, S. C.; Hernandez, O. *Tetrahedron Lett.* **1979**, *20*, 99.



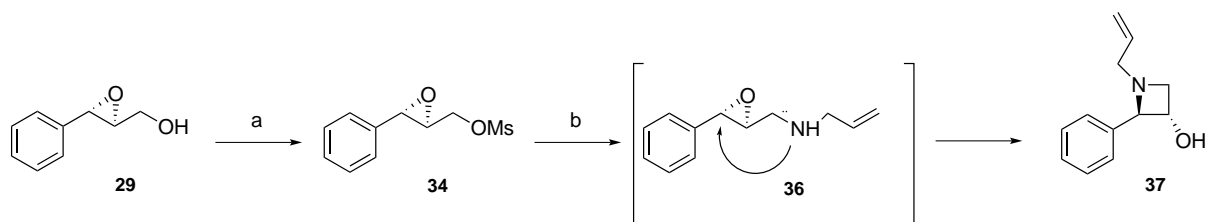
Scheme 2-8 Reagents and conditions: a) NaH, DMF, allyl bromide, -20 to 0 °C, 73% b) H₂PtCl₆, (MeO)₃SiH, toluene, 70 °C.

At this point we decided to abandon the synthesis of **27** and to convert the epoxy alcohol **29** into the corresponding mesyl derivative **34** that could undergo a nucleophilic substitution by the commercially available 3-aminopropyltriethoxysilane (APTES). In this way we could introduce the trialkoxysilane group, necessary for the attachment to the nanoparticles. This new strategy is shown in Scheme 2-9.



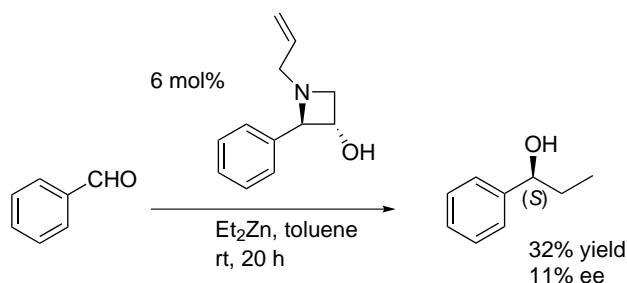
Scheme 2-9 A new strategy.

However, at first we focused on the synthesis of the corresponding free ligand, to test it as catalyst in homogeneous conditions, in order to examine the effect of the amine functionality instead of the ether. For this purpose mesylate epoxy alcohol **34** was reacted with an excess of allyl amine at 50 °C (Scheme 2-10). Surprisingly this reaction did not afford the expected amino derivative **36**, but the azetidine **37**, as confirmed by NMR and mass spectra. Evidently the amino derivative was very unstable and underwent an intramolecular nucleophilic epoxide ring-opening at the highly reactive benzylic position under the reaction conditions (Scheme 2-10).



Scheme 2-10 Reagents and conditions: a) MsCl, Et₃N, DMAP, CH₂Cl₂, >95% b) allyl amine (neat), 50 °C; after 24 hours compound **37** was isolated in 85% yield.

Anyway, since the chiral amino alcohol moiety is present in the obtained optically active azetidine **37**, we decided to evaluate also this compound as a ligand in the addition of Et₂Zn to benzaldehyde. Unfortunately the reaction proceeded in 32% yield with 11% ee (Scheme 2-11). The very low yield was due to the ubiquitous competing reductive pathway leading to benzyl alcohol.¹⁰⁶ Conceivably, in this case the rigidity of the amino alcohol structure prevents significant interactions with the diethylzinc. However, it is to be emphasized that azetidines represent an extraordinary class of strained compounds, having a wide range of known biological activities;¹⁰⁷ investigations about the unexpected reactivity observed (Scheme 2-10) are currently underway in our laboratory.

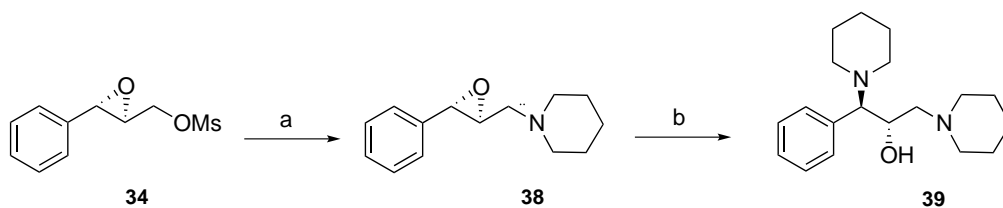


Scheme 2-11 Evaluation of **37**.

To avoid the azetidine formation, a further attempt was made removing the proton on nitrogen by employing a secondary amine, such as the available piperidine (Scheme 2-12). Subsequently, we could use diallyl amine instead of piperidine, in order to obtain the precursor of an anchorable alkoxy silane derivative.

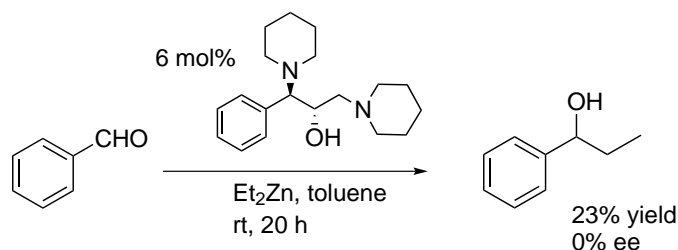
¹⁰⁶ Kitamura, M.; Okada, S.; Suga, S.; Noyori, R. *J. Am. Chem. Soc.* **1989**, *111*, 4028.

¹⁰⁷ a) Cromwell, N. H.; Phillips, B. *Chem. Rev.* **1979**, *79*, 331. b) Moore, J. A.; Ayers, R. S. *Chemistry of Heterocyclic compounds- Small Ring Heterocycles*; Hassner, A., Ed.; Wiley: New York, **1983**; Part 2, 1. c) De Kimpe, N. *Three- and Four-Membered Rings, With All Fused Systems Containing Three- and Four-Membered Rings. In Comprehensive Heterocyclic Chemistry II*; Padwa, A., Ed.; Elsevier: Oxford, **1996**; Vol. 1, Chapter 1.21.



Scheme 2-12 Reagents and conditions: a) piperidine (neat), 50 °C, 88% b) piperidine, LiClO₄, CH₃CN, 55 °C, >95%.

As reported for the ring opening of the epoxy ether **30**, also in this case the aminolysis was performed by using the piperidine/LiClO₄ system in acetonitrile at 55 °C, affording the desired amino alcohol in stereo- and regioselective manner (Scheme 2-12).



Scheme 2-13 Evaluation of **39**.

Using the amino alcohol **39** as ligand in our test reaction, we did not detect any catalytic effect: racemic 1-phenylethanol was obtained in 23% yield (Scheme 2-13). Therefore, we could conclude that the ether functionality is not replaceable by an amine in Pericas-type ligands.

At this point, the difficulty to make this type of ligands anchorable to magnetic nanoparticles prompted us to abandon this objective.

2.3 Ephedrine-type ligands

One of the advantages of the use of ephedrine derivatives **40** as chiral sources in asymmetric synthesis is that both enantiomers of ephedrine and norephedrine are available; thus both enantiomers of the chiral catalysts can be derived (Figure 2-4).

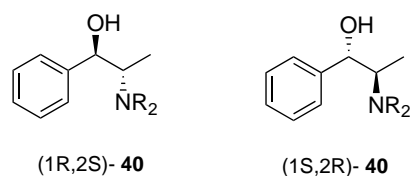
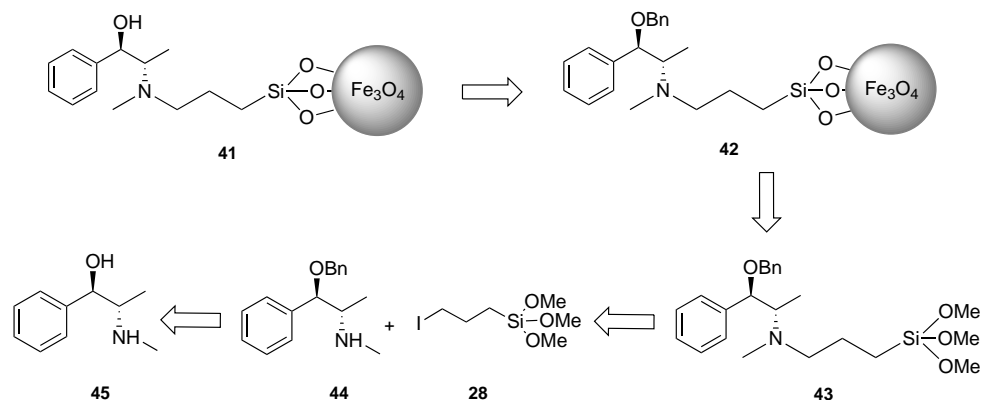


Figure 2-4 Ephedrine-type ligands.

Soai and co-workers have reported that chiral N,N-dialkylnorephedrine catalyze the enantioselective addition of dialkylzincs to aliphatic and aromatic aldehydes to afford optically active secondary alcohols.¹⁰⁸ Alkyl substituents on the (1S,2R)-N,N-di-*n*-alkylnorephedrine had a significant effect on the enantioselectivity of the addition of diethylzinc to 3-methylbutanal and nonanal. The optical purity of the product increases as the chain length of the N-*n*-alkyl substituent increases and peaks at a chain length of four carbons. As already mentioned in Chapter 1, (1S,SR)-N,N-dibutylnorephedrine (DBNE) has proven to be highly enantioselective for the addition to aliphatic aldehydes as well as to aromatic aldehydes (ee up to 95%).

Our objective was preparing an ephedrine derivative suitable to be attached to magnetite nanoparticles. For this purpose we planned to introduce an alkyl trimethoxysilane residue on the nitrogen atom of ephedrine **45**. Our initial strategy is shown in Scheme 2-14.

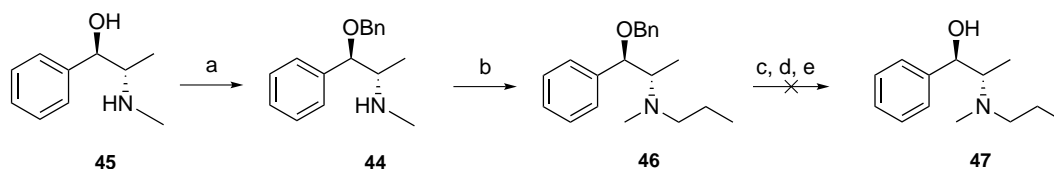


Scheme 2-14 Strategy to achieve a MNP-supported ephedrine-based ligand.

To develop the synthetic pathway to **41** and test the enantioselective catalytic efficiency of a free ligand similar to **43**, we prepared the amino alcohol **46** starting from ephedrine **45** (Scheme 2-15). It was necessary to protect the hydroxyl group as a benzyl ether to avoid side reactions in the

¹⁰⁸ See ref. 22.

presence of the trimethoxysilane moiety. This protecting group was chosen because it can usually be removed by catalytic hydrogenation, a reaction compatible with the stability of magnetite nanoparticles. In fact, much attention was required about the cleavage conditions, due to the instability of Fe₃O₄ in some environments (*e.g.* acid or oxidant conditions).¹⁰⁹



Scheme 2-15 Reagents and conditions: a) KH, THF, BnCl, 0 °C to rt, 92% b) K₂CO₃, *n*-PrI, CH₃CN, reflux, >95% c) H₂ (1 atm), Pd/C, MeOH d) H₂ (5 atm), Pd/C, MeOH e) Et₃SiH, Pd/C, MeOH.

Following a method already reported¹¹⁰ the ephedrine was benzylated in very good yield; then O-benzyl ephedrine **44** was N-alkylated with an alkyl group having a length comparable to our linker **28** (Scheme 2-15).

At this point we needed to remove the benzyl group to achieve the amino alcohol **46** available for evaluation as homogeneous catalyst in the addition of Et₂Zn to benzaldehyde. Unexpectedly, this step has revealed to be really crucial. In fact, using a simple catalytic hydrogenation (atmospheric pressure) the starting substrate was completely recovered, whereas the reaction at high pressure (5 atm) gave an inseparable mixture of products.

To overcome this problem we have attempted other methods for the debenzilation reaction. To the best of our knowledge, the only one compatible with nanoparticle stability was a Pd/C-induced catalytic transfer hydrogenation with triethylsilane.¹¹¹ Unfortunately also using this procedure a complex mixture of products was obtained.

At the moment this route is blocked at this crucial point, and the possibility of using other protecting groups, alternative to the benzyl ether, is under investigation in our laboratory.

¹⁰⁹ Vossen, J. L.; Kern, W. *Thin Film Processes*; Elsevier Science & Technology Books: Amsterdam, 1978.

¹¹⁰ Hutchison, P. C.; Heightman, T. D.; Procter, D. J.; *Org. Lett.*, 2002, 4, 4583.

¹¹¹ Mandal, P. K.; McMurray, J. S.; *J. Org. Chem.* 2007, 72, 6599.

2.4 Our approach to new amino alcohol ligands

In parallel we have focused on the design and synthesis of new β -amino alcohol ligands, having a fine-tunable catalytic site and a functionality (an alkoxy silane group) for their covalent anchoring to magnetite nanoparticles.

2.4.1 Early studies for the synthesis of supportable chiral amino alcohols

The approach chosen for the amino alcohol fragment synthesis is based on the regio- and stereocontrolled elaboration of optically active functionalized epoxides. At first it was considered appropriate to use as linker a long chain having a terminal double bond (Figure 2-5), in order to introduce a trialkoxysilane group by way of Pt-catalyzed hydrosilylation.

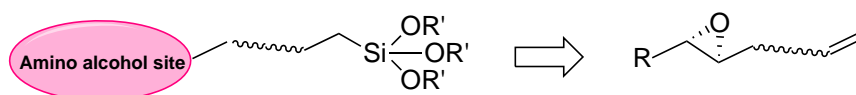
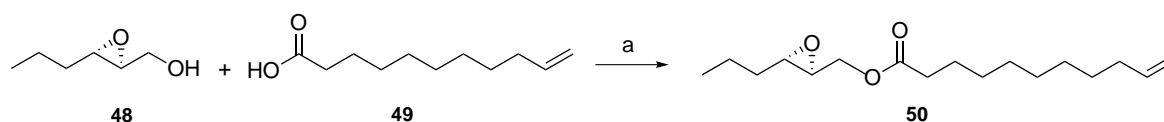


Figure 2-5 The initial idea.

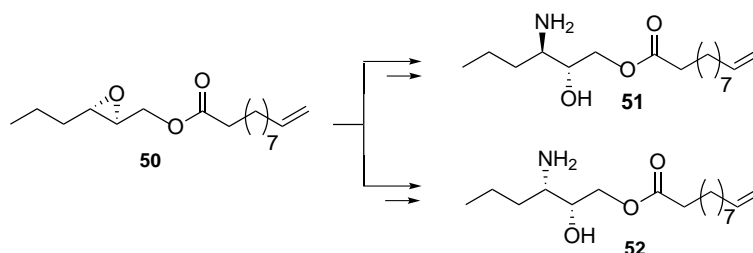
In view of these considerations, initially we have selected as precursors the epoxy alcohol **48**, easily accessible in enantioenriched form (94% ee) by Sharpless asymmetric epoxydation¹¹² of the commercially available *trans*-2-hexen-1-ol, and the 10-undecenoic acid **49**, which is also commercially available. A DCC/DMAP mediated coupling reaction provided ester **50**, containing both the desired functionalities, in high yield (Scheme 2-16).



Scheme 2-16 Reagents and conditions: a) DCC, DMAP, CH₂Cl₂, rt, 80%.

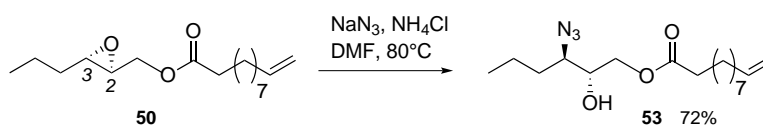
¹¹² See ref. 99.

The epoxide ring-opening carried out in two different conditions could lead to the stereoisomer amino alcohols, *anti* **51** and *syn* **52** (Scheme 2-17).



Scheme 2-17 Epoxide ring-opening affording *syn* and *anti* stereoisomeric amino alcohols.

Regioselective nucleophilic ring-opening by azide ion could provide an *anti* azido alcohol, precursor of the corresponding amino alcohol **51**. For this purpose, firstly epoxy ester **50** was treated with the LiClO₄/NaN₃ system in refluxing acetonitrile; unfortunately under these conditions a prominent hydrolysis of the ester group occurred. A classic system for epoxide ring-opening, widely employed in our group, was NaN₃/NH₄Cl in refluxing methanol; however, in this case it was necessary to change the solvent to avoid the risk of transesterification. Employing dimethoxyethane or *t*-butanol as solvents at temperature up to 80 °C, the reaction proceeded in very low yield (< 20%). To our pleasure, using dimethylformamide (DMF) as the solvent, the ring-opening reaction was quantitative and the azido alcohol **53**, arising from nucleophilic attack at C-3 position, was the main product, as determined by ¹H NMR analysis.

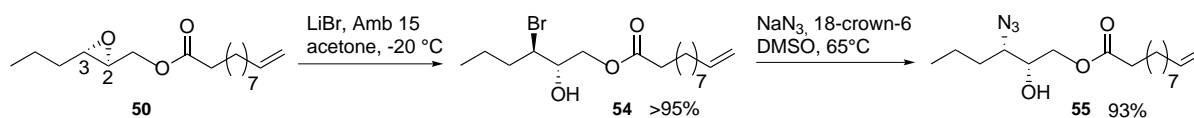


Scheme 2-18 Synthesis of the *anti* azido alcohol.

Instead, *syn* stereochemistry in **52** could be obtained through a double inversion of configuration at C-3, due to a previous ring-opening by bromide ion and a subsequent nucleophilic substitution by azide ion. For this purpose, initially epoxy ester **50** was treated with MgBr₂ in acetone at -20 °C. Unexpectedly this methodology, extensively studied in our group,¹¹³ didn't afford the corresponding 3-bromo derivative in a regioselective manner; a mixture of the two regioisomers

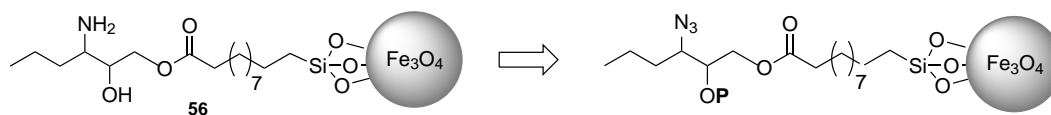
¹¹³ See ref. 55, 56.

was obtained. Conversely, a LiBr/Amberlyst 15 mediated ring-opening reaction provided the 3-bromo derivative **54** as the only product in quantitative yield. This methodology has already been reported on 2,3-epoxy alcohols:¹¹⁴ the regioselectivity is due to the chelating effect of the lithium, while the Amberlyst 15 (an acidic resin) activates the heterocyclic ring toward the opening. At this point, the bromo derivative **54** was subjected to nucleophilic substitution by NaN₃ in DMSO in the presence of 18-crown-6, affording the corresponding azido alcohol **55** with *syn* stereochemistry in excellent yield.



Scheme 2-19 Synthesis of the *syn* azido alcohol.

At this stage, the catalytic hydrogenation of azido alcohols **53** and **55** could provide the two simple diastereoisomeric amino alcohols **51** and **52**. However, our objective firstly was to develop a synthetic plan for supporting the amino alcohol fragment onto magnetite nanoparticles. Therefore the next step was to select an appropriate hydroxyl protecting group. We reasoned that the most convenient solution was a protecting group **P** removable by catalytic hydrogenation, simultaneously with the reduction of the azido moiety to amine, after anchoring to nanoparticles (Scheme 2-20). These cleavage conditions are also compatible with the presence of an ester bond in the molecule.

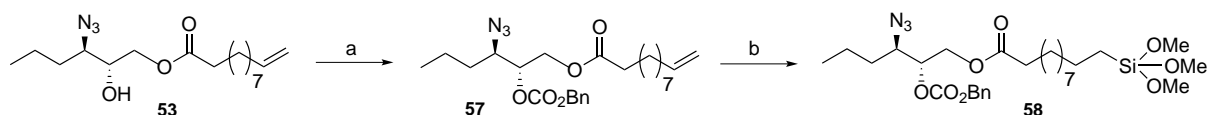


Scheme 2-20 Strategy to obtain a MNP-supported amino alcohol.

When we attempted to protect the hydroxyl group as benzyl ether using BnBr/NaH in THF, the ester hydrolysis was detected. So we turned our attention on the benzyloxycarbonyl group, whose introduction requires less basic conditions. However, using Et₃N and/or DMAP as base,

¹¹⁴ Bonini, C.; Giuliana, C.; Righi, G.; Rossi, L. *Synth. Comm.* **1992**, *22*, 13, 1863.

in different solvents (Et₂O, CH₂Cl₂, CH₃CN), the protection reaction proceeded in very low yield (up to 21%). Gratifyingly, treating the azido alcohol **53** with benzylchloroformate in the presence of N,N,N',N'-tetramethylethylenediamine (TMEDA) in CH₂Cl₂¹¹⁵ the desired product **57** was obtained in high yield.



Scheme 2-21 Reagents and conditions: a) ClCO₂Bn, TMEDA, CH₂Cl₂, rt, 85% b) H₂PtCl₆, (MeO)₃SiH, toluene, 70 °C, >95%.

Then, a Pt-catalyzed hydrosilylation reaction afforded the silane **58** in excellent yield (Scheme 2-21). At this point, before repeating the last two steps for the *syn* stereoisomer, we turned to study the covalent anchoring of **58** to magnetite nanoparticles.

It is known that alkoxy silane self-assembly can be successfully applied to exchange the original oleic acid ligand from the surface of iron oxide nanoparticles synthesized via the thermal decomposition method, without altering the nanoparticle morphology.¹¹⁶ Ligand exchange is performed by the covalent attachment of silanes to hydroxyl functions present on nanoparticle surface.

Some preliminary experiments have been carried out with a commercially available alkoxy silane, the 3-aminopropyltriethoxysilane (APTES). After reacting oleic acid-coated NPs with an excess of APTES in refluxing toluene under an argon atmosphere for 48 h, FTIR analysis confirmed the successful ligand exchange; the comparison of IR spectra of nanoparticles before and after modification with APTES is shown in Figure 2-6. The starting nanoparticles exhibit strong absorptions at 2922 and 2852 cm⁻¹, characteristic for the CH₂ chain of oleic acid, and two carboxylate stretching vibrations at 1543 and 1407 cm⁻¹.¹¹⁷ The strong IR band at 585 cm⁻¹ is characteristic of the Fe-O vibrations related to magnetite core.¹¹⁸

¹¹⁵ Adinolfi, M.; Barone, G.; Guariniello, L.; Iadonisi, A.; *Tetrahedron Letters*, **41**, 2000, 9305.

¹¹⁶ See ref. 91.

¹¹⁷ Lee, S.-Y.; Harris, M. T. J. *J. Colloid Interface Sci.* **2006**, *293*, 401.

¹¹⁸ Waldron, R. V. *Phys. Rev.* **1955**, *99*, 1727.

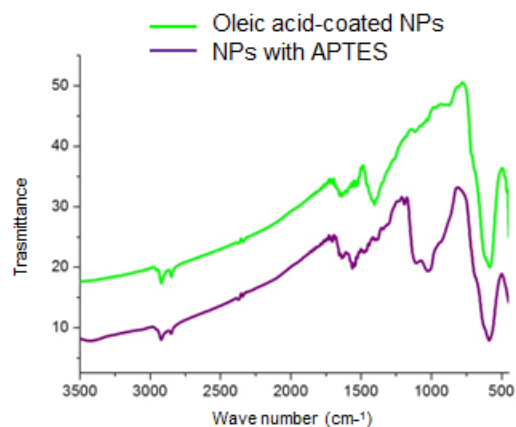
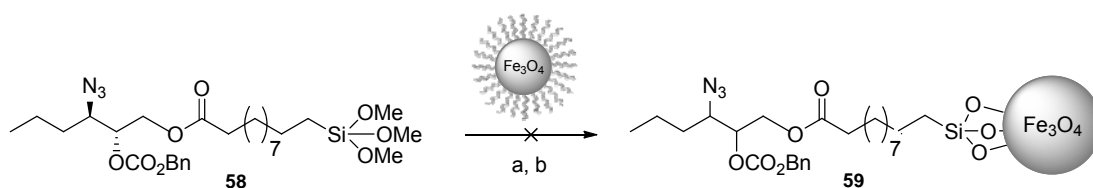


Figure 2-6 IR spectra of nanoparticles before and after modification with APTES.

After ligand exchange, a slight broadening of this band is observed, indicating the formation of Fe-O-Si bonds.¹¹⁹ Compared to the as synthesized NPs, some new bands are observed for silane-modified NPs. The most striking difference is the appearance of bands between 1000 and 1150 cm^{-1} , which are originated from Si-O vibrations, and two N-H bendings at 1633 and 1560 cm^{-1} .

Having this preliminary result, we attempted to use the same conditions to covalently anchor our amino alcohol precursor **58** to magnetite NPs. To our disappointment, also after 4 days of reaction, the IR spectrum of recovered NPs was almost identical to that of oleic acid-coated NPs. Not even using a catalytic amount of Et_3N better results have been obtained (Scheme 2-22).



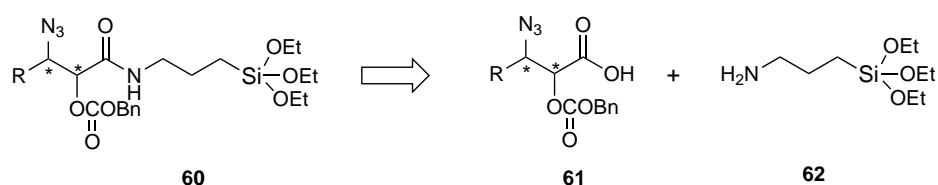
Scheme 2-22 Reagents and conditions: a) toluene, reflux, 4 days b) Et_3N , toluene, reflux, 4 days.

At this point we reasoned that the difficulty of anchoring could likely be due to a problem of steric hindrance, *i.e.* the presence of a too long and flexible chain in our ligand **58**. Therefore it was necessary to modify the linker structure in order to make possible the covalent immobilization onto nanoparticles.

¹¹⁹ Yamaura, M.; Camilo, R. L.; Sampaio, L. C.; Macedo, M. A.; Nakamura, M.; Toma, H. E. *J. Magn. Magn. Mater.* **2004**, 279, 210.

2.4.2 A different strategy: a short amide linker

In order to have a shorter and less flexible linker in our ligand, we have planned a new synthetic strategy. We have decided to use the commercially available APTES **62**, which is capable of reacting with a carboxylic acid to give an amide bond. Therefore it was necessary to modify the synthesis of our amino alcohol structures to introduce a carboxylic acid functionality available for the coupling reaction with the amino silane **62** (Scheme 2-23).



Scheme 2-23 The new strategy.

This choice was supported by an interesting example in the literature. In fact, Kohler and co-workers¹²⁰ have reported the synthesis and immobilization on iron oxide NPs of a trifluoroethyl ester-terminal poly(ethylene glycol) (PEG) silane. The authors suggest that the APTES coupled with PEG chains confers the stability of PEG layer and increases the PEG packing density on nanoparticle surface by establishing hydrogen bonding between the carbonyl and amine groups present within the layer structure (Figure 2-7).

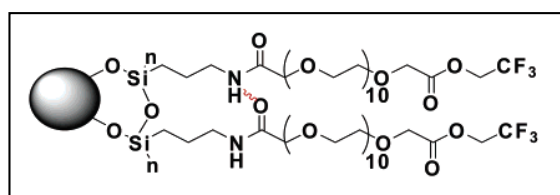
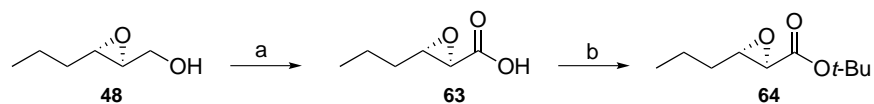


Figure 2-7 An example from literature.

To apply this strategy, epoxy alcohol **48** was transformed into the corresponding carboxylic acid **63**, using the $\text{NaIO}_4/\text{RuCl}_3$ system in a buffered environment (Scheme 2-24). This mild

¹²⁰ Kohler N.; Fryxell G. E.; Zhang M. J. *Am. Chem. Soc.* **2004**, *126*, 7206.

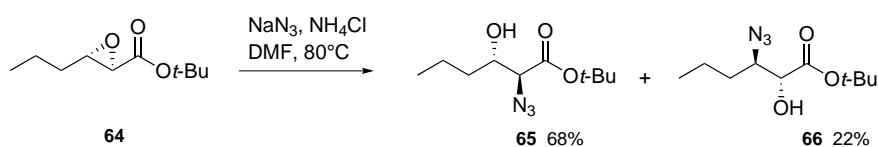
oxidation method¹²¹ was chosen because it is compatible with the presence of the epoxide moiety in the molecule.



Scheme 2-24 Reagents and conditions: a) NaIO₄, RuCl₃, CH₃CN/ CCl₄/ buffer pH 7, rt, 79%
b) Cl₃CC(=NH)O*t*-Bu, CH₂Cl₂, rt, 90%.

Before opening the epoxide ring, it was necessary to convert the carboxylic acid into ester. We have chosen a *t*-butyl ester for the possibility to hydrolyze it later by using trifluoroacetic acid (TFA); in fact, some preliminary experiments had shown that this treatment is compatible with the benzyloxycarbonyl protecting group, which will be introduced in the molecule as in the previous synthetic pathway. Using *t*-butyl 2,2,2-trichloroacetimidate, a known¹²² alcohol alkylation reagent, *t*-butyl ester **64** was obtained in high yield.

At this point, epoxy ester **64** was subjected to nucleophilic ring-opening with NaN₃/NH₄Cl in DMF at 80 °C, a system already used previously. This reaction afforded a mixture of *anti* azido alcohols **65** and **66**, where the regioisomer **65**, arising from nucleophilic attack at the more reactive α position, is predominant.



Scheme 2-25 Synthesis of the *anti* azido alcohols.

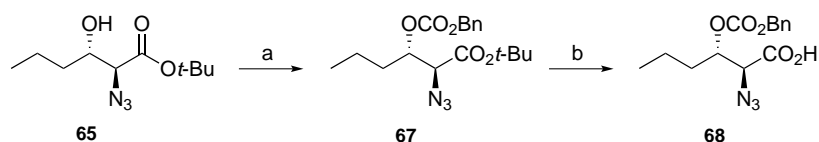
To attempt the anchoring to nanoparticles of this new type of ligand, amino alcohol precursor, three more steps were needed: 1) hydroxyl protection 2) *t*-butyl ester hydrolysis 3) amide bond formation with the APTES. We decided to explore this pathway starting from the azido alcohol **65** (Scheme 2-26).

¹²¹ Carlsen, P. H. J.; Katsuki, T.; Martin, V. S.; Sharpless, K. B. *J. Org. Chem.* **1981**, *46*, 3936

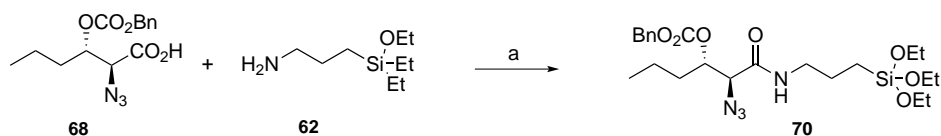
¹²² Supernant, S.; Lubell, W. D.; *J. Org. Chem.* **2006**, *71*, 848.

As seen before, the benzyloxycarbonyl protecting group meets our requirements for hydroxyl protection; the reaction conditions previously described were employed to obtain **67** in excellent yield. Then hydrolysis of the ester **67** was carried out with TFA in CH₂Cl₂, affording the desired carboxylic acid **68** in high yield. As expected, the benzyloxycarbonyl group proved to be stable in these conditions.

The carboxylic acid was reacted with APTES **62** to obtain the amide **70** (Scheme 2-27). The yield of this reaction was 35% using only the coupling agent EDC (*N*-ethyl-*N'*-(3-dimethylaminopropyl)carbodiimide), whereas it was increased to 43% employing the system EDC/HOBt (1-hydroxybenzotriazole). The best reaction conditions, however, involved the use of the coupling reagents EDC/HOAt (1-hydroxy-7-azabenzotriazole),¹²³ which afforded the desired product in 66% yield.



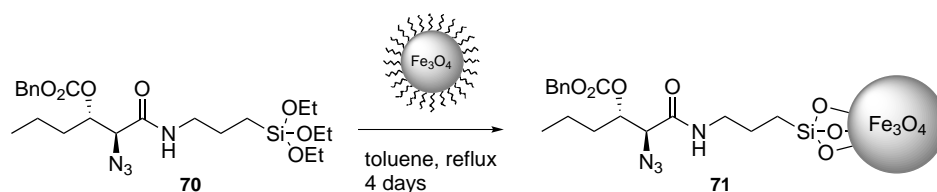
Scheme 2-26 Reagents and conditions: a) ClCO₂Bn, TMEDA, CH₂Cl₂, rt, >95% b) TFA, CH₂Cl₂, rt, 86%.



Scheme 2-27 Reagents and conditions: a) EDC/HOAt, CH₂Cl₂, rt, 66%.

At this point, a chiral amino alcohol precursor having a triethoxysilane group was available for anchoring to magnetite nanoparticles. To our pleasure, in this case the ligand exchange occurred successfully (Scheme 2-28).

¹²³ Carpino, L. A.; *J. Am. Chem. Soc.* **1993**, 115, 4397.



Scheme 2-28 Ligand exchange reaction.

Elemental analysis confirmed the presence of nitrogen on the surface of particles, and the determined nitrogen content allowed the calculation of the degree of ligand loading on the nanoparticles. It could be established in this way that the functionalization of nanoparticles was 0.31 mmol/g. IR spectrum of NPs after loading has shown, in particular, an absorption at 2114 cm^{-1} indicating the presence of the azido group on nanoparticle surface, and new bands between 1000 and 1150 cm^{-1} , due to the Si-O bonds.

Subjecting **71** to a catalytic hydrogenation reaction it was possible to obtain the desired magnetic nanoparticle-supported chiral amino alcohol. Therefore, at this time we could conclude that the employment of a short amide linker is a good choice, being able to allow the immobilization of an amino alcohol fragment on magnetite nanoparticles. In parallel, we have started to study the enantioselective catalytic activity of this type of ligands in homogeneous conditions, in order to optimize their structure.

2.4.3 Free ligands: the preliminary studies

At first we decided to investigate the influence of the regio- and stereochemistry of the amino alcohol fragment on catalytic activity. For this purpose, amino alcohols **72**, **73**, **74** and **75** have been synthesized in order to test them as chiral ligands. Also in this case we have chosen as reaction test the enantioselective addition of Et_2Zn to benzaldehyde, already seen before.

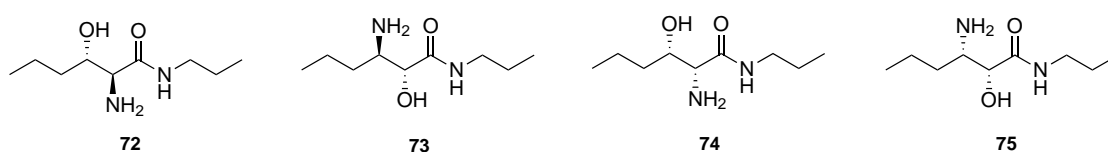
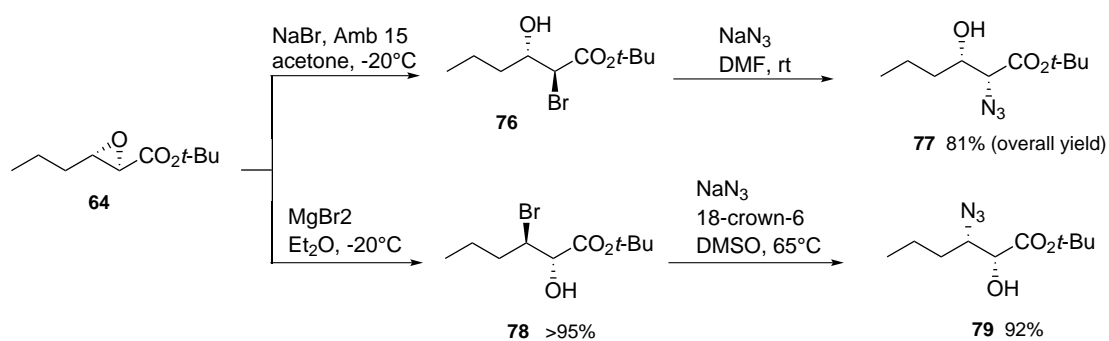


Figure 2-8 The first free ligands.

The key step for the synthesis of the *anti* amino alcohols **72** and **73** was the direct opening of the epoxy ester **64** with $\text{NaN}_3/\text{NH}_4\text{Cl}$, affording regioisomer azido alcohols **65** and **66**, as described above. Whereas, to obtain the *syn* stereochemistry in amino alcohols **74** and **75** the key step was a double configuration inversion, by a previous ring-opening by bromide ion and a subsequent nucleophilic substitution by azide ion.

When the epoxy ester **64** was reacted with the $\text{NaBr}/\text{Amberlyst 15}$ system¹²⁴ in acetone at $-20\text{ }^\circ\text{C}$, ^1H NMR analysis of the crude material revealed that the 2-bromo derivative **76** was the almost exclusive product, as expected given the high reactivity of the position adjacent to the carbonyl. The crude material was directly subjected to nucleophilic substitution by NaN_3 in DMF at room temperature; in fact, under these mild conditions the small amount of 3-bromo derivative present doesn't react. At this point a chromatographic separation afforded the *syn* azido alcohol **77** in very good yield referred to **64**.



Scheme 2-29 Synthesis of the *syn* azido alcohols.

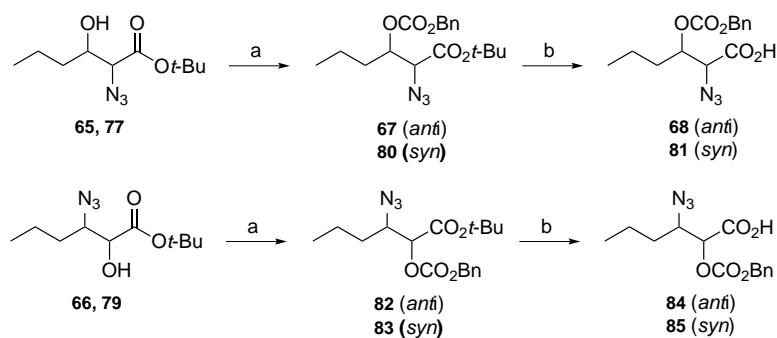
Using MgBr_2 in diethyl ether at $-20\text{ }^\circ\text{C}$,¹²⁵ the completely regioselective opening at C-3 position was obtained. The nucleophilic substitution by N_3^- ion on the 3-bromo derivative **78** required more drastic conditions, while still affording the corresponding *syn* azido alcohol **79** in excellent yield.

Azido alcohols **65**, **66**, **77** and **79** were then subjected to the same synthetic pathway in order to obtain the corresponding amino alcohols **72**, **73**, **74** and **75**. As already reported previously for the *anti* azido alcohol **65**, the first two steps were the hydroxyl protection as benzyl carbonate and the subsequent *t*-butyl ester hydrolysis (Scheme 2-30). This time, the carboxylic acids **68**, **81**,

¹²⁴ See ref. 57.

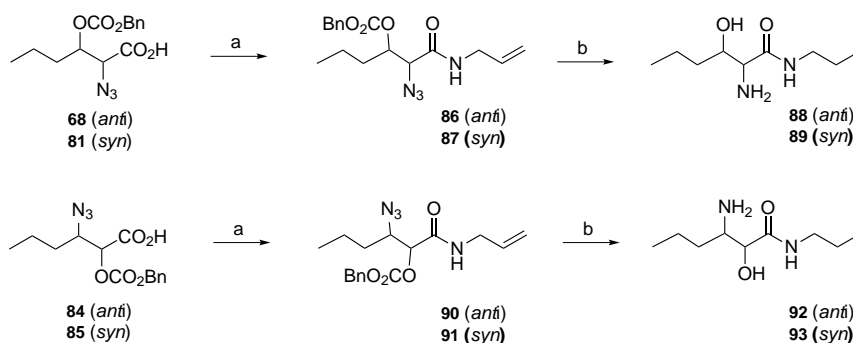
¹²⁵ See ref. 55, 56.

84 and **85** were reacted with allyl amine, an available amine having a length comparable with the APTES; employing also in this case the EDC/HOAt system in CH_2Cl_2 , the corresponding amides **86**, **87**, **90** and **91** were obtained in good yields (Scheme 2-31).



Scheme 2-30 Reagents and conditions: a) ClCO_2Bn , TMEDA, CH_2Cl_2 , rt, >95% b) TFA, CH_2Cl_2 , rt, 85-90%.

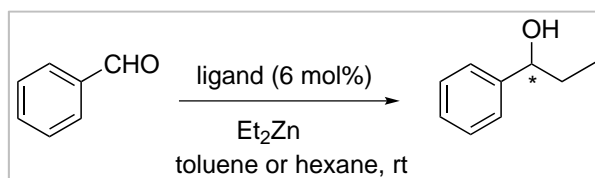
Then **86**, **87**, **90** and **91** were subjected to catalytic hydrogenation to deprotect the hydroxyl group and convert the azide moiety in amine (Scheme 2-31), affording the desired amino alcohols **88**, **89**, **92** and **93** in excellent yield. Under these reaction conditions, also the saturation of the terminal double bond occurred as expected.



Scheme 2-31 Reagents and conditions: a) EDC/HOAt, allyl amine, CH_2Cl_2 , rt, 70-74% b) H_2 (5 atm), Pd/C, EtOAc, >95%.

At this point, we were ready to test these simple, optically active amino alcohols, with different regio- and stereochemistry, in the addition of diethylzinc to benzaldehyde. In this case and throughout the study, the reaction test was carried out applying the conditions described by

Pericas,¹²⁶ *i.e.* employing a 6% molar amount of ligand and performing the reactions at room temperature in hexanes or toluene, depending on the ligand solubility (Scheme 2-32). Unfortunately these ligands, having a primary amine functionality, have shown no significant catalytic activity: in all cases (Table 2-1, entries 1, 2, 3, 4) reaction yields were slightly higher than that obtained in the absence of ligand (entry 5) and no asymmetric induction was observed.



Scheme 2-32 Test reaction.

entry	ligand	yield* (%)	ee (%)
1		41	0
2		39	0
3		44	0
4		40	0
5	-	24	0

*after 20 hours

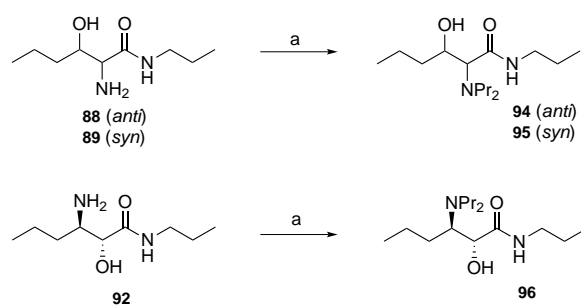
Table 2-1 Initial screening.

Relying on the numerous examples of amino alcohols ligands in the literature, where the amino group is tertiary, we decided to carry out the dialkylation on the nitrogen atom of the amino alcohols **88**, **89** and **92**. The one-step reaction with two equivalents of *n*-propyl iodide in

¹²⁶ See ref. 23.

refluxing acetonitrile in the presence of potassium carbonate¹²⁷ afforded the N,N-dipropyl amino alcohols **94**, **95** and **96** in moderate yields (Scheme 2-33).

Amino alcohols **94**, **95** and **96** were then evaluated as ligands in our reaction test. As Table 2-2 shows, using these new ligands, yields have increased significantly and although low enantiomeric excesses were observed (entries 1 and 3). More in detail, these preliminary results seemed to indicate that the amino alcohol regiochemistry has no particular influence on the catalytic efficiency (entries 1 and 3); whereas, the *syn* ligand (entry 2) is less efficient than the *anti* analogue (entry 1), in agreement with what previously established by Noyori, *i.e.* *anti* β -amino alcohols (which lead to *cis* disubstituted zinc chelates) are in general better ligands than the corresponding *syn* stereoisomers.¹²⁸



Scheme 2-33 Reagents and conditions: a) *n*-PrI, K₂CO₃, CH₃CN, reflux, 40-50%.

entry	ligand	yield* (%)	ee (%)	config.
1		84	28	R
2		74	0	-
3		86	27	S

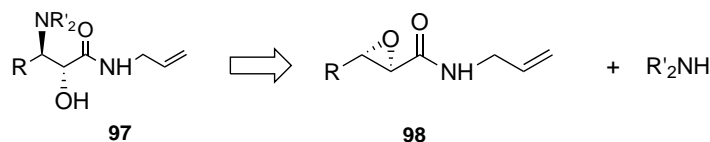
*after 20 hours

Table 2-2 Initial screening

¹²⁷ Soai K.; Yokoyama S.; Hayasaka T.; *J. Org. Chem.*, **1991**, 56, 4264.

¹²⁸ Noyori, R.; Kitamura, M. *Angew. Chem., Int. Ed. Engl.* **1991**, 30, 49.

Given the importance of a tertiary amino group in the ligand structure, we reasoned that we needed a more direct and convenient synthetic route: an aminolysis reaction on epoxy amide **98** seemed to be the best solution (Scheme 2-34), rather than the azidolysis reaction followed by reduction of the azido group to amine and subsequent alkylation.

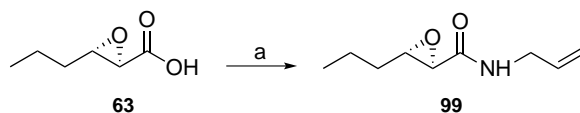


Scheme 2-34 Aminolysis reaction: the key step.

Interestingly, the amino alcohol **97** offers the possibility of systematic variations of steric and electronic properties, by varying the R and R' groups, in order to achieve an improved catalytic behavior.

2.4.4 Aminolysis: a methodological study¹²⁹

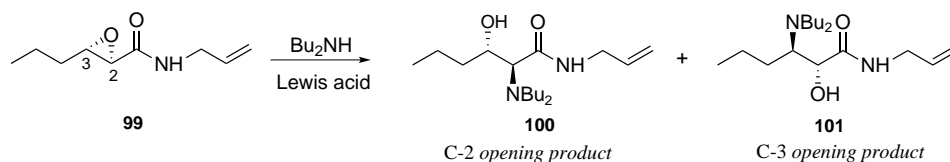
Despite the large number of studies on Lewis acid-promoted aminolysis of different functionalized epoxide rings, to the best of our knowledge, there are few reports concerning this reaction with 2,3-epoxy amides; this reaction has been explored only on particular substrates, often as a step in a more complex synthesis.¹³⁰ Initially, we carried out the reaction using the most popular methodologies employed in the aminolysis of functionalized epoxides, and the Bu_2NH , an amine often present in the structure of chiral ligands, as the nucleophile. The epoxy amide **99**, initially selected as the starting substrate, was provided by the coupling of carboxylic acid **63** with the allyl amine in excellent yield (Scheme 2-35).



Scheme 2-35 Reagents and conditions: a) EDC/HOAt, allyl amine, CH_2Cl_2 , rt, > 95%.

¹²⁹ Righi, G.; Mantíneo, A.; Suber, L.; Mari, A.; *Synlett*, **2012**, 23, 1947.

¹³⁰ (a) Sarabia, F.; Sánchez-Ruiz, A. *J. Org. Chem.* **2005**, *70*, 9514. (b) Pino-González, M. S.; Assiego, C. *Tetrahedron: Asymmetry* **2005**, *16*, 199. (c) Nikolai, A. K.; Hesse, M. *Helv. Chim. Acta* **2003**, *86*, 2028. (d) Prabhakaran, E. N.; Nageswara Rao, I.; Boruah, A.; Iqbal, J. *J. Org. Chem.* **2002**, *67*, 8247. (e) Valpuesta, M.; Durante, P.; Upez-Herrera, F. J. *Tetrahedron Lett.* **1995**, *36*, 4681.



entry	Lewis acid	reaction conditions	C-3:C-2 ratio*	yield (%)
1	LiClO ₄	CH ₃ CN, reflux, 12 h ¹³¹	-	no reaction
2	ZnCl ₂	CH ₃ CN, reflux, 12 h ¹³²	>95:5	60
3	Ti(O <i>i</i> -Pr) ₄	CH ₂ Cl ₂ , rt, 12 h ¹³³	-	no reaction
4	Ti(O <i>i</i> -Pr) ₄	THF, reflux, 12 h ¹³¹	-	no reaction
5	Ti(O <i>i</i> -Pr) ₄	neat, 50 °C, 12 h ¹³¹	>95:5	97

*Ratio determined by ¹H-NMR analysis of the crude materials.

Table 2-3 Attempts to the aminolysis of the 2,3-epoxy amide.

As reported in Table 2-3, using LiClO₄ in CH₃CN (entry 1), and Ti(O*i*-Pr)₄ in CH₂Cl₂ or THF (entries 3 and 4) the starting substrate **99** was completely recovered even at high temperature and with long reaction time, whereas the use of ZnCl₂ in refluxing CH₃CN gave only about 60% conversion (entry 2). Finally, by employing the amine as solvent in the presence of a small excess of Ti(O*i*-Pr)₄ (entry 5), the epoxy amide **99** was completely converted into the single amino alcohol derivative **101**. The regiochemistry of the reaction was established from NMR spectroscopic analysis; application of the spin-spin decoupling technique clearly showed that the oxirane opening occurred regioselectively at the C-3 position.

Inspired by other authors, the observed regioselectivity might be rationalized by proposing the formation of an intermediate titanium complex such as **A**, for which external nucleophiles show a very strong preference for attack at the C-3 position (Figure 2-9).¹³⁴

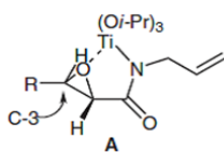


Figure 2-9 Proposed intermediate titanium complex.

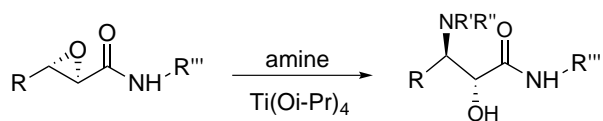
¹³¹ Azzena, F.; Calvani, F.; Crotti, P.; Gardelli, C.; Macchia, F.; Pineschi, M. *Tetrahedron* **1995**, *51*, 10601.

¹³² Duran, Pachon. L.; Gamez, P.; van Brussel, J. J. M.; Reedijk, J. *Tetrahedron Lett.* **2003**, *44*, 6025.

¹³³ Chong, J. M.; Sharpless, K. B. *J. Org. Chem.* **1985**, *50*, 1560.

¹³⁴ Caron, M.; Sharpless, K. B. *J. Org. Chem.* **1985**, *50*, 1557.

At this point, we have considered interesting to carry out a systematic study on the $\text{Ti}(\text{O}i\text{-Pr})_4$ -promoted regio- and stereoselective aminolysis of 2,3-epoxy amides. In order to verify the general applicability of this methodology, the 2,3-epoxy amides **102**, **103**, **104** and **105** (Table 2-4) were prepared¹³⁵ to investigate the influence of steric hindrance and electronic effects of the substituent R on the heterocyclic ring. Furthermore, the reaction was tested with a range of amines such as the cyclic piperidine and morpholine, the more branched diisopropylamine, and the aromatic aniline.



entry	substrate	R	R'''	amine	C-3 product	T (°C)	yield (%)*
1	99	<i>n</i> -Pr	allyl	Bu ₂ NH	101	rt	97
2	99	<i>n</i> -Pr	allyl	piperidine	106	rt	95
3	99	<i>n</i> -Pr	allyl	morpholine	107	rt	89
4	99	<i>n</i> -Pr	allyl	<i>n</i> -hexylamine	108	rt	92
5	99	<i>n</i> -Pr	allyl	<i>c</i> -hexylamine	109	rt	75
6	99	<i>n</i> -Pr	allyl	aniline	110	60	88
7	102	<i>n</i> -Pr	Me	Bu ₂ NH	111	rt	97
8	103	<i>n</i> -Pr	Bn	Bu ₂ NH	112	rt	93
9	104	<i>c</i> -Hex	allyl	Pr ₂ NH	113	rt	98
10	104	<i>c</i> -Hex	allyl	<i>i</i> -Pr ₂ NH	114	80	no reaction
11	104	<i>c</i> -Hex	allyl	Bu ₂ NH	115	rt	98
12	104	<i>c</i> -Hex	allyl	piperidine	116	rt	97
13	104	<i>c</i> -Hex	allyl	morpholine	117	rt	87
14	104	<i>c</i> -Hex	allyl	benzylamine	118	50	85
15	105	Ph	allyl	Bu ₂ NH	119	rt	98
16	105	Ph	allyl	piperidine	120	rt	98

* Yields of the isolated compounds.

Table 2-4. $\text{Ti}(\text{O}i\text{-Pr})_4$ -promoted aminolysis of 2,3-epoxy amides.

¹³⁵ All the substrates were prepared starting from the corresponding optically active allylic alcohols (see the Experimental section 2.6.3), by the synthetic pathway already described for the substrate **99** with R=propyl. For the substrate with R=cyclohexyl the appropriate alcohol is not commercially available and it was synthesized from the cyclohexanecarboxaldehyde, by an Horner-Emmons reaction followed by a reduction of the ester using diisobutylaluminum hydride (DIBAL); see Barrett, A. G. M.; Doubleday, W. W.; Tustin, G. J. *Tetrahedron*, **1996**, 52, 48, 15325.

As shown in Table 2-4, all the examined reactions gave only one detectable regioisomer, regardless of the steric hindrance of R. The method failed using the bulky diisopropylamine (entry 10), whereas it worked very well not only with primary and secondary acyclic amines (entries 1, 4, 5, 7-9, 11, 14 and 15), but also with cyclic amines (entries 2, 3, 12, 13 and 16). It is worth noting that the reaction occurred with almost quantitative yield at room temperature in most cases.

In summary, a new and general regioselective aminolysis of 2,3-epoxy amides has been developed; it seems to have a wide applicability, due to the large range of compatible substituents on the heterocyclic ring, and the simple and mild reaction conditions used.

2.4.5 Screening of free ligands: effect of the R and R' groups.

A set of amino alcohols **97**, synthesized using the methodology described above (Table 2-4), was evaluated in the standard addition of Et₂Zn to benzaldehyde.

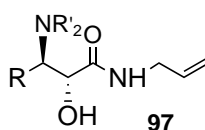
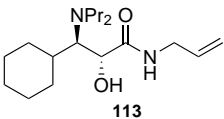
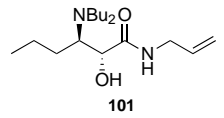
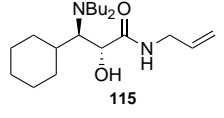
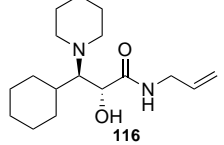
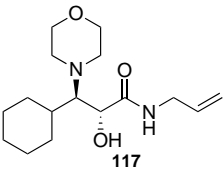
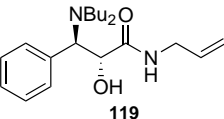
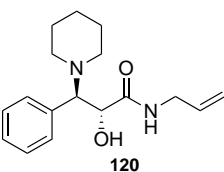


Figure 2-10 Free ligands.

Some conclusions can be drawn from the results summarized in Table 2-5. Firstly, the increase in steric hindrance of the alkyl chain R has a positive effect on the catalytic behavior (entries 2 and 3); whereas an acyclic amino group seems to give better results than a cyclic one (entries 3, 4 and 5). With R=*n*-propyl or *o*-hexyl (entries 1-5), yields in general were good, in particular with ligand **115** (entry 3), even if the level of asymmetric induction remained very moderate. It is noteworthy that a lower catalytic activity was registered with R=phenyl. This result was completely unexpected since the amino alcohol **120** has a structure very similar to the very efficient Pericas-type ligand **31** (Scheme 2-5), except for the amide moiety. Therefore, it was reasonable to hypothesize that a carbonyl group adjacent to the amino alcohol site has a very unfavorable effect on the formation of the chiral complex which differentiates the enantiofaces of the aldehyde in the transition state.

entry	ligand	yield* (%)	ee (%)**
1	 113	87	25
2	 101	88	29
3	 115	93	31
4	 116	78	16
5	 117	80	15
6	 119	61	7
7	 120	50	4

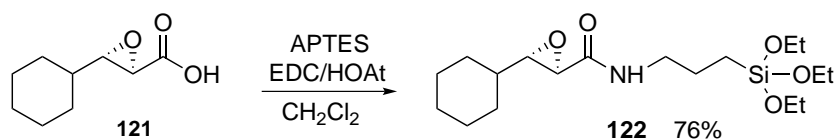
*after 20 hours. ** (*S*)-1-Phenyl-1-propanol was predominantly obtained in all instances.

Table 2-5. Screening of free ligands.

However, in light of these results, before concentrating our efforts on the structural optimization of ligands containing a dibutylamino substituent and a bulky alkyl group, we decided to support this type of ligand on MNPs, in order to verify that the catalytic efficiency is not perturbed by the immobilization.

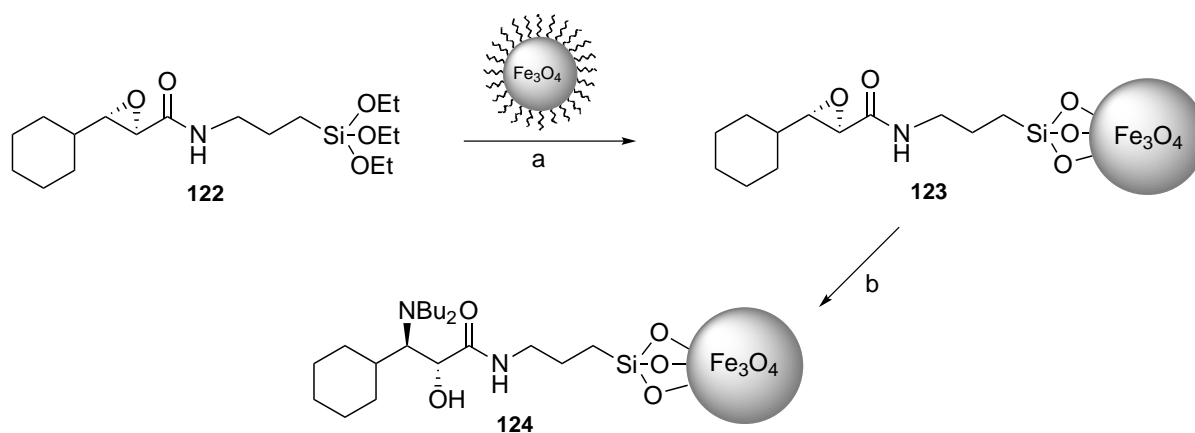
2.4.6 The first MNP-supported amino alcohol catalyst

At this point the best ligand achieved was the amino alcohol **115**. With the aim of preparing the corresponding MNP-supported catalyst, the carboxylic acid **121** was reacted with the APTES, to obtain an anchorable derivative **122** (Scheme 2-36). In fact, the mild conditions developed for the aminolysis of 2,3-epoxy amides seemed suitable to be applied to magnetite nanoparticle-immobilized substrates. In this way, we could obtain directly the desired MNP-supported amino alcohol by a regio- and stereocontrolled opening of the anchored epoxide.



Scheme 2-36 An anchorable epoxide derivative.

The immobilization of **122** onto MNPs was carried out employing the ligand exchange conditions developed previously and was then followed by the Ti(*Oi*-Pr)₄-promoted aminolysis of the epoxide ring in **123**. Bu₂NH was selected as the nucleophile given the considerations reported in the paragraph above. Nitrogen elemental analysis, performed before and after the aminolysis reaction, allowed to determine the amount of the amino alcohol ligand present on the nanoparticle surface (0.46 mmol/g).



Scheme 2-37 Reagents and conditions: a) toluene, reflux, 4 days b) Ti(*Oi*-Pr)₄, Bu₂NH (neat), rt.

HR-SEM analysis (Figure 2-11) of the magnetite nanoparticles after the two functionalization steps showed that no significant increase of the individual particle size occurred, *i.e.* the particles remained separated.

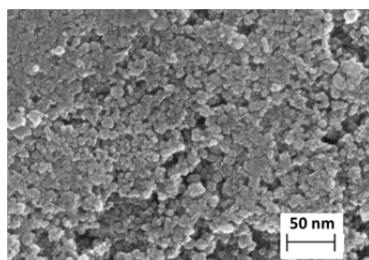
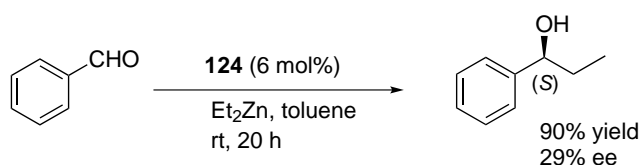


Figure 2-11 HR-SEM image of functionalized nanoparticles **124**.

Finally, the MNP-supported amino alcohol **124** was tested as catalyst in the standard enantioselective addition of Et_2Zn to benzaldehyde. Notably, the functionalized nanoparticles have been shown to be readily dispersible in toluene (the reaction solvent). The catalytic behavior of the supported catalyst was very similar to that of the corresponding homogeneous catalyst: 1-phenyl-1-propanol was obtained in very good yield and a comparable enantiomeric excess.



Scheme 2-38 Evaluation of the supported catalyst **124**.

This preliminary result seemed to indicate that amino alcohol catalysis could be successfully transferred to the surface of magnetic nanoparticles. Moreover, the functionalized nanoparticles could be easily removed from the reaction mixture by adding methanol and applying an external magnet, as expected. With this result in hand, the next step was the optimization of a supportable amino alcohol, in order to obtain a satisfactory level of enantioselectivity.

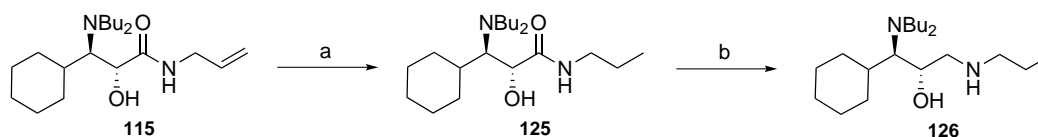
2.4.7 Optimization of the free ligands

To verify our hypothesis about the negative effect of the carbonyl group on enantioselectivity, we have considered to follow two different routes:

* removing the carbonyl group (**route A**)

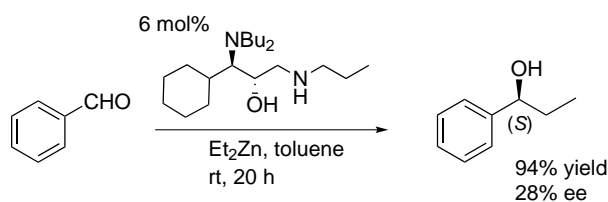
* introducing a spacer between the carbonyl group and the amino alcohol moiety (**route B**).

Firstly, we decided to subject the amino alcohol **115** to a reduction reaction of the carbonyl group. A first attempt in this direction was carried out employing LiAlH_4 in refluxing THF, but the substrate was completely recovered unchanged. Then we tried to use a BH_3 -THF solution at 70 °C, as reported in the literature for the reduction of an α -hydroxy β -amino amide.¹³⁶ To avoid possible complications in this reaction, the double bond present in **115** was previously reduced by a catalytic hydrogenation (Scheme 2-39); then the desired product **126** was obtained in moderate yield.



Scheme 2-39 Reagents and conditions: a) H_2 (1 atm), Pd/C, MeOH, > 95% b) BH_3 -THF, THF, reflux, 43%.

The amino alcohol obtained in this way was then evaluated in our reaction test, again affording 1-phenyl-1-propanol in excellent yield but with very low enantiomeric excess (Scheme 2-40).

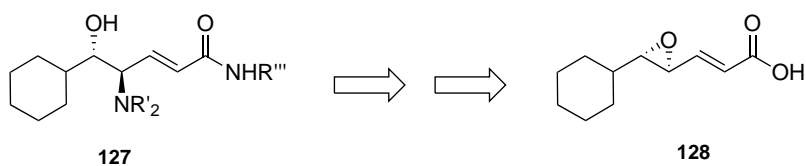


Scheme 2-40 Evaluation of **126**.

Therefore the **route A** failed; on the other hand, we had already found previously that the catalytic efficiency decreases drastically replacing the ether functionality with an amine in a Pericas-type ligand (Scheme 2-13). We have then focused on the **route B**.

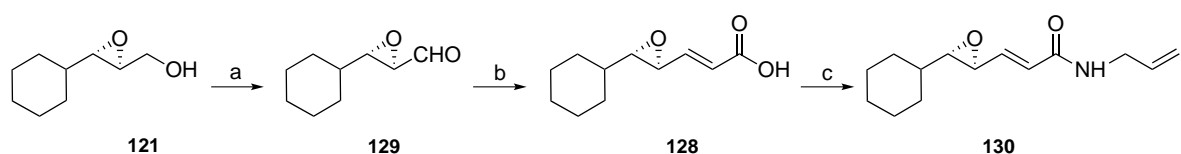
¹³⁶ Vu, A. T.; *Bioorg. Med. Chem. Lett.*, **2009**, 19,2464

In particular, we considered appropriate to use a double bond as a spacer between the carbonyl group and the amino alcohol moiety and have selected the optically active unsaturated epoxide acid **128** as precursor of the amino alcohol **127**. In fact we expected the double bond to make the epoxide ring-opening regioselective. Moreover we have reasoned that the double bond, conferring rigidity to the ligand structure, could later help the assembly of ligand chains on the nanoparticle surface.



Scheme 2-41 Ligand with the double bond as a spacer.

To synthesize **128**, the epoxy alcohol **121** was firstly oxidized by using DMSO/ SO₃-pyridine complex, a mild method which afforded the aldehyde **129** in very good yield. Then the α,β -unsaturated carboxylic moiety was obtained by an Horner Emmons reaction with diethylphosphonoacetic acid in the presence of *n*-BuLi in THF (Scheme 2-42).¹³⁷ Unsaturated epoxy acid **128** was reacted with the allyl amine in the presence of the coupling system EDC/HOAt affording the amide **130** in good yield.



Scheme 2-42 Reagents and conditions: a) SO₃-pyr/DMSO, Et₃N, CH₂Cl₂, 0 °C, 88% b) (EtO)₂POCH₂COOH, *n*-BuLi, THF, -70 °C, 75% c) allyl amine, EDC/HOAt, CH₂Cl₂, 72%.

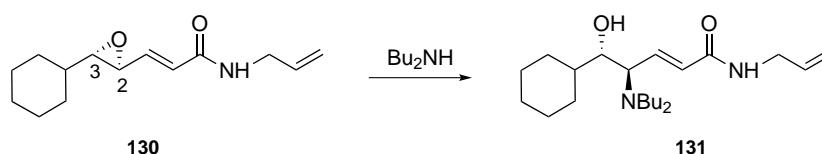
At this point, it was necessary to carry out the aminolysis of the epoxide ring, possibly in a regiocontrolled fashion. With respect to the nucleophile, the Bu₂NH was our first choice, due to the results obtained in the previous screening of ligands (Table 2-5). To the best of our knowledge, only one example of aminolysis of a substrate quite similar to **130**, which used Al₂O₃

¹³⁷ Gerspacher, M.; Lewis, C.; Ball, H. A.; Howes, C.; Subramanian, N.; Ryffel, K.; Fozard, J. R.; *J. Med. Chem.*, **2003**, *46*, 3508.

as Lewis acid, has been reported in the literature.¹³⁸ However, we expected to achieve easily the attack of the amine at the allylic position, given its high reactivity towards the nucleophilic substitutions.

In spite of these considerations, we needed to try different reaction conditions, summarized in Table 2-6, before achieving the desired amino alcohol **131** in good yield. Using Al₂O₃ in THF (entry 1), Ti(O*i*-Pr)₄ in neat Bu₂NH (entries 2 and 3), and ZnCl₂ in CH₃CN (entry 4), the starting substrate **130** was completely recovered even at high temperature and with long reaction time. Finally, by employing LiClO₄ in refluxing CH₃CN (entry 5), the epoxy amide **130** was completely converted into the single amino alcohol derivative **131**. The regiochemistry of the reaction was established by NMR spectroscopic analysis.

To our pleasure, when the amino alcohol **131** was tested in the enantioselective addition of diethylzinc to benzaldehyde, very satisfactory results were achieved. In fact, (*S*)-1-phenyl-1-propanol was obtained in nearly quantitative yield and excellent enantiomeric excess (Scheme 2-43).

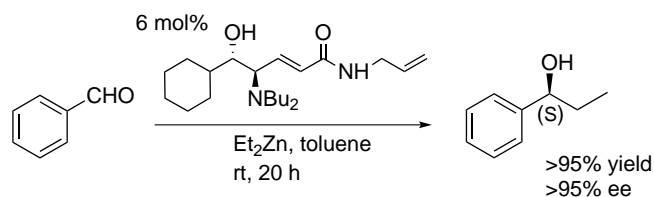


entry	Lewis acid	reaction conditions	yield (%)
1	Al ₂ O ₃	THF, reflux	no reaction
2	Ti(O <i>i</i> -Pr) ₄	neat, 60 °C	no reaction
3	Ti(O <i>i</i> -Pr) ₄	neat, 80 °C	no reaction
4	ZnCl ₂	CH ₃ CN, reflux	no reaction
5	LiClO ₄	CH ₃ CN, reflux	>95*

*Only C-2 opening product was detected by ¹H-NMR analysis of the crude material

Table 2-6. Attempts to the aminolysis.

¹³⁸ Noguchi, M.; Yoshioka, M.; Kakimoto, S.; Kajigaeshi, S.; *Bull. Chem. Soc. Jpn.*, **1987**, *60*, 3261.

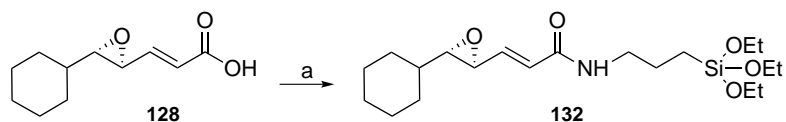


Scheme 2-43 Evaluation of **131**.

Obviously, the issue of reaction scope, with respect to the aldehyde substrate, needs further investigations; however, we have finally found the optimized amino alcohol that satisfies two fundamental requirements: ligand **131** is a very efficient asymmetric catalyst in our reaction test, the enantioselective addition of Et_2Zn to benzaldehyde, and can be easily supported onto magnetite nanoparticles in order to obtain a magnetically recoverable, recyclable “chiral nanocatalyst”.

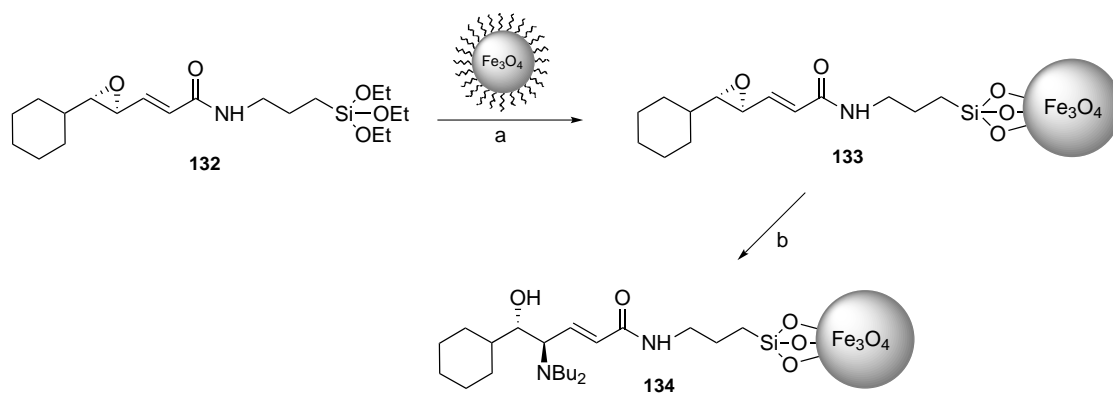
2.4.8 First MNP-supported enantioselective amino alcohol catalyst

At this point we were ready to prepare the MNP-supported catalyst corresponding to **131**, following the synthetic pathway previously developed. For this purpose, the unsaturated epoxy acid **128** was transformed into an anchorable derivative, the amide **132** (Scheme 2-44).



Scheme 2-44 Reagents and conditions: a) APTES, EDC/HOAt, CH_2Cl_2 , rt, 57%.

After immobilization onto the nanoparticles, by ligand exchange in refluxing toluene, the epoxide in **133** was subjected to ring-opening employing Bu_2NH and LiClO_4 in CH_3CN , a system that has proven to be completely regioselective (Scheme 2-45). After the two functionalization steps, HR-SEM images showed no changes in either nanoparticle size or morphology (Figure 2-12).



Scheme 2-45 Reagents and conditions: a) toluene, reflux, 4 days b) LiClO_4 , Bu_2NH , CH_3CN , 55°C .

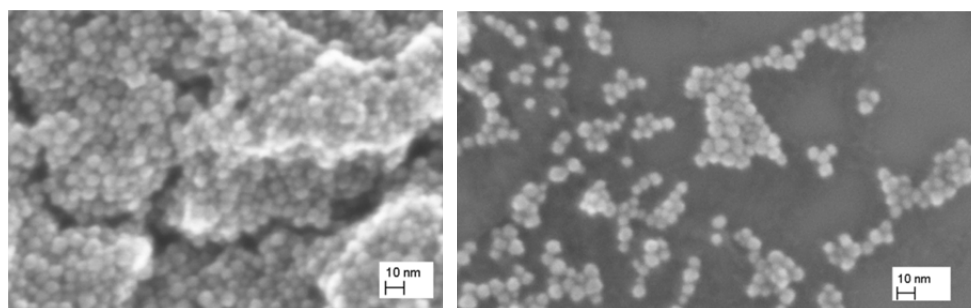
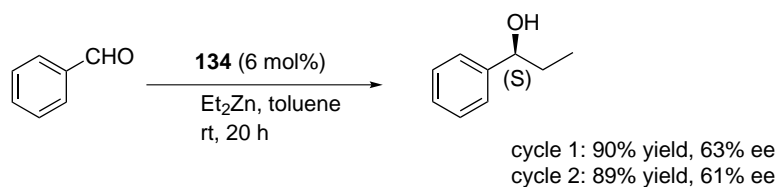


Figure 2-12 HR-SEM images of functionalized nanoparticles **134**.

The functionalized nanoparticles **134**, where the loading of the amino alcohol was 0.39 mmol/g, were then evaluated in our reaction test (Scheme 2-46, cycle 1). In comparison to the free ligand **131**, the supported amino alcohol **134** allowed the formation of 1-phenyl-1-propanol in a comparable 90% yield, while the enantioselectivity was inferior: to our disappointment only 63% enantiomeric excess was obtained. **134** was easily magnetically recovered and then used in a next run giving a comparable result (Scheme 2-46, cycle 2).



Scheme 2-46 Evaluation of **134**.

Experiments aimed at improving the efficiency of the supported catalyst in terms of enantioselectivity are currently underway. In particular the attention is now focused on the influence of the catalyst density onto the nanoparticle surface; in fact it is known that the molecular order of immobilized catalysts has an important effect on their activity and selectivity.¹³⁹ The catalyst density onto nanoparticle surface can be varied by modifying ligand exchange reaction conditions, such as type of solvent, reaction time and alkoxy silane concentration.¹⁴⁰

2.5 Conclusion

Several attempts have failed to immobilize well-known asymmetric amino alcohol catalysts, such as Pericas-type ligands and ephedrine derivatives, onto magnetite nanoparticles in order to make them readily recoverable by magnetic decantation.

In parallel, it has been carried out a study aimed at identify a new, efficient, optically active β -amino alcohol ligand, having a structure suitable for the immobilization on magnetite nanoparticles. As a result of this study, the optimized homogeneous amino alcohol catalyst **131** has been designed and synthesized, which is capable of catalyzing the asymmetric addition of diethylzinc to benzaldehyde with nearly quantitative yield and ee > 95%. Thus the corresponding supported amino alcohol **134** has been prepared and evaluated as an asymmetric catalyst in the same reaction giving a comparable yield but a lower enantiomeric excess. Efforts to improve the enantioselectivity are currently underway. The next step will be an in depth study of catalyst recyclability.

2.6 Experimental section

2.6.1 General information

All chromatographic purifications were performed on silica gel (230–400 mesh). Thin layer chromatography (TLC) was performed on pre-coated silica gel 60 F254 plates and visualization was achieved by inspection under UV light (Mineralight UVG 11 254 nm) followed by staining with phosphomolybdic acid dip [polyphosphomolybdic acid (12 g), ethanol (250 mL)] or

¹³⁹ Tollner, K.; Popovitz-Biro, R.; Lahav, M.; Milstein, D. *Science* **1997**, *278*, 2100.

¹⁴⁰ Onclin, S.; Ravoo, B. J.; Reinhoudt, D. N. *Angew. Chem., Int. Ed.* **2005**, *44*, 6282.

Ninhydrin dip [ninhydrin (5 g), sulfuric acid (5 mL), *n*-butanol (100mL)]. Organic solvents used for the chemical synthesis and for chromatography were of analytical grade. Benzaldehyde was freshly distilled before use. For all known compounds the spectral characteristics were in agreement with those reported in the literature.

¹H NMR spectra were recorded using a Varian Mercury 300 (300 MHz). Residual solvent peaks were used as internal references for ¹H NMR spectra: chloroform (δ 7.26 ppm), acetone (δ 2.05 ppm) and methanol (δ 3.31 ppm). Chemical shifts (δ) are reported in parts per million (ppm) and coupling constants (J) are reported in Hz. Splitting patterns are designated as s, singlet; bs, broad singlet; d, doublet; bd, broad doublet; dd, doublet of doublets; ddd, doublet of doublet of doublets; t, triplet; dt, doublet of triplets; q, quartet; m, multiplet. ¹³C spectra were recorded using a Varian Mercury 300 (75 MHz). Chemical shifts (δ) are reported in parts per million (ppm) relative to the internal standard of the residue solvent peak: chloroform (77.00), acetone (δ 30.83 ppm) and methanol (49.05). Optical rotations were measured on a digital polarimeter Jasco DIP-370 with a cell path length of 1 cm; solution concentrations are reported in grams per 100 ml. FT-IR spectra (400-4000 cm⁻¹) were recorded on a IR Prestige 21 Shimadzu FT-IR spectrophotometer using KBr pellets. Elemental analyses for C, H, and N were performed on an EA 1110 CHNS-O Instrument. SEM images were obtained with a Leo 1530 FE-SEM; a few drops of sample dispersion in hexane were deposited on a graphite substrate and the solvent let to evaporate at room temperature.

2.6.2 Synthesis of Fe₃O₄ nanoparticles

Iron(III) acetylacetonate (0.706 g, 2 mmol), 1,2-hexadecanediol (2.87 g, 10 mmol), oleic acid (2.1 mL, 6 mmol), oleylamine (2.8 mL, 6 mmol) and benzyl ether (20 mL) were mixed at room temperature under argon. The reaction mixture was warmed at 200 °C for 2 h and then to reflux for 1h. After cooled to room temperature, the dark-brown mixture was treated with ethanol under air, and a dark-brown material was precipitated from the solution. The MNPs were removed using an external magnetic field, washed several times with EtOH and dried *in vacuo*. Elemental analysis: C 14.10%, H 2.28%, N 0.03%; IR (KBr/cm⁻¹) ν_{\max} : 2922, 2852, 1543, 1407, 585.

2.6.3 Synthesis of amino alcohol ligands

The starting optically active epoxy alcohols were prepared from the corresponding allylic alcohols according to the procedure described by Sharpless *et al.*:¹⁴¹

(2S,3S)-3-phenyl-2,3-epoxy-propan-1-ol (29): white solid (53% yield); $[\alpha]_D^{25} = -49.7$ ($c=2.0$ in CHCl_3); $^1\text{H NMR}$ (300 MHz, CDCl_3) δ : 7.46-7.17 (5H, m, Ph), 4.05 (1H, ddd, $J=4.0, 6.2, 12.0$ Hz, $\text{CH}_a\text{H}_b\text{OH}$), 3.93 (1H, d, $J=2.1$ Hz, PhCH), 3.79 (1H, ddd, $J = 4.0, 6.2, 12.0$ Hz, $\text{CH}_a\text{H}_b\text{OH}$), 3.24 (1H, ddd, $J=2.1, 4.0$ Hz, CHCH_2OH), 2.56 (1H, t, $J=6.2$ Hz, OH); $^{13}\text{C NMR}$ (75 MHz CDCl_3) δ : 136.8, 128.6, 128.4, 125.8, 62.6, 61.4, 55.8.

(2S,3S)- 2,3-epoxy-hexan-1-ol (48): colourless oil (88% yield); $[\alpha]_D^{25} = -44.1$ ($c = 1.1$, CHCl_3); $^1\text{H NMR}$ (300 MHz, CDCl_3) δ : 3.92 (1H, dd, $J = 2.2, 12.4$ Hz, $\text{CH}_a\text{H}_b\text{OH}$), 3.63 (1H, dd, $J = 3.3, 12.4$ Hz, $\text{CH}_a\text{H}_b\text{OH}$), 2.97-2.86 (2H, m, CH-O-CH), 2.3 (1H, bs, OH), 1.57-1.3 (4H, m, $\text{CH}_2 \times 2$), 0.97 (3H, t, $J = 7.3$ Hz, CH_3); $^{13}\text{C NMR}$ (75 MHz CDCl_3) δ : 61.9, 58.7, 55.9, 33.5, 19.1, 13.7

(2S,3S)-3-cyclohexyl-2,3-epoxy-propan-1-ol (48a): colourless oil (90% yield); $[\alpha]_D^{25} = -32.5$ ($c = 2.2$, CDCl_3); $^1\text{H NMR}$ (300 MHz, CDCl_3) δ : 3.87-3.76 (1H, m, $\text{CH}_a\text{H}_b\text{OH}$), 3.55-3.44 (1H, m, $\text{CH}_a\text{H}_b\text{OH}$), 2.98 (1H, bs, OH), 2.92 (1H, ddd, $J 2.5, 4.9, 7.4$ Hz, CHCH_2OH), 2.68 (1H, dd, $J = 2.5, 6.8$ Hz, cyclohexyl-CH), 1.84-0.93 (11H, m, cyclohexyl); $^{13}\text{C NMR}$ (75 MHz, CDCl_3) δ : 62.1, 60.4, 57.6, 39.5, 29.6, 28.9, 26.2, 25.6, 25.5.

(2S,3S)-2-phenyl-3-(propoxymethyl)oxirane (30). A solution of the epoxy alcohol **29** (600 mg, 4.0 mmol) in THF (10 mL) was added to a suspension of sodium hydride (60% in mineral oil, 240 mg, 6.0 mmol) in THF (20 mL) at -20 °C under argon. The mixture was stirred for 20 min, and propyl iodide (0.78 mL, 8.0 mmol) was syringed into the mixture. After being stirred for 12 h at -20 °C, the mixture was allowed to reach room temperature and stirred for another hour. NH_4Cl saturated solution was carefully added drop-wise. The aqueous solution was extracted with CH_2Cl_2 and the combined organic extracts were dried and concentrated *in vacuo*. The residual oil was chromatographed using hexane:EtOAc (95:5-90:10) as eluent to give 522 mg (68%) of **30** as an oil. $^1\text{H NMR}$ (300 MHz, CDCl_3) δ : 7.50-7.19 (m, 5H, Ph), 3.85-3.75 (m, 2H, Ph-CHO and $\text{CHCH}_a\text{H}_b\text{O}$), 3.57 (dd, 1H, $J = 11.6, 5.6$, $\text{CHCH}_a\text{H}_b\text{O}$), 3.50 (t, 2H, $J = 6.6$, OCH_2CH_2), 3.22 (m, 1H, OCHCH_2O), 1.64 (m, 2H, CH_2CH_3), 0.95 (t, 3H, $J = 7.15$, CH_3); $^{13}\text{C NMR}$ (75 MHz, CDCl_3) δ : 136.9, 128.3, 128.0, 125.5, 73.1, 70.4, 61.0, 55.6, 22.8, 10.3.

¹⁴¹ See ref. 99 and 135.

(1R,2R)-1-phenyl-1-(piperidinyl)-3-propoxypropan-2-ol (31). Piperidine (0.74 mL, 7.2 mmol) was syringed into a mixture of **30** (137 mg, 0.71 mmol) and LiClO₄ (1.17 g, 11.1 mmol) in acetonitrile (2.5 mL) at 55 °C. After the mixture was stirred for 24 h at 55 °C, H₂O was added, and the aqueous layer was extracted with CH₂Cl₂. The combined organic extracts were dried and concentrated *in vacuo*. The residual oil was chromatographed using hexane: EtOAc (90:10-80:20) as eluent to give 190 mg (> 95%) of **31**. $[\alpha]_D^{25} = -16.3$ (c=2.9 in CHCl₃); ¹H NMR (300 MHz, CDCl₃) δ: 7.40-7.21 (m, 5H, Ph), 4.49 (ddd, 1H, *J* = 7.2, 6.3, 3.6, CHOH), 3.41-3.16 (5H, m, CHN, CH_aCH_bO, OCH₂CH₃), 2.75 (bs, 1H, OH), 2.68-2.44 (m, 4H, CH₂N x2), 1.73-1.32 (m, 8H), 0.89 (t, 3H, *J* = 7.7, CH₃); ¹³C NMR (75 MHz, CDCl₃) δ: 129.3, 127.8, 127.3, 73.1, 73.0, 71.7, 68.4, 51.8, 26.3, 24.5, 22.7, 10.4.

(1R,2R)-1-(dibutylamino)-1-phenyl-3-propoxypropan-2-ol (32). Compound **30** (150 mg, 0.78 mmol), LiClO₄ (1.28 g, 12.1 mmol), and Bu₂NH (1.32 mL, 10 mmol) in acetonitrile (2.0 mL) were stirred at 55 °C for 24 h. The workup was identical to the one described for **31** to give 250 mg (> 95%) of **32** as an oil after chromatography using hexane:EtOAc (90:10-80:20) as eluent; ¹H NMR (300 MHz, CDCl₃) δ: 7.39-7.14 (m, 5H, Ph), 4.32 (ddd, 1H, *J* = 7.1, 6.3, 3.3, CHOH), 3.70 (d, 1H, *J* = 7.1, CHN), 3.53 (dd, 1H, *J* = 9.3, 3.3, CH_aCH_bO), 3.43-3.22 (m, 3H, CH_aCH_bO, CH₂O), 2.50 (m, 2H, CH₂N), 2.22 (m, 2H, CH₂N), 1.70-1.05 (m, 10H), 0.97-0.70 (m, 9H). ¹³C NMR (75 MHz, CDCl₃) δ: 129.6, 127.8, 127.2, 73.1, 73.0, 69.1, 66.5, 49.8, 29.5, 22.8, 20.5, 13.9, 10.5.

(2S,3S)-2-((allyloxy)methyl)-3-phenyloxirane (33). A solution of the epoxy alcohol **29** (495 mg, 3.3 mmol) in DMF (3 mL) was added to a suspension of sodium hydride (60% in mineral oil, 160 mg, 3.9 mmol) in DMF (4 mL) at -20 °C under argon. The mixture was stirred for 20 min, and allyl bromide (0.4 mL, 4.3 mmol) was syringed into the mixture. After being stirred for 12 h at -20 °C, the mixture was allowed to reach room temperature and stirred for another hour. NH₄Cl saturated solution was carefully added drop-wise. The aqueous solution was extracted with CH₂Cl₂ and the combined organic extracts were dried and concentrated *in vacuo*. The residual oil was chromatographed using hexane:EtOAc (95:5-90:10) as eluent to give 458 mg (73%) of **33**. ¹H NMR (300 MHz, CDCl₃) δ: 7.45-6.95 (m, 5H, Ph), 6.09-5.65 (m, 1H, CH=), 5.40-5.09 (m, 2H, CH₂=), 4.09 (m, 2H, OCH₂CH=), 3.87-3.67 (m, 2H, Ph-CHO and CH_aH_bO), 3.59 (dd, 1H, *J* = 11.0, 5.0, CH_aH_bO), 3.22 (m, 1H, OCHCH₂O); ¹³C NMR (75 MHz, CDCl₃) δ: 136.7, 134.2, 128.3, 128.1, 128.0, 125.0, 117.12, 72.1, 69.6, 60.9, 55.6.

((2S,3S)-3-phenyloxiranyl)methyl methanesulfonate (34). To a solution of the epoxy alcohol **29** (300 mg, 2.0 mmol) in CH₂Cl₂ (6.5 mL), Et₃N (0.56 mL, 4.0 mmol) and a catalytic amount of

DMAP were added. After being stirred at 0°C, methane sulfonyl chloride (0.15 mL, 2.0 mmol) was added dropwise. After 2 h, the reaction was quenched with ice cold water; the mixture was extracted with CH₂Cl₂ and the organic layer was washed with saturated aqueous NH₄Cl and brine and then dried over Na₂SO₄. The solvent was removed *in vacuo* to give 430 mg (> 95%) of **34**; ¹H NMR (300 MHz, CDCl₃) δ: 7.43-7.17 (m, 5H, Ph), 4.59 (d, 1H, J = 12.1, CH_aH_bO), 4.27 (dd, 1H, J = 12.1, 6.05, CH_aH_bO), 3.87 (d, 1H, Ph-CHO), 3.33 (m, 1H, OCH₂CH₂), 3.1 (s, 3H, CH₃); ¹³C NMR (75 MHz, CDCl₃) δ: 128.6, 128.5, 125.6, 69.0, 58.6, 56.3, 37.8.

(2R,3S)-1-allyl-2-phenylazetid-3-ol (37). Compound **34** (400 mg, 1.75 mmol) was reacted with allyl amine (0.26 mL, 3.51 mmol) at 50 °C for 24 hours. Allyl amine was evaporated *in vacuo* and the crude material was purified on silica gel (hexane/EtOAc, 70:30-60:40) affording 276 mg (85%) of **37**; [α]_D²⁵ = -102.8 (c=2.3 in CHCl₃); ¹H NMR (300 MHz, CDCl₃) δ: 7.42-7.18 (m, 5H, Ph), 5.70 (m, 1H, CH=), 5.06 (m, 2H, CH₂=), 4.09 (m, 1H, CHOH), 3.77 (d, 1H, J = 6.0, Ph-CHN), 3.70 (m, 1H, CH_aH_bCHOH), 3.28 (dd, 1H, J = 13.2, 6.0, CH_aH_bN), 3.00 (dd, 1H, J = 13.2, 6.6, CH_aH_bN), 2.71 (m, 1H, CH_aH_bCHOH); ¹³C NMR (75 MHz, CDCl₃) δ: 140.3, 134.0, 128.4, 127.6, 127.0, 117.7, 78.7, 69.9, 61.2, 60.0. MS (TOF ES⁺) m/z: 190 (M⁺+1, 100).

1-(((2S,3S)-3-phenyloxiranyl)methyl)piperidine (38). Compound **34** (260 mg, 1.14 mmol) was reacted with piperidine (0.23 mL, 2.28 mmol) at 50 °C for 12 hours. The crude material was purified on silica gel (hexane/EtOAc, 70:30-60:40) affording 218 mg (88%) of **38**; ¹H NMR (300 MHz, CDCl₃) δ: 7.47-6.98 (m, 5H, Ph), 3.59 (d, 1H, Ph-CHO), 3.16 (m, 1H, OCH₂CH₂), 2.71 (dd, 1H, J = 13.2, 3.8, CH_aH_bN), 2.62-2.28 (m, 5H, CH_aH_bN and CH₂N x2), 1.69-1.25 (m, 6H); ¹³C NMR (75 MHz, CDCl₃) δ: 140.9, 128.7, 125.9, 61.5, 61.0, 57.3, 55.2, 26.1, 24.3.

(1R,2S)-1-phenyl-1,3-di(piperidinyl)propan-2-ol (39). Compound **38** (170 mg, 0.78 mmol), LiClO₄ (1.28 g, 12.1 mmol), and piperidine (1.32 mL, 10 mmol) in acetonitrile (2.0 mL) were stirred at 55 °C for 24 h. The workup was identical to the one described for **31** to give 234 mg (>95%) of **32** after chromatography using CH₂Cl₂/MeOH (95:5) as eluent; ¹H NMR (300 MHz, CDCl₃) δ: 7.46-7.01 (m, 5H, Ph), 4.22 (m, 1H, CHOH), 3.52 (d, 3H, J = 7.7, CHN), 2.75-2.00 (m, 10 H, CH_aH_bN and CH₂N x4), 1.70-1.20 (m, 12H); ¹³C NMR (75 MHz, CDCl₃) δ: 137.0, 129.9, 128.0, 127.3, 68.6, 65.9, 63.8, 55.0, 50.3, 26.1, 24.3.

(1R,2S)-O-benzyl ephedrine (44). To a solution of potassium hydride (370 mg, 9.22 mmol) in THF (5 mL) was added (1R,2S)-ephedrine (1.03g, 6.24 mmol) in THF (10 mL) dropwise. After 16 hours, benzyl bromide (0.70 mL, 5.92 mmol) was added. After 5 hours, the reaction was quenched with *i*-PrOH (5 mL) and water (15 mL). The aqueous layer was extracted with Et₂O;

the combined organic layers were dried and concentrated *in vacuo*. The crude product was purified by flash chromatography using CH₂Cl₂/MeOH as eluent (90:10-70:30), affording **44** (1.45g, 92%) as a colourless oil; ¹H NMR (300 MHz, CDCl₃) δ: 7.43-7.27 (m, 5H, Ph), 4.55 (d, 1H, J = 11.8, CH_aH_bPh), 4.38 (d, 1H, J = 5.3, CHPh), 4.30 (d, 1H, J = 11.8, CH_aH_bPh), 2.84-2.78 (m, 1H, CHCH₃), 2.35 (s, 3H, CH₃N), 1.11 (d, 3H, J = 6.4, CHCH₃); ¹³C NMR (75 MHz, CDCl₃) δ: 140.2, 138.9, 128.8, 128.7, 128.1, 127.9, 127.9, 84.0, 71.2, 60.5, 34.2, 15.4.

(1R,2S)-O-benzyl-N-propyl ephedrine (46). To a solution of compound **44** (150 mg, 0.58 mmol) in acetonitrile (6 mL), propyl iodide (0.11 mL, 1.15 mmol) and potassium carbonate (158 mg, 15 mmol) were added. The reaction mixture was heated to reflux and stirred for 20 hours. Then the reaction mixture was filtered and concentrated *in vacuo*. The crude product was purified by flash chromatography using hexane/EtOAc (80:20), affording 164 mg (96%) of **46**. ¹H NMR (300 MHz, CDCl₃) δ: 7.42-7.11 (m, 5H, Ph), 4.50 (d, 1H, J = 5.3, CHPh), 4.43 (d, 1H, J = 11.6, CH_aH_bPh), , 4.30 (d, 1H, J = 11.6, CH_aH_bPh), 2.84-2.78 (m, 1H, CHCH₃), 2.35 (s, 3H, CH₃N), 1.42-1.12 (m, 2H), 1.09 (d, 3H, J = 7.1, CHCH₃), 0.75 (t, 3H, J = 7.15, CH₂CH₃); ¹³C NMR (75 MHz, CDCl₃) δ: 140.2, 138.9, 128.2, 128.0, 127.6, 127.5, 127.0, 83.0, 70.5, 63.7, 56.3, 37.9 22.6, 21.2, 20.9, 14.1, 11.6, 8.7.

((2S,3S)-3-propyloxiran-2-yl)methyl undec-10-enoate (50). A solution of epoxy alcohol **48** (1.0 g, 8.6 mmol), 10-undecenoic acid (1.6 g, 8.6 mmol), DCC (2.1 g, 10.3 mmol) and DMAP (catalytic amount) in CH₂Cl₂ (10 mL) was stirred at room temperature for 12 h under argon. The solution was filtered and then concentrated *in vacuo*. The residue was chromatographed using hexane:EtOAc (95:5) as eluent to give 1.92 g (80%) of **50**; ¹H NMR (300 MHz, CDCl₃) δ: 5.78 (m, 1H, CH₂=CH), 5.06-4.84 (m, 2H, CH₂=CH), 4.33 (dd, 1H, J = 3.3, 12.1, CH_aH_bO), 3.90 (dd, 1H, J = 6.0, 12.1, CH_aH_bO), 2.93 (m, 1H, CH₂CH-O), 2.82 (ddd, 1H, J = 2.2, 5.5, 11.0, OCHCH₂O), 2.31 (t, 2H, J = 7.15, COCH₂), 2.01 (m, 2H, CH₂CH=), 1.68-1.18 (m, 16H), 0.93 (t, 3H, J = 7.15, CH₃); ¹³C NMR (75 MHz, CDCl₃) δ: 173.4, 139.1, 114.2, 64.6, 56.4, 55.3, 34.1, 33.9, 33.7, 29.4, 29.3, 29.2, 29.1, 29.0, 25.0, 19.3, 13.9.

(2R,3R)-3-azido-2-hydroxyhexyl undec-10-enoate (53). To a solution of compound **50** (900 mg, 3.19 mmol) in DMF (25 mL), NaN₃ (2.2 g, 34.4 mmol) and NH₄Cl (2.1 g, 38.7 mmol) were added and the reaction mixture was heated to 80 °C for 16 h. Et₂O and brine were added. The aqueous layer was extracted with Et₂O. The combined organic extracts were dried and concentrated *in vacuo*. The residual oil was chromatographed using hexane:EtOAc (90:10-80:20) as eluent to give 750 mg (72%) of **53**. ¹H NMR (300 MHz, CDCl₃) δ: 5.80 (m, 1H, CH₂=CH), 5.07-4.86 (m, 2H, CH₂=CH), 4.28 (dd, 1H, J = 3.3, 12.1, CH_aH_bO), 4.14 (dd, 1H, J = 6.6, 12.1,

CH_aH_b-O), 3.82 (m, 1H, CHOH), 3.44 (m, 1H, CHN₃), 2.58 (bs, 1H, OH), 2.35 (t, 2H, J = 7.15, COCH₂), 2.01 (m, 2H, CH₂CH=), 1.68-1.18 (m, 16H), 0.93 (t, 3H, J = 7.15, CH₃); ¹³C NMR (75 MHz, CDCl₃) δ: 173.7, 139.3, 114.4, 71.2, 65.5, 64.7, 34.9, 33.8, 33.7, 29.4, 29.3, 29.2, 29.1, 29.0, 24.3, 19.0, 13.9.

(2S,3R)-3-bromo-2-hydroxyhexyl undec-10-enoate (54). LiBr (180 mg, 2.1 mmol) and Amberlyst 15 (225 mg, 1.05 mmol) were added to a solution of compound **50** (300 mg, 1.05 mmol) in acetone (5 mL) at -20 °C. After stirring for 24 h, the solution was filtered and concentrated *in vacuo*. EtOAc was added and the mixture was washed with brine. The organic layer was dried and the solvent was removed *in vacuo* giving 371 mg (97%) of **54**, without the need of purification : ¹H NMR (300 MHz, CDCl₃) δ: 5.80 (m, 1H, CH₂=CH), 5.07-4.87 (m, 2H, CH₂=CH), 4.36 (dd, 1H, J = 3.3, 12.1, CH_aH_bO), 4.24 (dd, 1H, J = 6.6, 12.1, CH_aH_b-O), 4.05 (m, 1H, CHBr), 3.86 (m, 1H, CHOH), 2.81 (bs, 1H, OH), 2.34 (t, 2H, J = 7.15, COCH₂), 2.01-1.18 (m, 18H), 0.93 (t, 3H, J = 7.15, CH₃); ¹³C NMR (75 MHz, CDCl₃) δ: 174.0, 138.9, 114.0, 72.6, 66.1, 57.8, 35.8, 35.7, 34.0, 33.6, 29.3, 29.2, 29.1, 28.7, 24.7, 20.6, 13.2.

(2R,3S)-3-azido-2-hydroxyhexyl undec-10-enoate (55). A solution of compound **54** (150 mg, 0.41 mmol), NaN₃ (107 mg, 1.65 mmol) and 18-crown-6 (108 mg, 0.41 mmol) in DMSO (1.0 mL) was stirred at 65 °C under argon for 12 h. The mixture was diluted with Et₂O and washed several times with water and brine. The organic layer was then dried and concentrated *in vacuo*. Chromatographic purification, using hexane/EtOAc (90:10) as eluent, afforded 125 mg (93%) of **55**. ¹H NMR (300 MHz, CDCl₃) δ: 5.80 (m, 1H, CH₂=CH), 5.07-4.86 (m, 2H, CH₂=CH), 4.19-4.13 (m, 2H, CH_aH_bO), 3.80 (m, 1H, CHOH), 3.31 (m, 1H, CHN₃), 2.60 (bs, 1H, OH), 2.33 (t, 2H, J = 7.15, COCH₂), 2.01 (m, 2H, CH₂CH=), 1.68-1.18 (m, 16H), 0.93 (t, 3H, J = 7.15, CH₃); ¹³C NMR (75 MHz, CDCl₃) δ: 173.7, 139.0, 114.0, 71.2, 65.5, 63.3, 34.2, 33.8, 33.6, 29.4, 29.3, 29.2, 29.1, 28.9, 24.3, 19.0, 13.9.

(2R,3R)-3-azido-2-((benzyloxycarbonyl)oxy)hexyl undec-10-enoate (57). TMEDA (0.18 mmol) and benzyl chloroformate (0.33 mmol) were added, under argon and at 0 °C, to a solution of compound **53** (100 mg, 0.30 mmol) in CH₂Cl₂ (3.0 mL). Then the reaction mixture was allowed to reach the room temperature. After 12 h, the mixture is diluted with CH₂Cl₂, washed with water, dried and concentrated *in vacuo*. The crude material was purified by flash chromatography with petroleum ether/Et₂O (95:5) as eluent, affording 118 mg of **57** (85%). ¹H NMR (300 MHz, CDCl₃) δ: 5.83 (m, 1H, CH₂=CH), 5.18 (s, 2H, CH₂-Ph), 5.09-4.90 (m, 3H, CH₂=CH and CH-O), 4.46 (dd, 1H, J = 3.3, 12.1, CH_aH_bO), 4.20 (dd, 1H, J = 6.6, 12.1, CH_aH_b-O), 3.65 (m, 1 H, CHN₃), 2.29 (t, 2H, J = 7.1, COCH₂), 2.06 (m, 2H, CH₂CH=), 1.68-1.18 (m,

16H), 0.96 (t, 3H, J = 7.1, CH₃); ¹³C NMR (75 MHz, CDCl₃) δ: 173.1, 154.3, 139.0, 133.4, 128.6, 128.5, 114.0, 76.9, 69.5, 62.1, 61.9, 33.8, 33.7, 32.6, 29.1, 28.9, 28.8, 24.6, 19.3, 13.6.

(2R,3R)-3-azido-2-((benzyloxycarbonyl)oxy)hexyl 11-(trimethoxysilyl)undecanoate (58).

Toluene and hydrogen hexachloroplatinate (IV) hydrate (catalytic amount) were added to compound **57** (100 mg, 0.20 mmol) under argon. Subsequently, trimethoxysilane (0.050 mL, 0.40 mmol) was syringed into the mixture and the mixture was heated to 70°C for 24 h. After cooling to room temperature, the mixture was filtered by applying argon pressure. The solvent and the trimethoxysilane in excess were removed *in vacuo* affording 228 mg (98%) of **58**: ¹H NMR (300 MHz, CDCl₃) δ: 5.18 (s, 2H, CH₂-Ph), 4.97 (m, 1H, CH-O), 4.35 (dd, 1H, J = 3.3, 12.1, CH₂H_bO), 4.16 (dd, 1H, J = 6.6, 12.1, CH_aH_c-O), 3.65 (m, 1 H, CHN₃), 3.56 (s, 9H, OCH₃ x3), 2.26 (t, 2H, J = 7.1, COCH₂), 1.75-1.10 (m, 20H), 0.96 (t, 3H, J = 7.1, CH₃); 0.64 (t, 2H, J = 8.6, CH₂Si); ¹³C NMR (75 MHz, CDCl₃) δ: 173.2, 154.3, 133.6, 128.6, 128.5, 76.9, 70.0, 61.2, 61.1, 33.9, 33.8, 29.5, 29.4, 29.3, 29.1, 28.9, 28.8, 24.6, 19.1, 13.6, 6.6. IR (neat, cm⁻¹) ν_{max}: 2926 (CH₂), 2853 (CH₂), 2115 (N₃), 1750 (C=O), 1457, 1261, 1100-1000 (Si-O).

General procedure for the oxidation of epoxy alcohol to epoxy acid by

RuCl₃/NaIO₄. The epoxy alcohol (1 mmol) was dissolved in CCl₄ (2 mL), CH₃CN (2 mL) and phosphate buffer (pH = 7, 0.2 M, 3 mL) with vigorous stirring. Then NaIO₄ (3.0 mmol) and RuCl₃ (5 mg) were added. After 12 h, CH₂Cl₂ and water were added. The organic layer was separated and the aqueous layer was extracted several times with CH₂Cl₂. The combined organic extracts were dried, concentrated and then filtered on a celite pad. The solvent was removed *in vacuo* affording the desired product.

(2R,3S)-3-propyloxirane-2-carboxylic acid (63): obtained from the epoxy alcohol **48** in 79% yield; ¹H NMR (300 MHz, CDCl₃) δ: 10.9 (bs, 1H, COOH), 3.23 (d, 1H, J = 1.6, COCH-O), 3.14 (dt, 1H, J = 1.6, 3.8, Pr-CH-O), 1.62-1.36 (m, 4H), 0.92 (t, 3H, J = 7.1, CH₃). ¹³C NMR (75 MHz, CDCl₃) δ: 174.7, 58.7, 52.4, 33.2, 18.8, 13.5.

(2R,3S)-3-cyclohexyloxirane-2-carboxylic acid (121): obtained from the epoxy alcohol **48b** in 80% yield; ¹H NMR (300 MHz, CDCl₃) δ: 10.6 (bs, 1H, COOH), 3.25 (d, 1H, J = 1.7, COCH-O), 2.95 (dd, 1H, J = 1.6, 3.8, O). ¹³C NMR (75 MHz, CDCl₃) δ: 175.5, 58.5, 54.7, 39.6, 28.8, 26.2, 25.6, 25.5.

(2R,3S)-3-phenyloxirane-2-carboxylic acid (121a): obtained from the epoxy alcohol **29** in 61% yield; ¹H NMR (300 MHz, CDCl₃) δ: 9.03 (bs, 1H, COOH), 7.16-7.73 (m, 5H, Ph), 4.15 (d,

1H, J = 1.6, Ph-CHO), 3.55 (d, 1H, J = 1.6, COCH-O), Hex-CH-O), 1.00-1.90 (m, 11H). ¹³C NMR (75 MHz, CDCl₃) δ: 173.6, 134.5, 129.6, 129.3, 128.8, 128.7, 125.9, 58.2, 56.1.

(2R,3S)-tert-butyl 3-propyloxirane-2-carboxylate (64). A solution of epoxy acid **63** (230 mg, 1.77 mmol) and *tert*-butyl 2,2,2-trichloroacetimidate (0.63 mL, 3.54 mmol) in CH₂Cl₂ (8 mL), was stirred at room temperature for 48 h. Then the reaction mixture was concentrated *in vacuo* and the residue was purified by flash chromatography with hexane/EtOAc (98:2) as eluent, affording 296 mg (90%) of **64**. ¹H NMR (300 MHz, CDCl₃) δ: 3.09-2.99 (m, 2H, CH-O-CH), 1.65-1.35 (m, 13H), 0.92 (t, 3H, J = 7.1, CH₃); ¹³C NMR (75 MHz, CDCl₃) δ: 168.2, 82.0, 57.8, 53.5, 33.3, 28.0, 19.0, 13.6.

Epoxide ring-opening of (2R,3S)-tert-butyl 3-propyloxirane-2-carboxylate by NaN₃/NH₄Cl. To a solution of compound **64** (320 mg, 1.72 mmol) in DMF (10 mL), NaN₃ (1.20 g, 18.6 mmol) and NH₄Cl (1.13 g, 21.2 mmol) were added and the reaction mixture was heated to 80 °C for 4 h. Then Et₂O and brine were added. The organic layer was separated and the aqueous layer was extracted with Et₂O. The combined organic extracts were dried and concentrated *in vacuo*. Chromatographic purification of the crude material, using hexane:EtOAc (95:5) as eluent, allowed to obtain the two regioisomer azido alcohols **65** (268 mg, 68%) and **66** (88 mg, 22%). **(2S,3S)-tert-butyl 2-azido-3-hydroxyhexanoate (65)**: ¹H NMR (300 MHz, CDCl₃) δ: 3.91 (m, 1H, CHOH), 3.78 (d, 1H, J = 5.4, CHN₃), 2.65 (bs, 1H, OH), 1.65-1.31 (m, 13H), 0.92 (t, 3H, J = 7.1, CH₃); ¹³C NMR (75 MHz, CDCl₃) δ: 168.0, 83.4, 71.5, 66.6, 35.0, 27.9, 18.5, 13.7. **(2R,3R)-tert-butyl 3-azido-2-hydroxyhexanoate (66)**: ¹H NMR (300 MHz, CDCl₃) δ: 4.22 (dd, 1H, J = 3.1, 5.5, CHOH), 3.49 (dt, 1H, J = 3.3, 9.9, CHN₃), 3.14 (d, 1H, J = 5.5, OH), 1.60-1.35 (m, 13H), 0.95 (t, 3H, J = 7.1, CH₃); ¹³C NMR (75 MHz, CDCl₃) δ: 168.2, 83.5, 72.8, 63.2, 32.0, 27.9, 19.5, 13.6.

(2S,3S)-tert-butyl 2-bromo-3-hydroxyhexanoate (76). NaBr (221 mg, 2.15 mmol) and Amberlyst 15 (232 mg, 1.07 mmol) were added to a solution of compound **64** (200 mg, 1.07 mmol) in acetone (5 mL) at -20 °C. After stirring for 24 h, the solution was filtered and concentrated *in vacuo*. EtOAc was added and the mixture was washed with brine. The organic layer was dried and the solvent was removed *in vacuo* giving the desired product, which will be used in the next reaction as crude material. ¹H NMR (300 MHz, CDCl₃) δ: 4.03 (d, 1H, J = 7.1, 5.5, CHBr), 3.95 (m, 1H, CHOH), 2.82 (d, 1H, J = 6.3, OH), 1.80-1.35 (m, 13H), 0.96 (t, 3H, J = 7.1, CH₃).

(2R,3S)-tert-butyl 2-azido-3-hydroxyhexanoate (77). To a solution of the crude product **76** (280 mg) in DMF (1 mL), NaN₃ (272 mg, 4.19 mmol) was added and the mixture was stirred at room temperature under argon for 16 h. The mixture was diluted with Et₂O and washed several times with water and brine. The organic layer was then dried and concentrated *in vacuo*. Chromatographic purification, using hexane/EtOAc (90:10) as eluent, afforded 198 mg of **77**. ¹H NMR (300 MHz, CDCl₃) δ: 4.00 (m, 1H, CHOH), 3.7 (d, 1H, J = 3.3, CHN₃), 2.12 (d, 1H, J = 6.1, OH), 1.75-1.35 (m, 13H), 0.94 (t, 3H, J = 7.1, CH₃). ¹³C NMR (75 MHz, CDCl₃) δ: 168.0, 83.4, 71.5, 66.3, 35.0, 27.9, 18.5, 13.7.

(2S,3R)-tert-butyl 3-bromo-2-hydroxyhexanoate (78). To a solution of compound **64** (185 mg, 1 mmol) in Et₂O (15 mL) at -20°C under argon, MgBr₂ (260 mg, 1 mmol) was added and the mixture was stirred for 12 h. The mixture was diluted with Et₂O and washed with water and brine. The organic layer was dried and concentrated *in vacuo* affording 260 mg (97%) of **78**, without need of chromatographic purification. ¹H NMR (300 MHz, CDCl₃) δ: 4.28 (dd, 1H, J = 2.8, 6.2, CHOH), 4.20 (dt, 1H, J = 2.8, 9.9, CHBr), 3.24 (d, 1H, J = 6.2, OH), 1.78-1.42 (m, 13H), 0.94 (t, 3H, J = 7.1, CH₃). ¹³C NMR (75 MHz, CDCl₃) δ: 170.3, 83.8, 74.3, 57.2, 36.0, 28.0, 20.9, 13.3.

(2R,3S)-tert-butyl 3-azido-2-hydroxyhexanoate (79). A solution of compound **78** (137 mg, 0.51 mmol), NaN₃ (133 mg, 2.05 mmol) and 18-crown-6 (135 mg, 0.51 mmol) in DMSO (1.0 mL) was stirred at 65 °C under argon for 12 h. The mixture was diluted with Et₂O and washed several times with water and brine. The organic layer was then dried and concentrated *in vacuo*. Chromatographic purification, using hexane/EtOAc (90:10) as eluent, afforded 107 mg (92%) of **79**. ¹H NMR (300 MHz, CDCl₃) δ: 4.07 (dd, 1H, J = 2.1, 5.3, CHOH), 3.45 (m, 1H, CHN₃), 3.09 (d, 1H, J = 5.3, OH), 1.98-1.38 (m, 13H), 0.94 (t, 3H, J = 7.1, CH₃). ¹³C NMR (75 MHz, CDCl₃) δ: 168.0, 83.5, 72.7, 63.0, 31.9, 27.6, 19.4, 13.6.

General procedure for the protection of the hydroxyl with a benzyloxycarbonyl group. TMEDA (0.6 mmol) and benzyl chloroformate (1.1 mmol) were added, under argon and at 0 °C, to a solution of the substrate (1.0 mmol) in CH₂Cl₂ (10 mL). Then the reaction mixture was allowed to reach the room temperature. After completion of the reaction, the mixture was diluted with CH₂Cl₂, washed with water, dried and concentrated *in vacuo*. The crude material was purified by flash chromatography using hexane/Et₂O (95:5) as eluent.

(2S,3S)-tert-butyl 2-azido-3-(((benzyloxy)carbonyl)oxy)hexanoate (67): obtained from **65** in >95% yield; ¹H NMR (300 MHz, CDCl₃) δ: 7.37 (m, 5H, Ph), 5.18 (s, 2H, CH₂Ph), 5.06 (m, 1H, CH-O), 4.15 (d, 1H, J = 4.7, CHN₃), 1.80-1.20 (m, 13 H), 0.94 (t, 3H, J = 7.1, CH₃). ¹³C NMR (75 MHz, CDCl₃) δ: 168.0, 154.5, 134.9, 128.5, 83.7, 76.9, 69.8, 64.4, 32.0, 27.9, 18.3, 13.6.

(2R,3S)-tert-butyl 2-azido-3-(((benzyloxy)carbonyl)oxy)hexanoate (80): obtained from **77** in 95% yield; ¹H NMR (300 MHz, CDCl₃) δ: 7.37 (m, 5H, Ph), 5.20-5.00 (m, 3H, CH₂Ph and CH-O), 3.75 (d, 1H, J = 3.7, CHN₃), 1.82-1.35 (m, 13H), 0.95 (t, 3H, J = 7.1, CH₃). ¹³C NMR (75 MHz, CDCl₃) δ: 168.0, 154.5, 134.9, 128.4, 83.5, 77.4, 69.8, 63.7, 33.4, 27.9, 18.3, 13.7.

(2R,3R)-tert-butyl 3-azido-2-(((benzyloxy)carbonyl)oxy)hexanoate (82): obtained from **66** in >95% yield; ¹H NMR (300 MHz, CDCl₃) δ: 7.42-7.34 (m, 5H), 5.22 (s, 2H, CH₂Ph), 5.05 (d, J = 3.4, CH-O), 3.67 (dt, 1H, J = 3.4, 9.9, CHN₃), 1.85-1.35 (m, 13 H), 0.95 (t, 3H, J = 7.1, CH₃). ¹³C NMR (75 MHz, CDCl₃) δ: 167.9, 154.2, 134.8, 128.5, 83.3, 77.7, 70.2, 61.4, 31.4, 27.8, 19.4, 13.5.

(2R,3S)-tert-butyl 3-azido-2-(((benzyloxy)carbonyl)oxy)hexanoate (83): obtained from **79** in >95% yield; ¹H NMR (300 MHz, CDCl₃) δ: 7.40-7.36 (m, 5H, Ph), 5.20 (s, 2H, CH₂Ph), 4.96 (d, J = 3.1, CH-O), 3.62 (m, 1H, CHN₃), 1.82-1.35 (m, 13 H), 0.95 (t, 3H, J = 7.1, CH₃). ¹³C NMR (75 MHz, CDCl₃) δ: 167.8, 154.3, 134.8, 128.6, 128.5, 83.3, 77.3, 70.1, 61.7, 31.4, 27.7, 19.4, 13.6.

General procedure for the hydrolysis of t-butyl ester. TFA (3 mL) was added to a solution of the substrate (1 mmol) in CH₂Cl₂ (6 mL) at 0 °C. Then the reaction mixture was allowed to reach the room temperature and stirred for 12 h. The mixture was diluted with CH₂Cl₂, washed with water and brine, dried and concentrated *in vacuo*. The crude material was purified by flash chromatography using CH₂Cl₂/MeOH (90:10-80:20) as eluent.

(2S,3S)-2-azido-3-(((benzyloxy)carbonyl)oxy)hexanoic acid (68): obtained from **67** in 86% yield; ¹H NMR (300 MHz, CDCl₃) δ: 9.04 (bs, 1H, COOH), 7.40-7.36 (m, 5H, Ph), 5.27-5.10 (m, 3H, CH-O and CH₂Ph), 4.38 (d, 1H, J = 3.9, CHN₃), 1.62-1.28 (m, 4H), 0.95 (t, 3H, J = 7.1, CH₃). ¹³C NMR (75 MHz, CDCl₃) δ: 172.0, 154.5, 135.7, 128.6, 77.6, 70.1, 63.8, 31.9, 18.4, 13.6.

(2R,3S)-2-azido-3-(((benzyloxy)carbonyl)oxy)hexanoic acid (81): obtained from **80** in 90% yield; ¹H NMR (300 MHz, CDCl₃) δ: 7.40-7.36 (m, 5H, Ph), 5.24-5.16 (m, 3H, CH-O and CH₂Ph), 3.94 (d, 1H, J = 3.4, CHN₃), 1.83-1.62 (m, 2H), 1.48-1.32 (m, 2H), 0.96 (t, 3H, J = 7.1, CH₃). ¹³C NMR (75 MHz, CDCl₃) δ: 173.2, 154.8, 135.1, 128.8, 77.6, 70.3, 63.4, 33.5, 18.7, 13.9.

(2R,3R)-3-azido-2-(((benzyloxy)carbonyloxy)hexanoic acid (84): obtained from **82** in 88% yield; $^1\text{H NMR}$ (300 MHz, CDCl_3) δ : 10.4, (bs, 1H, COOH), 7.40-7.36 (m, 5H, Ph), 5.25 (s, 2H, CH_2Ph), 5.18 (d, 1H, $J = 3.1$, CH-O), 3.77 (dt, 1H, $J = 3.1, 9.9$, CHN_3), 1.90-1.33 (m, 4H), 0.96 (t, 3H, $J = 7.1$, CH_3). $^{13}\text{C NMR}$ (75 MHz, CDCl_3) δ : 172.9, 154.5, 134.8, 128.9, 77.3, 70.9, 61.8, 31.7, 19.7, 13.8.

(2R,3S)-3-azido-2-(((benzyloxy)carbonyloxy)hexanoic acid (85): obtained from **83** in 85% yield; $^1\text{H NMR}$ (300 MHz, CDCl_3) δ : 7.36 (m, 5H, Ph), 5.24 (s, 2H, CH_2Ph), 5.12 (d, 1H, $J = 3.0$, CH-O), 3.78 (m, 1H, CHN_3), 1.83-1.47 (m, 4H), 0.96 (t, 3H, $J = 7.1$, CH_3). $^{13}\text{C NMR}$ (75 MHz, CDCl_3) δ : 173.1, 154.5, 134.8, 129.2, 129.0, 77.3, 70.8, 62.3, 31.2, 19.7, 13.6.

General procedure for the amidation reaction. A solution of EDC (230 mg, 1.2 mmol) and HOAt (177 mg, 1.3 mmol) in CH_2Cl_2 (5 mL) was added to a solution of the carboxylic acid (1.0 mmol) and amine (1.26 mmol) in CH_2Cl_2 (5 mL) at rt under argon. After 2 hours, the solvent was removed *in vacuo* and the crude material was purified by flash chromatography using hexane/EtOAc (90:10-80:20) as eluent.

(2S,3S)-2-azido-1-oxo-1-(3-triethoxysilylpropylamino)hexan-3-yl benzyl carbonate (70): obtained from **68** and 3-aminopropyltriethoxysilane in 66% yield; $^1\text{H NMR}$ (300 MHz, CDCl_3) δ : 7.40-7.28 (m, 5H, Ph), 6.54 (bs, 1H, NH), 5.30 (m, 1H, CH-O), 5.16 (s, 2H, CH_2Ph), 4.40 (d, 1H, $J = 3.3$, CHN_3), 3.80 (q, 6H, $J = 7.1$, $\text{CH}_2\text{O} \times 3$), 3.22 (q, 2H, $J = 2.2$, CH_2NH), 1.80-1.10 (m, 15H), 0.96 (t, 3H, $J = 7.1$, CH_3), 0.60 (t, 2H, $J = 6.6$, CH_2Si); $^{13}\text{C NMR}$ (75 MHz, CDCl_3) δ : 165.2, 154.4, 135.0, 128.6, 128.2, 78.6, 69.9, 66.2, 58.4, 41.9, 34.3, 27.4, 18.4, 14.7, 13.7, 7.6; IR (neat, cm^{-1}) ν_{max} : 2926, 2854, 2115, 1644, 1594, 1482, 1390, 1296, 1150-1000, 968.

(2S,3S)-1-(allylamino)-2-azido-1-oxohexan-3-yl benzyl carbonate (86): obtained from **68** and ally amine in 74% yield; $^1\text{H NMR}$ (300 MHz, CDCl_3) δ : 7.41-7.26 (m, 5H, Ph), 6.52 (bs, 1H, NH), 5.84-5.64 (m, 1H, CH=), 5.32-5.15 (m, 3H, $\text{CH}_2=$ and CH-O), 4.78 (s, 2H, CH_2Ph), 4.42 (d, 1H, $J = 3.3$, CHN_3), 3.89 (m, 2H, CH_2N), 1.57-1.20 (m, 4H), 0.96 (t, 3H, $J = 7.1$, CH_3). $^{13}\text{C NMR}$ (75 MHz, CDCl_3) δ : 165.2, 154.4, 140.0, 135.0, 128.6, 128.2, 116.9, 77.6, 69.9, 66.4, 41.8, 33.3, 18.4, 13.6.

(2R,3S)-1-(allylamino)-2-azido-1-oxohexan-3-yl benzyl carbonate (87): obtained from **81** and ally amine in 70% yield; $^1\text{H NMR}$ (300 MHz, CDCl_3) δ : 7.37 (m, 5H, Ph), 6.46 (bs, 1H, NH), 5.82-5.69 (m, 1H, CH=), 5.22-5.07 (m, 5H, $\text{CH}_2=$, CH-O and CH_2Ph), 4.12 (m, 1H, CH- N_3),

3.84 (m, 2H, CH₂N), 1.70-1.40 (m, 4H), 0.95 (t, 3H, J = 7.1, CH₃).¹³C NMR (75 MHz, CDCl₃) δ: 165.2, 154.4, 140.0, 135.0, 128.5, 128.2, 116.8, 78.7, 69.9, 66.1, 41.8, 33.3, 18.6, 13.7.

(2R,3R)-1-(allylamino)-3-azido-1-oxohexan-2-yl benzyl carbonate (90): obtained from **84** and ally amine in 73% yield; ¹H NMR (300 MHz, CDCl₃) δ: 7.48 (m, 5H, Ph), 6.38 (bs, 1H, NH), 5.86-5.73 (m, 1H, CH=), 5.28-5.15 (m, 3H, CH₂= and CH-O), 4.70 (s, 2H, CH₂Ph), 4.15 (m, 1H, CH-N₃), 3.84 (m, 2H, CH₂N), 1.75-1.40 (m, 4H), 0.95 (t, 3H, J = 7.1, CH₃).¹³C NMR (75 MHz, CDCl₃) δ: 165.8, 154.4, 140.9, 135.7, 128.9, 127.3, 116.9, 78.6, 70.8, 65.3, 42.2, 31.4, 19.1, 13.6.

(2R,3S)-1-(allylamino)-3-azido-1-oxohexan-2-yl benzyl carbonate (91): obtained from **85** and ally amine in 70% yield; ¹H NMR (300 MHz, CDCl₃) δ: 7.46 (m, 5H, Ph), 6.35 (bs, 1H, NH), 5.75-5.69 (m, 1H, CH=), 5.19-5.07 (m, 5H, CH₂=, CH-O and CH₂Ph), 4.17 (m, 1H, CH-N₃), 3.81 (m, 2H, CH₂N), 1.75-1.40 (m, 4H), 0.96 (t, 3H, J = 7.1, CH₃).¹³C NMR (75 MHz, CDCl₃) δ: 165.8, 154.4, 140.9, 135.7, 128.5, 127.6, 116.9, 78.6, 70.8, 65.3, 42.4, 31.5, 19.5, 13.5.

(2R,3S)-N-allyl-3-propyloxirane-2-carboxamide (99): obtained from **63** and allyl amine in 95% yield; ¹H NMR (300 MHz, CDCl₃) δ: 6.32 (bs, 1H, NH), 5.84-5.62 (m, 1H, CH=), 5.18-4.99 (m, 2H, CH₂=) 3.76 (m, 2H, CH₂NH), 3.14 (d, 1H, J = 1.6, COCH-O), 2.94-2.83 (m, 1H, PrCH-O), 1.68-1.30 (m, 4H), 0.87 (t, J=6.6, CH₃); ¹³C NMR (75 MHz, CDCl₃) δ: 168.6, 133.8, 116.6, 59.5, 55.4, 41.2, 33.8, 19.1, 13.8.

(2R,3S)-N-methyl-3-propyloxirane-2-carboxamide (102): obtained from **63** and methyl amine (2 M solution in THF) in 84% yield. ¹H NMR (300 MHz, CDCl₃) δ: 6.22 (bs, 1H, NH), 3.11 (d, 1H, J = 1.6, COCH-O), 2.94-2.82 (m, 1H, PrCH-O), 2.78 (d, 3H, J = 2.1, CH₃N), 1.68-1.25 (m, 4H), 0.90 (t, J=6.6, CH₃); ¹³C NMR (75 MHz, CDCl₃) δ: 168.9, 59.2, 55.1, 33.8, 26.8, 19.1, 13.8.

(2R,3S)-N-benzyl-3-propyloxirane-2-carboxamide (103): obtained from **63** and benzyl amine in >95% yield. ¹H NMR (300 MHz, CDCl₃) δ: 7.37-7.05 (m, 5H, Ph), 6.35 (bs, 1H, NH), 4.42 (d, 1H, J = 14.5, CH₂H_bPh), 4.39 (d, 1H, J = 14.5, CH_aH_bPh), 3.10 (d, 1H, J = 1.6, COCH-O), 2.93-2.82 (m, 1H, PrCH-O), 1.68-1.26 (m, 4H), 0.90 (t, J=6.6, CH₃); ¹³C NMR (75 MHz, CDCl₃) δ: 168.2, 139.7, 128.4, 128.1, 126.8, 58.6, 55.2, 43.8, 26.4, 19.2, 13.8.

(2R,3S)-N-allyl-3-cyclohexyloxirane-2-carboxamide (104): obtained from **121** and allyl amine in 92% yield. ¹H NMR (300 MHz, CDCl₃) δ: 6.20 (bs, 1H, NH), 5.91-5.69 (m, 1H, CH=), 5.30-5.05 (m, 2H, CH₂=) 3.85 (m, 2H, CH₂NH), 3.28 (d, 1H, J = 1.9, COCH-O), 2.75 (dd, 1H, J =

1.9, 6.1, cyclohexyl-CH-O), 1.88-1.60 (m, 6H), 1.42-1.01 (m, 5H); ^{13}C NMR (75 MHz, CDCl_3) δ : 168.8, 133.9, 116.8, 63.9, 54.5, 41.2, 39.7, 29.2, 28.9, 26.3, 25.7, 25.6.

(2R,3S)-N-allyl-3-phenyloxirane-2-carboxamide (105): obtained from **121a** and allyl amine in 86% yield. ^1H NMR (300 MHz, CDCl_3) δ : 7.41-7.08 (m, 5H, Ph), 6.57 (bs, 1H, NH), 5.88-5.64 (m, 1H, CH=), 5.18-4.97 (m, 2H, CH_2 =), 3.94 (m, 2H, CH_2N), 3.80 (d, 1H, $J = 1.6$, PhCH-O), 3.43 (d, 1H, $J = 1.6$, COCH-O); ^{13}C NMR (75 MHz, CDCl_3) δ : 167.6, 133.7, 131.6, 129.2, 128.8, 128.6, 127.2, 125.9, 116.5, 59.1, 42.6, 41.9.

General procedure for the azido group reduction and the hydroxyl deprotection by catalytic hydrogenation. A solution of the substrate (1 mmol) in AcOEt (2 mL) was hydrogenated at 5 atm over 10% Pd/C (catalytic amount) for 16 h at room temperature. Then the solution was filtered on a celite pad to eliminate the catalyst and concentrated *in vacuo*, affording the desired product.

(2S,3S)-2-amino-3-hydroxy-N-propylhexanamide (88): obtained from **86** in >95% yield; ^1H NMR (300 MHz, CDCl_3) δ : 6.45 (bs, 1H, NH), 3.80 (dt, 1H, $J = 3.1, 6.9$, CHOH), 3.35-3.15 (m, 3H, CHN_3 and CH_2N), 2.40 (bs, 3H, OH and NH_2), 1.50-1.35 (m, 6H), 1.12 (t, 3H, $J = 7.3$), 0.96 (t, 3H, $J = 7.1$). ^{13}C NMR (75 MHz, CDCl_3) δ : 165.2, 72.9, 58.6, 34.6, 33.9, 18.6, 14.6, 13.9.

(2R,3S)-2-amino-3-hydroxy-N-propylhexanamide (89): obtained from **87** in > 95% yield; ^1H NMR (300 MHz, CDCl_3) δ : 6.37 (bs, 1H, NH), 4.05 (m, 1H, CHOH), 3.42 (d, 1H, $J = 6.5$, CHN), 3.19 (m, 2H, CH_2N), 2.70 (bs, 2H, NH_2), 2.12 (bs, 1H, OH), 1.55-1.40 (m, 6H), 0.98 (m, 6H). ^{13}C NMR (75 MHz, CDCl_3) δ : 165.2, 72.1, 58.2, 34.5, 33.9, 18.4, 14.6, 13.7.

(2R,3R)-3-amino-2-hydroxy-N-propylhexanamide (92): obtained from **90** in > 95% yield; ^1H NMR (300 MHz, CDCl_3) δ : 6.39 (bs, 1H, NH), 4.52 (d, 1H, $J = 3.1$, CHOH), 3.31 (m, 1H, CHN), 3.12 (m, 2H, CH_2N), 2.75 (bs, 2H, NH_2), 1.63-1.20 (m, 7H), 0.91 (m, 6H). ^{13}C NMR (75 MHz, CDCl_3) δ : 165.2, 72.9, 56.3, 34.5, 33.1, 19.2, 14.7, 13.8.

(2R,3S)-3-amino-2-hydroxy-N-propylhexanamide (93): obtained from **91** in > 95% yield. ^1H NMR (300 MHz, CDCl_3) δ : 6.90 (bs, 1H, NH), 4.55 (m, 1H, CHOH), 3.27 (m, 1H, CHN), 3.15 (m, 2H, CH_2N), 2.7 (bs, 1H, OH), 1.63-1.20 (m, 6H), 0.91 (m, 6H); ^{13}C NMR (75 MHz, CDCl_3) δ : 165.2, 71.8, 55.3, 35.5, 33.1, 19.2, 18.5, 14.2, 13.8.

General procedure for the N,N-dialkylation reaction. A mixture of the substrate (1.0 mmol), alkyl halide (2.0 mmol), K_2CO_3 (2.0 mol) and CH_3CN (5 mL) was refluxed for 48 h.

The reaction mixture was cooled to room temperature and filtered. The filtrate was concentrated *in vacuo* and the residue was purified by flash chromatography using hexane/EtOAc (70:30-60:40).

(2S,3S)-2-(dipropylamino)-3-hydroxy-N-propylhexanamide (94): obtained from **88** in 50% yield. ¹H NMR (300 MHz, CDCl₃) δ: 7.54 (bs, 1H, NH), 4.42 (bs, 1H, OH), 3.92 (m, 1H, CHOH), 3.28 (m, 2H, CONHCH₂), 3.08 (d, 1H, J = 5.0, CHN), 2.54 (t, 4H, J = 7.7, CH₂N x2), 1.7-1.27 (m, 6H), 1.13 (t, 3H, J = 7.1), 0.99-0.80 (m, 9H).

(2R,3S)-2-(dipropylamino)-3-hydroxy-N-propylhexanamide (95): obtained from **89** in 43% yield. ¹H NMR (300 MHz, CDCl₃) δ: 7.50 (bs, 1H, NH), 4.04 (bs, 1H, OH), 3.90 (m, 1H, CHOH), 3.28 (m, 2H, CONHCH₂), 3.12 (d, 1H, J = 5.0, CHN), 2.55 (t, 4H, J = 7.7, CH₂N x2), 1.7-1.27 (m, 6H), 1.13 (t, 3H, J = 7.1), 0.99-0.81 (m, 9H).

(2R,3R)-3-(dipropylamino)-2-hydroxy-N-propylhexanamide (96): obtained from **92** in 40% yield. ¹H NMR (300 MHz, CDCl₃) δ: 7.31 (bs, 1H, NH), 4.09 (d, 1H, J = 4.4, CHOH), 3.28 (m, 2H, CONHCH₂), 2.55 (t, 4H, J = 7.7, CH₂N x2), 2.11 (m, 1H, CHN), 1.6-0.8 (m, 18H).

General procedure for the regioselective Ti(O-*i*Pr)₄-mediated aminolysis reaction of epoxy amides. A mixture of the 2,3-epoxy amide (1.0 mmol), amine (excess, 1 mL) and Ti(O-*i*Pr) (1.5 mmol) was stirred at the required temperature for 12 h. After this time, EtOAc was added and the organic layer was washed with an aqueous tartaric acid solution (0.5 M), dried and concentrated *in vacuo*. The crude product was purified by flash chromatography (CH₂Cl₂/MeOH, 95:5, 0.2% NH₄OH); see **Table 2-4**.

(2R,3R)-N-allyl-3-(dibutylamino)-2-hydroxyhexanamide (101): obtained from **99** and Bu₂NH in > 95% yield. ¹H NMR (300 MHz, CDCl₃) δ: 7.80 (bs, 1H, NH), 5.85-5.69 (m, 1H, CH=), 5.20-5.04 (m, 2H, CH₂=), 4.59 (bs, 1H, OH), 3.89 (d, 1H, J = 7.1, CHOH), 3.85-3.76 (m, 2H, CH₂NH), 2.81 (m, 1H, CHN), 2.67-2.21 (m, 4H, CH₂N x2), 1.65-1.09 (m, 12H), 0.95-0.80 (m, 9H); ¹³C NMR (75 MHz, CDCl₃) δ: 173.4, 133.9, 116.5, 68.8, 63.6, 51.1, 41.5, 31.4, 27.5, 21.2, 20.5, 13.9.

(2R,3R)-N-allyl-2-hydroxy-3-(piperidin-1-yl)hexanamide (106): obtained from **99** and piperidine in 95% yield. ¹H NMR (300 MHz, CDCl₃) δ: 8.10 (bs, 1H, NH), 5.86-5.67 (m, 1H, CH=), 5.22-5.01 (m, 2H, CH₂=), 4.30 (bs, 1H, OH), 3.88 (d, 1H, J = 7.1, CHOH), 3.84-3.76 (m, 2H, CH₂NH), 2.76-2.54 (m, 3H, CHN and CH₂N), 2.51-2.34 (m, 2H, CH₂N), 1.81-1.11 (m,

10H), 0.83 (t, 3H, J = 7.1); ¹³C NMR (75 MHz, CDCl₃) δ: 173.5, 133.9, 116.1, 68.6, 67.4, 50.5, 41.3, 27.8, 26.5, 24.3, 21.2, 14.1.

(2R,3R)-N-allyl-2-hydroxy-3-morpholinohexanamide (107): obtained from **99** and morpholine in 89% yield. ¹H NMR (300 MHz, CDCl₃) δ: 7.39 (bs, 1H, NH), 5.91-5.74 (m, 1H, CH=), 5.23-5.09 (m, 2H, CH₂=), 4.11 (d, 1H, J = 7.1, CHOH), 3.91-3.86 (m, 2H, CH₂NH), 3.76-3.57 (m, 4H, CH₂O x2), 2.76-2.64 (m, 3H, CHN and CH₂N), 2.63-2.53 (m, 2H, CH₂N), 1.81-1.31 (m, 4H), 0.85 (t, 3H, J = 7.1); ¹³C NMR (75 MHz, CDCl₃) δ: 173.4, 133.8, 116.5, 69.1, 67.4, 66.8, 50.0, 41.5, 27.8, 20.9, 14.2.

(2R,3R)-N-allyl-3-(hexylamino)-2-hydroxyhexanamide (108): obtained from **99** and *n*-hexyl amine in 92% yield. ¹H NMR (300 MHz, CDCl₃) δ: 7.69 (bs, 1H, CONH), 5.85-5.69 (m, 1H, CH=), 5.20-5.04 (m, 2H, CH₂=), 4.21 (bs, 1H, OH), 4.01 (d, 1H, J = 7.2, CHOH), 3.85-3.78 (m, 2H, COCH₂NH), 3.05-2.91 (m, 1H, CHN), 2.67-2.21 (m, 3H, CH₂N and NH), 1.65-1.21 (m, 12H), 0.97-0.85 (m, 6H); ¹³C NMR (75 MHz, CDCl₃) δ: 172.4, 133.9, 116.3, 68.8, 56.8, 53.1, 41.2, 31.2, 27.5, 23.1, 21.2, 20.3, 17.9, 13.9.

(2R,3R)-N-allyl-3-(cyclohexylamino)-2-hydroxyhexanamide (109): obtained from **99** and *c*-hexyl amine in 75% yield. ¹H NMR (300 MHz, CDCl₃) δ: 0.74–2.02 (m, 17 H), 2.51 (m, 1 H, NH), 3.06–3.22 (m, 2 H, CHN and CHN), 3.89 (m, 2 H, CH₂N), 4.04 (m, 1 H, CHOH), 5.06–5.24 (m, 2 H, CH₂=), 5.73–5.87 (m, 1 H, CH=), 7.21 (bs, 1 H, CONH). ¹³C NMR (75 MHz, CDCl₃) δ: 13.9, 19.1, 24.9, 25.0, 31.0, 33.5, 34.3, 41.0, 53.9, 56.4, 71.3, 116.1, 133.9, 172.1.

(2R,3R)-N-allyl-2-hydroxy-3-(phenylamino)hexanamide (110): obtained from **99** and aniline in 88% yield. ¹H NMR (300 MHz, CDCl₃) δ: 0.87 (t, 3H, J = 7.1), 1.24–1.57 (m, 4 H), 3.72–3.99 (m, 4 H, CHN, CH₂NH and NH), 4.28 (d, J = 1.6 Hz, CHOH), 5.04–5.27 (m, 2 H, CH₂=), 5.66–5.88 (m, 1 H, CH=), 6.57–6.78 (m, 3 H, Ph), 7.00 (bs, 1 H, CONH), 7.07–7.21 (m, 3 H, Ph). ¹³C NMR (75 MHz, CDCl₃) δ: 14.2, 19.7, 31.6, 33.9, 41.3, 41.6, 55.5, 72.3, 113.8, 116.8, 117.5, 129.6, 133.9, 147.3, 172.7.

(2R,3R)-3-(dibutylamino)-2-hydroxy-N-methylhexanamide (111): obtained from **102** and Bu₂NH in >95% yield. ¹H NMR (300 MHz, CDCl₃) δ: 6.09 (bs, 1H, NH), 3.91 (d, 1H, J = 7.2, CHOH), 2.82 (m, 1H, CHN), 2.79 (d, 3H, J = 3.1, CH₃NH), 2.65-2.20 (m, 4H, CH₂N x2), 1.65-1.21 (m, 12H), 0.90 (m, 9H); ¹³C NMR (75 MHz, CDCl₃) δ: 173.4, 68.8, 63.6, 51.5, 31.4, 27.4, 25.7, 21.1, 20.4, 13.9.

(2R,3R)-N-benzyl-3-(dibutylamino)-2-hydroxyhexanamide (112): obtained from **103** and Bu₂NH in 93% yield. ¹H NMR (300 MHz, CDCl₃) δ: 7.37-7.05 (m, 5H, Ph), 6.39 (bs, 1H, NH), 4.62 (bs, 1H, OH), 4.42 (d, 1H, J = 14.5, CH₂H_bPh), 4.39 (d, 1H, J = 14.5, CH₂H_bPh), 3.91 (d, 1H, J = 7.1, CHOH), 2.78 (m, 1H, CHN), 2.65-2.23 (m, 4H, CH₂N x2), 1.67-1.15 (m, 12H), 0.88 (m, 9H); ¹³C NMR (75 MHz, CDCl₃) δ: 168.2, 139.7, 128.5, 128.1, 126.8, 68.8, 63.6, 55.4, 40.8, 31.4, 27.5, 21.2, 20.5, 13.9.

(2R,3R)-N-allyl-3-cyclohexyl-3-(dipropylamino)-2-hydroxypropanamide (113): obtained from **104** and Pr₂NH in >95% yield; ¹H NMR (300 MHz, CDCl₃) δ: 7.31 (bs, 1H, NH), 5.91-5.68 (m, 1H, CH=), 5.32-5.03 (m, 2H, CH₂=), 4.11 (d, 1H, J = 4.4, CHOH), 3.82 (m, 2H, CH₂NH), 2.79-2.33 (m, 5H, CHN and CH₂N x2), 2.20 (bs, 1H, OH), 1.97-0.83 (m, 15H), 0.81 (t, 6H, J = 7.1); ¹³C NMR (75 MHz, CDCl₃) δ: 173.5, 134.2, 116.9, 71.4, 67.7, 55.4, 41.7, 37.6, 31.0, 26.8, 26.4, 26.1, 23.9, 11.7.

(2R,3R)-N-allyl-3-cyclohexyl-3-(dibutylamino)-2-hydroxypropanamide (115): obtained from **104** and Bu₂NH in >95% yield; ¹H NMR (300 MHz, CDCl₃) δ: 7.33 (bs, 1H, NH), 5.92-5.68 (m, 1H, CH=), 5.21-5.06 (m, 2H, CH₂=), 4.83 (bs, 1H, OH), 4.12 (m, 1H, CHOH), 3.86 (m, 2H, CH₂NH), 2.74-2.33 (m, 4H, CH₂N x2), 2.31 (m, 1H, CHN), 1.96-0.85 (m, 19H), 0.82 (t, 6H, J = 7.1); ¹³C NMR (75 MHz, CDCl₃) δ: 173.4, 134.1, 116.9, 70.9, 67.7, 53.1, 41.6, 37.5, 32.8, 30.9, 26.7, 26.4, 26.2, 20.6, 14.2.

(2R,3R)-N-allyl-3-cyclohexyl-2-hydroxy-3-(piperidin-1-yl)propanamide (116): obtained from **104** and piperidine in >95% yield; ¹H NMR (300 MHz, CDCl₃) δ: 7.67 (bs, 1H, NH), 5.93-5.62 (m, 1H, CH=), 5.36-4.85 (m, 2H, CH₂=), 4.57 (bs, 1H, OH), 4.03 (d, 1H, J = 6.0, CHOH), 3.93-3.59 (m, 2H, CH₂NH), 2.91-2.18 (m, 5H, CHN and CH₂N x2), 2.18-0.63 (m, 17H). ¹³C NMR (75 MHz, CDCl₃) δ: 173.8, 134.3, 116.6, 73.9, 67.4, 51.7, 41.6, 36.9, 33.0, 36.6, 27.3, 26.6, 26.2, 24.7.

(2R,3R)-N-allyl-3-cyclohexyl-2-hydroxy-3-morpholinopropanamide (117): obtained from **104** and morpholine in 87% yield; ¹H NMR (300 MHz, CDCl₃) δ: 7.41 (bs, 1H, NH), 5.87-5.65 (m, 1H, CH=), 5.24-5.02 (m, 2H, CH₂=), 4.15 (d, 1H, J = 4.3, CHOH), 3.96-3.74 (m, 2H, COCH₂NH), 3.69-3.44 (m, 4H, CH₂O x2), 2.75-2.57 (m, 4H, CH₂N x2), 2.53 (dd, 1H, J = 4.3, 9.0, CHN), 2.12-1.78 (m, 3H), 1.76-1.44 (m, 3H), 1.36-0.80 (m, 5H); ¹³C NMR (75 MHz, CDCl₃) δ: 173.8, 134.1, 116.8, 75.0, 67.9, 50.8, 41.6, 36.4, 32.6, 30.5, 26.6, 26.3, 26.2.

(2R,3R)-N-allyl-3-(benzylamino)-3-cyclohexyl-2-hydroxypropanamide (118): obtained from **104** and benzyl amine in 85% yield; ^1H NMR (300 MHz, CDCl_3) δ : 0.84–1.97 (m, 13 H), 3.17 (m, 1 H, CHN), 3.76–4.12 (m, 4 H, CH_2NH and CH_2Ph), 4.65 (d, 1H, $J = 5.6$ Hz, CHOH), 5.05–5.33 (m, 2 H, $\text{CH}_2=$), 5.76–5.94 (m, 1 H, $\text{CH}=\text{}$), 6.76 (bs, 1 H, NH), 7.08–7.68 (m, 5 H, Ph). ^{13}C NMR (75.4 MHz, CDCl_3) δ : 26.0, 26.2, 28.4, 29.5, 30.2, 41.3, 47.1, 51.4, 63.9, 70.2, 116.3, 126.8, 128.1, 128.4, 130.6, 134.3, 175.0.

(2R,3R)-N-allyl-3-(dibutylamino)-2-hydroxy-3-phenylpropanamide (119): obtained from **105** and Bu_2NH in >95% yield. ^1H NMR (300 MHz, CDCl_3) δ : 7.69 (bs, 1H, NH), 7.30-7.12 (m, 5H, Ph), 5.56-5.37 (m, 1H, $\text{CH}=\text{}$), 4.99-4.82 (m, 2H, $\text{CH}_2=$), 4.44 (d, 1H, $J = 7.1$, CHOH), 3.91 (d, 1H, $J = 7.1$, CHN), 3.78-3.49 (m, 2H, CH_2NH), 2.63-2.44 (m, 2H, CH_2N), 2.37-2.17 (m, 2H, CH_2N), 1.48-1.05 (m, 8H), 0.81 (t, 6H, $J = 7.1$); ^{13}C NMR (75 MHz, CDCl_3) δ : 172.4, 134.1, 129.8, 128.6, 128.0, 116.5, 69.5, 67.7, 50.0, 41.6, 29.2, 20.8, 14.1.

(2R,3R)-N-allyl-2-hydroxy-3-phenyl-3-(piperidin-1-yl)propanamide (120): obtained from **105** and piperidine in >95% yield. ^1H NMR (300 MHz, CDCl_3) δ : 7.89 (bs, 1H, NH), 7.48-6.95 (m, 5H, Ph), 5.66-5.40 (m, 1H, $\text{CH}=\text{}$), 5.08-4.77 (m, 2H, $\text{CH}_2=$), 4.58 (d, 1H, $J = 7.1$, CHOH), 4.10 (bs, 1H, OH), 3.80-3.41 (m, 3H, CHN and COCH_2NH), 2.64-2.08 (m, 4H, $\text{CH}_2\text{N} \times 2$), 1.78-0.99 (m, 6H); ^{13}C NMR (75 MHz, CDCl_3) δ : 172.4, 133.9, 129.3, 127.8, 127.7, 116.5, 71.5, 68.3, 51.4, 41.3, 26.3, 26.2, 24.2.

(2R,3S)-3-cyclohexyl-N-(3-(triethoxysilyl)propyl)oxirane-2-carboxamide (122): obtained from **121** and 3-aminopropyltriethoxysilane, using the general procedure described for the amidation reaction, in 76% yield. ^1H NMR (300 MHz, CDCl_3) δ : 6.28 (bs, 1H, NH), 3.77 (q, 6H, $J = 7.1$, $\text{CH}_2\text{O} \times 3$), 3.26-3.12 (m, 3H, O-CH-CO and CH_2NH), 2.70 (dd, 1H, $J = 6.0, 2.2$, ι -Hex-CH-O) 1.90-1.45 (m, 13H), 1.17 (t, 9H, $J = 7.1$, $\text{CH}_3 \times 3$), 0.55 (t, 2H, $J = 7.7$, CH_2Si); ^{13}C NMR (75 MHz, CDCl_3) δ : 165.2, 58.5, 55.19, 41.8, 39.9, 29.5, 28.7, 26.3, 25.5, 22.7, 18.2, 7.7; IR (CDCl_3 , cm^{-1}) ν_{max} : 2975, 2927, 1654, 1640, 1528, 1383, 1260, 1150-1000, 968, 724, 695.

(2R,3R)-3-cyclohexyl-3-(dibutylamino)-2-hydroxy-N-propylpropanamide (125). A solution of **115** (100 mg, 0.30 mmol) in MeOH (1 mL) was hydrogenated at atmospheric pressure over 10% of palladium on carbon for 12 hours at room temperature; then the solution was filtered on a Celite pad and concentrated *in vacuo* affording 95 mg (> 95%) of **125**. ^1H NMR (300 MHz, CDCl_3) δ 0.69-0.83 (m, 9H, $\text{CH}_3 \times 3$), 0.85-1.97 (m, 21H); 2.22-2.67 (m, 4H, $\text{CH}_2\text{N} \times 2$); 2.86 (m, 2H, CHN and OH); 3.05-3.31 (m, 2H, CONHCH_2), 3.75 (d, 1H, $J = 6.9$, CHOH); 7.71 (bs, 1H, NH). ^{13}C NMR (75 MHz, CDCl_3) δ 13.9, 14.0, 14.4, 20.6, 21.2, 22.8, 27.4, 31.2, 40.8, 51.1, 63.7.

(1R,2S)-1-cyclohexyl-1-(dibutylamino)-3-(propylamino)propan-2-ol (126). To a solution of compound **125** (143 mg, 0.42 mmol) in THF (0.5 mL), borane-tetrahydrofuran complex (1.0 M solution in THF, 0.84 mmol) was added dropwise at 0 °C under an argon atmosphere. The reaction mixture was refluxed for 12 hours. The reaction was quenched by addition of 6 M HCl aqueous solution at 0 °C. Then the solvent was concentrated *in vacuo* and 25% NaOH aqueous solution was added to the residue. The aqueous layer was extracted with diethyl ether and the combined organic extracts were washed with brine and dried. The solvent was removed *in vacuo* and the crude product was purified by flash chromatography using hexane/EtOAc (80:20-60:40), affording 56 mg (43%) of **126**; ¹H NMR (300 MHz, CDCl₃) δ: 0.69-0.83 (m, 9H, CH₃ x3), 0.86-1.97 (m, 21H); 2.07-2.86 (m, 8H, CH₂N x2, CH₂NH, NCH₂CHOH); 2.96 (m, 1H, CHN), 3.74 (ddd, 1H, J = 9.7, 7.4, 2.8, CHOH); ¹³C NMR (300 MHz, CDCl₃) δ 13.9, 14.0, 14.4, 20.6, 21.2, 22.8, 27.4, 31.74; 50.66; 51.57; 52.89; 63.69; 69.3.

(2R,3S)-3-cyclohexyloxirane-2-carbaldehyde (129). To a solution of epoxy alcohol **121** (10 mmol) in CH₂Cl₂ (75 mL), Et₃N (5.6 ml, 40 mmol) was added and the mixture was then stirred at 0° C. After 10 min, a solution of pyridine-SO₃ (4.77 g, 30 mmol) in DMSO (30 mL) was added to the reaction mixture. After 2 h, the mixture was diluted with 200 mL of Et₂O and 410 mL of hexane and washed with aq. NaHCO₃ (190 mL). The combined organic layers were washed with 1 M NaH₂PO₄ and brine, and then dried and concentrated *in vacuo*, affording 1.34 g (88%) of **129**.

(E)-3-((2S,3S)-3-cyclohexyloxiran-2-yl)acrylic acid (128). A solution of aldehyde **129** (438 mg, 2.84 mmol) in THF (8.0 mL) was added dropwise to a stirred solution of *n*-BuLi (4.26 mL of a 1.6 M hexane solution, 6.82 mmol) and diethylphosphonoacetic acid (0.50 mL, 3.12 mmol) in THF (21 mL) under an argon atmosphere at -70°C. After 2 hours the reaction mixture was allowed to reach the room temperature and then stirred for 12 hours. HCl aqueous solution (0.1 M, 100 mL) was added to the reaction mixture and the aqueous layer was extracted several times with Et₂O. The combined organic extracts were dried and concentrated *in vacuo*. The crude product was purified by flash chromatography using CH₂Cl₂/MeOH (90:10), affording **128** in 75% yield; ¹H NMR (300 MHz, CDCl₃) δ: 11.12 (bs, 1H, OH), 6.75 (dd, 1H, J = 6.7, 15.6, CH=), 6.07 (d, 1H, J = 15.6, CHCOOH), 3.27 (dd, 1H, J = 6.7, 1.5, O-CHCH=), 2.69 (dd, 1H, J = 1.5, 6.7, *c*-Hex-CH-O), 2.19-0.96 (m, 11H); ¹³C NMR (300 MHz, CDCl₃) δ 170.7, 147.4, 122.3, 65.6, 54.7, 31.2, 29.2, 28.5, 25.3.

(E)-N-allyl-3-((2S,3S)-3-cyclohexyloxiran-2-yl)acrylamide (130): obtained from **128** and allyl amine, using the general procedure previously described for amidation reaction, in 72% yield; ¹H NMR (300 MHz, CDCl₃) δ: 6.67 (m, 1H, CH₂CH=), 6.26 (d, 1H, J = 3.4, COCH=), 5.86-5.64

(m, 2H, CHCH= and NH), 5.14 (m, 2H, CH₂=), 3.96-3.72 (m, 2H, CH₂N), 3.23 (dd, 1H, J = 1.4, 0.4, O-CHCH=), 2.63 (m, 1H, *ε*-Hex-CH-O), 2.03-0.85 (m, 11H); ¹³C NMR (300 MHz, CDCl₃) δ 164.9, 141.1, 134.0, 125.2, 116.7, 66.2, 55.4, 42.1, 29.6, 28.9, 26.3, 25.7.

(4R,5S,E)-N-allyl-5-cyclohexyl-4-(dibutylamino)-5-hydroxypent-2-enamide (131): compound **130** (160 mg, 0.67 mmol), LiClO₄ (1.10 g, 10.4 mmol), and Bu₂NH (1.30 mL, 6.7 mmol) in acetonitrile (2.0 mL) were stirred at 55 °C for 24 h. The workup was identical to the one described for **31** to give 236 mg (>95%) of **131** after chromatography using CH₂Cl₂/MeOH (95:5) as eluent; [α]²⁵_D = -12.3 (c=3.6 in CHCl₃); ¹H NMR (300 MHz, CDCl₃) δ: 6.71 (dd, 1H, J = 15.9, 9.9 O-CHCH=), 6.11 (bs, 1H, NH), 5.91 (d, 1H, J = 15.4, COCH=), 5.81 (m, 1H, CH₂CH=), 5.16 (m, 2H, CH₂=), 3.91 (m, 2H, CH₂NH), 3.42 (m, 1H, CHOH), 3.12 (m, 1H, CHN), 2.85 (bs, 1H, OH), 2.55-2.28 (m, 4H, CH₂N x2), 1.88-0.93 (m, 19H), 0.85 (t, 6H, J = 7.1, CH₃x2); ¹³C NMR (300 MHz, CDCl₃) δ 165.1, 140.5, 134.0, 127.3, 116.4, 74.4, 64.6, 50.41, 41.9, 38.9, 29.7, 29.2, 27.5, 26.4, 26.1, 25.8, 20.3, 13.9.

(E)-3-((2S,3S)-3-cyclohexyloxiran-2-yl)-N-(3-(triethoxysilyl)propyl)acrylamide (132): obtained from **128** and 3-aminopropyltriethoxysilane, using the general procedure previously described for amidation reaction, in 57% yield; ¹H NMR (300 MHz, CDCl₃) δ: 6.56 (dd, 1H, J = 14.8, 6.6, O-CHCH=), 6.18 (bs, 1H, NH), 6.03 (d, 1H, J = 14.8, COCH=), 3.76 (q, 6H, J = 7.1, OCH₂ x3), 3.23 (m, 2H, =CHCH-O and CH₂NH), 2.63 (m, 1H, *ε*-Hex-CH-O), 1.85-1.50 (m, 13H), 1.17 (t, 9H, J = 7.1, CH₃ x3), 0.59 (t, 2H, J = 7.7, CH₂Si); ¹³C NMR (300 MHz, CDCl₃) δ 164.7, 140.2, 125.5, 65.8, 58.3, 55.19, 41.8, 39.9, 29.4, 28.7, 26.0, 25.5, 25.3, 22.7, 18.2, 7.7; IR (CDCl₃, cm⁻¹) ν_{max}: 3035, 2935, 2395, 1676, 1643, 1536, 1428, 1251, 1229, 1205, 1150-1000, 930, 824, 704.

2.6.4 Evaluation of free ligands in the enantioselective addition of diethylzinc to benzaldehyde

To a solution of the chiral amino alcohol (0.06 mmol, 6 mol %) in hexane or toluene (2 mL) the benzaldehyde (1 mmol) was added at room temperature. The mixture was stirred for 20 min and then cooled to 0 °C. Diethylzinc (2.5 mL of a 1.0 M hexanes solution, 2.5 mmol) was added dropwise. Then the reaction mixture was allowed to reach the room temperature and stirred for the corresponding reaction time under argon. The reaction was quenched by the addition of a saturated NH₄Cl solution (10 mL). The mixture was then extracted with CH₂Cl₂. The combined organic extracts were dried and concentrated *in vacuo*. The crude product was purified by flash

chromatography using hexane/EtOAc (90:10) as eluent. Enantiomeric excesses were determined by measurement of the optical rotation and comparison with the reported value for (*S*)-1-phenylpropanol ($[\alpha]_{\text{D}} = -40.74$ ($c = 5.2$, CHCl_3) for 90% ee).¹⁴²

2.6.5 Functionalization of magnetite nanoparticles

General procedure for alkoxy silane loading onto magnetite nanoparticles. Oleic acid-coated magnetite nanoparticles (100 mg) were dispersed in toluene (20 mL) and the alkoxy silane (0.1 mmol) was then added. This mixture was refluxed for 4 days under an argon atmosphere. Dry EtOH was added and the reaction vessel was placed in proximity of an external magnet until the solution became clear. The solution was then separated from the nanoparticles, which were washed several times with toluene and acetone and dried *in vacuo*. Siloxane loading was determined by elemental analysis.

Magnetite nanoparticles functionalized with (2*S*,3*S*)-2-azido-1-oxo-1-(3-triethoxysilylpropylamino)hexan-3-yl benzyl carbonate 70 (71): elemental analysis revealed a 1.73 weight% content of N corresponding to a loading of 0.31 mmol/g. IR (KBr/cm⁻¹) ν_{max} : 2930, 2114, 1720, 1640, 1527, 1480, 1387, 1228, 1120-1030, 938, 583.

Magnetite nanoparticles functionalized with (2*R*,3*S*)-3-cyclohexyl-N-(3-(triethoxysilyl)propyl)oxirane-2-carboxamide 122 (123): elemental analysis revealed a 0.63 weight% content of N corresponding to a loading of 0.46 mmol/g. IR (KBr/cm⁻¹) ν_{max} : 2923, 2851, 1718, 1652, 1528, 1383, 1260, 1098, 1024, 867, 639, 576.

Magnetite nanoparticles functionalized with (E)-3-((2*S*,3*S*)-3-cyclohexyloxiran-2-yl)-N-(3-(triethoxysilyl)propyl)acrylamide 132 (133): elemental analysis revealed a 0.54 weight% content of N corresponding to a loading of 0.39 mmol/g. IR (KBr/cm⁻¹) ν_{max} : 2925, 2390, 1670, 1535, 1428, 1228, 1150-1000, 580.

Magnetite nanoparticle-supported amino alcohol ligand 124: 50 mg of functionalized nanoparticles **123** were easily dispersed in 1 mL of Bu₂NH and Ti(O-*i*Pr) (15 μL , 0.05 mmol) was added. The reaction mixture was stirred at room temperature for 72 h under an argon atmosphere. Then MeOH was added and the reaction vessel was placed in the proximity of an external magnet until the solution became clear. The nanoparticles were separated from the

¹⁴² See ref. 22.

solution, washed several times with MeOH and acetone and dried *in vacuo*. Nitrogen elemental analysis: 1.27%. IR (KBr/cm⁻¹) ν_{\max} : 2927, 2852, 1718, 1652, 1555, 1465, 1383, 1264, 1191, 1098, 1024, 574.

Magnetite nanoparticle-supported amino alcohol ligand 134: 100 mg of functionalized nanoparticles **133** were dispersed in acetonitrile (2 mL) and LiClO₄ (63 mg, 0.60 mmol) and Bu₂NH (66 μ L, 0.39 mmol) were added. The reaction mixture was stirred at 55 °C under an argon atmosphere for 24 h. Then MeOH was added and the reaction vessel was placed in the proximity of an external magnet until the solution became clear. The nanoparticles were separated from the solution, washed several times with acetonitrile, MeOH and acetone and dried *in vacuo*. Nitrogen elemental analysis: 1.04%. IR (KBr/cm⁻¹) ν_{\max} : 2925, 2390, 1670, 1535, 1465, 1230, 1150-1000, 580.

2.6.6 Evaluation of MNP-supported ligands in the enantioselective addition of diethylzinc to benzaldehyde

The catalyst-loaded nanoparticles (6 mol%) were dispersed in toluene (2 mL) and the benzaldehyde (1 mmol) was added at room temperature. The mixture was stirred for 20 min and then cooled to 0 °C. Diethylzinc (2.5 mL of a 1.0 M hexanes solution, 2.5 mmol) was added dropwise. Then the reaction mixture was allowed to reach the room temperature and stirred for the corresponding reaction time under argon. The reaction was quenched by the addition of a saturated NH₄Cl solution (10 mL). The reaction vessel was placed over an external magnet until the reaction mixture became transparent. The solution was separated from the nanoparticles and then extracted with CH₂Cl₂. The combined organic extracts were dried and concentrated *in vacuo*. The crude product was purified by flash chromatography using hexane/EtOAc (90:10) as eluent. Enantiomeric excesses were determined by measurement of the optical rotation and comparison with the reported value for (*S*)-1-phenylpropanol ($[\alpha]_D = -40.74$ (c=5.2, CHCl₃) for 90% ee).¹⁴³

¹⁴³ See ref. 22

3 Magnetic nanoparticle-supported N-heterocyclic carbene catalysts

3.1 Introduction

During my third year of PhD I spent six months in the laboratory of Professor Stephen Connon, at the School of Chemistry, University of Dublin Trinity College. His group is interested mainly in the development of new organocatalysts and new methodologies of high synthetic utility; in particular N-heterocyclic carbene catalysis, which involves *umpolung* intermediates, is one of the key research topics.¹⁴⁴ Recently, in collaboration with Professor Y. Gun'ko, they have also attached organocatalysts (DMAP analogues and cinchona alkaloid derivatives) to magnetic nanoparticles, as mentioned in Chapter 1.^{145,146} In this context, I focused my work on the synthesis of magnetic nanoparticle-supported N-heterocyclic carbenes and their evaluation as recyclable catalysts in the oxidative esterification reaction of aldehydes.

3.1.1 N-Heterocyclic carbenes as organocatalysts: oxidative esterification of aldehydes

N-heterocyclic carbenes (Figure 3-1) are by far the most studied members of the family of nucleophilic carbenes.¹⁴⁷

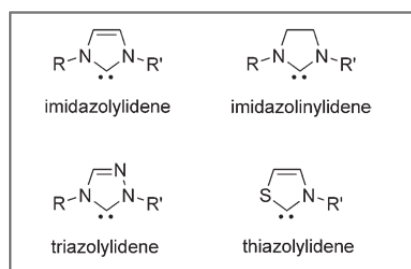


Figure 3-1 General structures of N-heterocyclic carbenes.

¹⁴⁴ a) Rose, C. A.; Gundala, S.; Fagan, C. L.; Franz, J. F.; Connon, S. J.; Zeitler, K. *Chem. Sci.* **2012**, *3*, 735. b) Rose, C. A.; Gundala, S.; Zeitler, K.; Connon, S. J.; *Synthesis* **2011**, 190. c) O'Toole, S. E.; Rose, C. A.; Gundala, S.; Zeitler, K.; Connon, S. J.; *J. Org. Chem.* **2011**, *76*, 347. d) Baragwanath, L.; Rose, C. A.; Zeitler, K.; Connon, S. J.; *J. Org. Chem.* **2009**, *74*, 9214. e) O'Toole, S. E., Connon, S. J. *Org. Biomol. Chem.* **2009**, *7*, 3584. f) Noonan, C.; Baragwanath, L.; Connon, S. J.; *Tetrahedron Lett.* **2008**, *49*, 4003.

¹⁴⁵ Dálaigh, C. O.; Corr, S. A.; Gun'ko, Y.; Connon, S. J.; *Angew. Chem. Int. Ed.* **2007**, *46*, 4329.

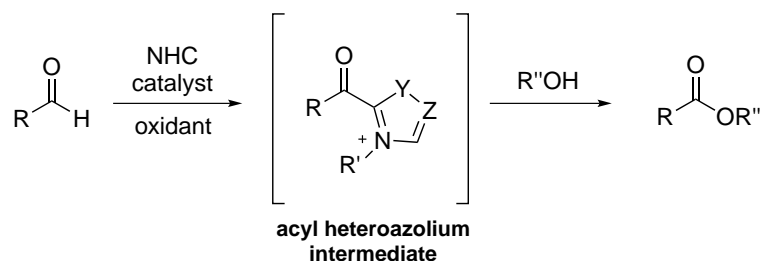
¹⁴⁶ See section 1.3.1 and ref. 82, 86.

¹⁴⁷ a) Bourissou, D.; Guerret, O.; Gabba, F. P.; Bertrand, G.; *Chem. Rev.* **2000**, *100*, 39. b) Herrmann, W. A.; *Angew. Chem.* **2002**, *114*, 1342; *Angew. Chem. Int. Ed.* **2002**, *41*, 1290. c) Diez-Gonzalez, S.; Nolan, S. P.; *Coord. Chem. Rev.* **2007**, *251*, 874.

They are generally known as excellent ligands for metal-based catalysis, but there is also increasing interest in the role of nucleophilic carbenes as organocatalysts. In fact metal-free catalyzed processes are often more economical and environmentally friendly. N-heterocyclic carbenes (NHCs) have been studied for their ability to promote primarily the benzoin condensation;¹⁴⁸ however, in the last few years it has been reported a tremendous increase of their scope.¹⁴⁹

A very attractive methodology is the oxidative transformation of alcohols or aldehydes to esters under mild conditions using NHC catalysts. The addition of the NHC catalyst to aldehydes in the presence of a suitable oxidant gives the acyl azolium intermediates, which are capable of transferring their acyl group to an alcohol nucleophile to produce the corresponding esters (Scheme 3-1). A number of oxidants, such as MnO₂ and organic electron acceptors, have been used to carry out the aldehyde to ester conversion.

This strategy of accessing to activated acylating agents allows streamlining synthetic routes and has potential applications with nucleophiles that undergo fast background reactions with acid chlorides or anhydrides.



Scheme 3-1 NHC-catalyzed oxidative esterification of aldehydes.

NHCs derived from thiazolium ions have been shown to catalyze the oxidative esterification of aldehydes with simple alcohols.¹⁵⁰ The proposed mechanism is shown in Scheme 3-2: deprotonation of thiazolium salt **A** gives rise to carbene **B**, the addition of which to benzaldehyde gives the Breslow intermediate **C**.¹⁵¹ In the presence of a suitable oxidant, **C** can be diverted from the benzoin condensation pathway through the formation of 2-benzoyl thiazolium

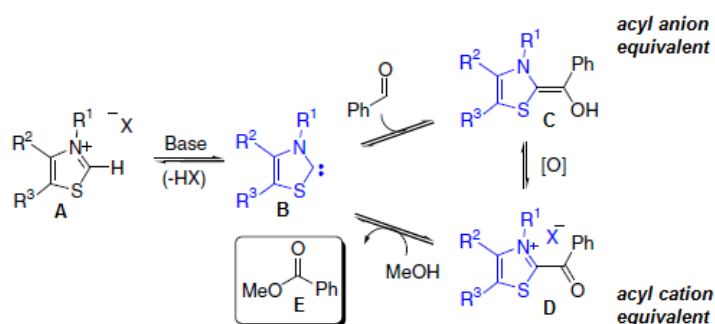
¹⁴⁸ Enders, D.; Balensiefer, T.; *Acc. Chem. Res.* **2004**, *37*, 534.

¹⁴⁹ Marion, N.; Diez-Gonzalez, S.; Nolan, S. P. *Angew. Chem. Int. Ed.* **2007**, *46*, 2988.

¹⁵⁰ Kluger, R. *Chem. Rev.* **1987**, *87*, 863.

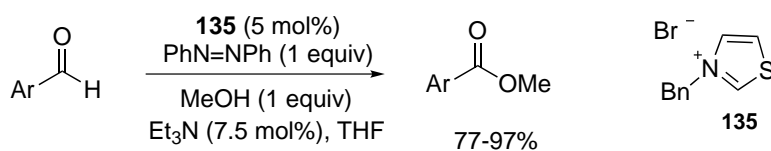
¹⁵¹ (a) Breslow, R. J. *Am. Chem. Soc.* 1957, *79*, 1762; (b) Breslow, R. J. *Am. Chem. Soc.* **1958**, *80*, 3719.

ion **D** which is capable of transferring its acyl group to an alcohol nucleophile to give the ester **E** and regenerate the catalyst.



Scheme 3-2 Proposed mechanism of nucleophilic carbene-catalyzed aldehyde esterification.

Connon *et al.*¹⁵² have reported the first synthetically useful protocol for the oxidative esterification of aromatic aldehydes with equimolar amounts of primary and secondary alcohols catalyzed by N-heterocyclic carbenes. Thiazolium precatalysts **135** proved superior to the triazolium analogues and can be employed at low loadings (5 mol%), in the presence of catalytic amounts of Et₃N and azobenzene as the stoichiometric oxidant at room temperature (Scheme 3-3).



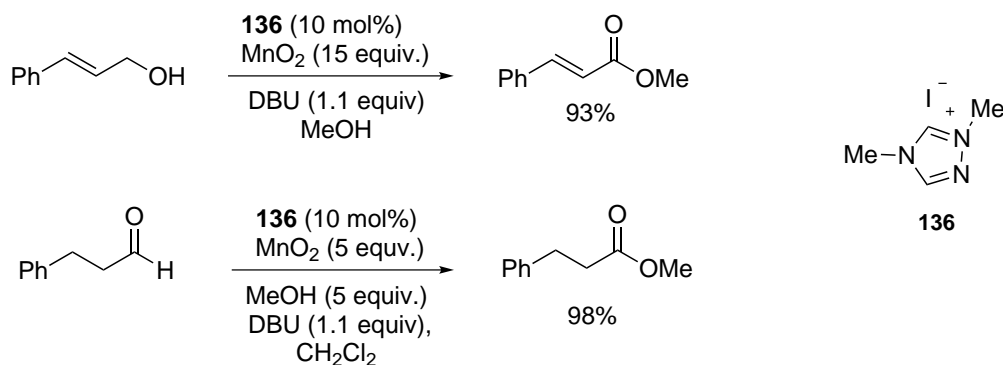
Scheme 3-3 Protocol developed by Connon *et al.*

Scheidt and coworkers have reported that NHCs catalyze the oxidation of allylic and benzylic alcohols as well as saturated aldehydes to esters in excellent yields with manganese (IV) oxide as the oxidant.¹⁵³ The oxidation proceeds under mild conditions, with 10% loading of the simple triazolium salt precatalyst **136** in the presence of 1,8-diazabicycloundec-7-ene (DBU) as base (Scheme 3-4). It has been proven that substrates containing potentially epimerizable centers are oxidized while preserving stereochemical integrity.

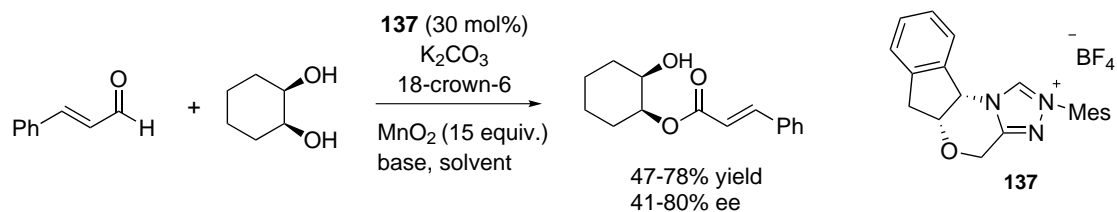
¹⁵² See ref. 144 f.

¹⁵³ a) Maki, B.E.; Chan, A.; Phillips, E. M.; Scheidt, K. A.; *Org. Lett.* **2007**, *9*, 371. b) Maki, B.E.; Scheidt, K.A.; *Org. Lett.* **2008**, *10*, 4331.

Importantly, the acyl heteroazolium intermediate presents the opportunity to create a chiral environment around the activated carbonyl, lending this method to asymmetric applications; for example the chiral triazolium **137** was employed in the desymmetrization of *meso*-diols (Scheme 3-5).



Scheme 3-4 Protocol developed by Scheidt *et al.*



Scheme 3-5 Desymmetrization of *cis*-1,2-cyclohexane diol.

3.2 Results and discussion

Initially, we were intrigued by the possibility of attaching an appropriate heteroazolium salt to cobalt ferrite-manganese dioxide core-shell nanoparticles ($\text{CoFe}_2\text{O}_4@\text{MnO}_2$), to obtain a recyclable, multifunctional “nanosystem” **138** where (Figure 3-2):

- * theazolium salt is able to generate an efficient NHC catalyst
- * the MnO_2 shell acts as the oxidant in the oxidative esterification of aldehydes,
- * the magnetic core, consisting of cobalt ferrite, allows the easy separation from the reaction mixture.

In this way, for the first time, both the organocatalyst and the oxidant could be easily recovered applying an external magnetic field. Furthermore, it was conceivable that the high spatial proximity, between the oxidant and the catalyst on the surface, could have a beneficial effect on the reaction.

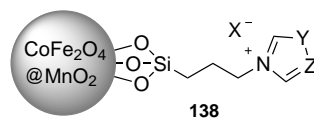
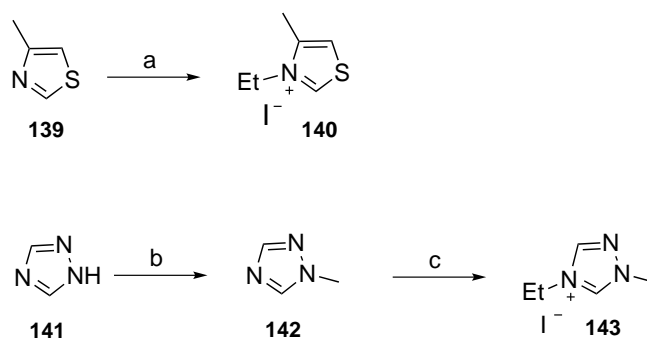


Figure 3-2 Heteroazolium salt (precatalyst) supported onto $\text{CoFe}_2\text{O}_4@\text{MnO}_2$ NPs.

As is typical for all the metal oxides,¹⁵⁴ MnO_2 surface presents a large number of hydroxyl groups that are suitable for the supporting of the catalyst by means of covalent Si-O bonds; therefore it seemed appropriate to introduce in the azolium structure an alkoxy silane group to be exploited for the immobilization on the nanoparticles. $\text{CoFe}_2\text{O}_4@\text{MnO}_2$ nanoparticles (about 120 nm-sized)¹⁵⁵ were prepared and characterized by the group of Professor Y. Gun'ko (School of Chemistry, University of Dublin Trinity College).

3.2.1 Preliminary studies

At first the azolium salts **140** and **143** were synthesized and tested as homogeneous catalysts in the oxidative esterification of benzaldehyde with methanol, using MnO_2 as the oxidant, in order to optimize the reaction conditions and select the best catalyst to support on nanoparticles.



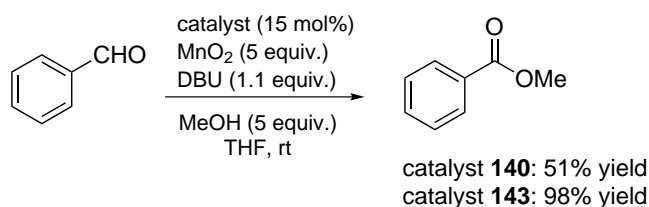
Scheme 3-6 Reagents and conditions: a) EtI (neat), 70 °C, 53% b) 1. NaOMe, MeOH, 56 °C, 2. MeI, reflux; 31% c) EtI (neat), 50 °C, 35%.

¹⁵⁴ Mc Cafferty, E.; Wightman, J. P.; *Surf. Interface Anal.* **1998**, *26*, 549.

¹⁵⁵ The cobalt ferrite core was about 100 nm-sized, thickness of the MnO_2 shell was about 20 nm.

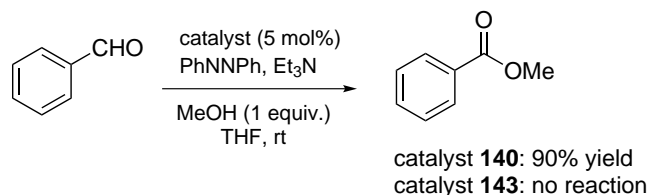
The commercially available 4-methylthiazole **139** was reacted with an excess of ethyl iodide at 70 °C, giving the thiazolium salt **140** in fairly good yield (Scheme 3-6). The conversion of (1H)-1,2,4-triazole **141** to its sodium salt with methanolic sodium methoxide was followed by reaction with iodomethane, affording the 1-methyl-1,2,4-triazole **142** as the only product. Then 1-methyl-1,2,4-triazole was quaternized at N-4 by reaction with ethyl iodide under neat reaction conditions, to produce the triazolium salt **143** in moderate yield (Scheme 3-6).

The two precatalysts were then evaluated in the reaction test (Scheme 3-7), employing five equivalents of MnO₂ under an argon atmosphere as described by Scheidt and coworkers.



Scheme 3-7 Evaluation of homogeneous catalysts in the presence of MnO₂ as the oxidant.

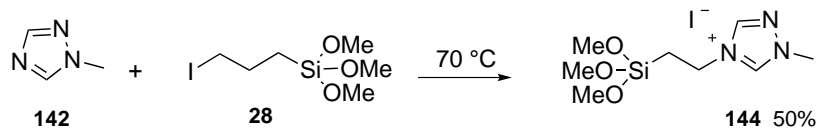
Using the thiazolium salt **140** the reaction yield was 51%, whereas employing the triazolium salt **143** the methyl ester was obtained in 98% yield, hereby confirming that this reaction is particularly sensitive to azolium structure. Also the behavior of the two catalysts in the presence of azobenzene as the oxidant under an argon atmosphere was studied (Scheme 3-8): **143** gave no product whereas using **140** the yield increased up to 90%.



Scheme 3-8 Evaluation of homogeneous catalysts in the presence of azobenzene as the oxidant.

Therefore, it has been confirmed that a triazolium precatalyst is superior to the thiazolium analogue in the presence of MnO₂ and DBU, while exactly the opposite occurs when the system azobenzene/Et₃N is used. In view of these results, we turned to synthesize a triazolium salt having a trimethoxysilane group that is capable of covalently attaching to MnO₂ surface (Scheme

3-9); **144** was obtained in quite good yield by reacting the 1-methyl-1,2,4-triazole **142** with the commercially available iodopropyltrimethoxysilane **28** at 70 °C.

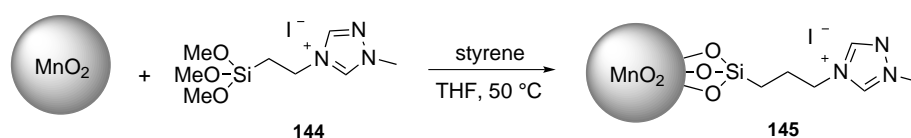


Scheme 3-9 Synthesis of an anchorable triazolium precatalyst.

Initially we decided to use simple MnO₂ nanoparticles as support for **144**; in fact, first of all, we intended to verify that

- * the triazolium salt is an efficient precatalyst also when it is immobilized on nanoparticle surface,
- * MnO₂ on the nanoparticle surface can exert the role of oxidant in the NHC-catalyzed esterification of benzaldehyde with methanol.

For this purpose, MnO₂ nanoparticles (about 50 nm-sized) were prepared by a simple precipitation technique using KMnO₄ and EtOH¹⁵⁶ and were then treated with excess trimethoxysilane derivative **144** in THF at 50 °C. The loading step proceeded cleanly and could be quantitatively and conveniently monitored (0.40 mmol/g loading, consistent between batches) by ¹H NMR spectroscopy in the presence of styrene as an internal standard, following a method developed and reported earlier by Connon *et al.*¹⁵⁷ FTIR analysis clearly confirmed that the catalyst has been successfully immobilized onto the nanoparticles; in the IR spectrum for the catalyst-loaded nanoparticles additional stretches due to the triazolium salt (in particular: 1580 cm⁻¹, 800-1100 cm⁻¹) were noted.

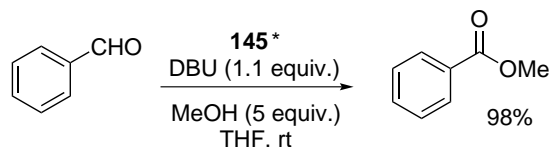


Scheme 3-10 Immobilization of the azolium salt onto manganese dioxide NPs.

¹⁵⁶ Subramanian, V.; Zhu, H.; Wei, B.; *Chemical Physics Letters*, **2008**, *453*, 242.

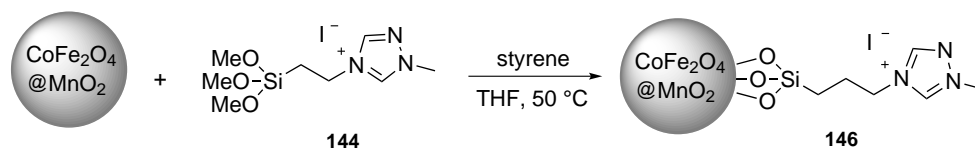
¹⁵⁷ See ref. 145.

Functionalized nanoparticles were then evaluated in our reaction test (Scheme 3-11). Gratifyingly, **145** (at 7 mol% catalyst loading, *ca.* 2 equivalents of MnO₂) exhibited high catalytic activity, allowing the smooth and quantitative conversion of benzaldehyde to the corresponding methyl ester at room temperature under an argon atmosphere.



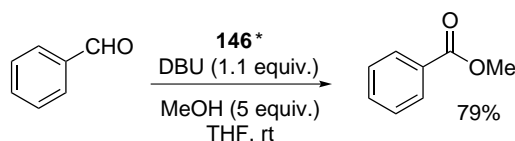
Scheme 3-11 Preliminary test. * 7 mol% catalyst loading, *ca.* 2 equivalents of MnO₂.

This excellent result has encouraged us to immobilize the triazolium salt **144** onto the CoFe₂O₄@MnO₂ magnetic nanoparticles (Scheme 3-12); also in this case the loading process occurred successfully and was quantified (0.22 mol/g) by ¹H NMR spectroscopy using styrene as an internal standard.



Scheme 3-12 Immobilization of the azolium salt onto magnetic core-shell NPs.

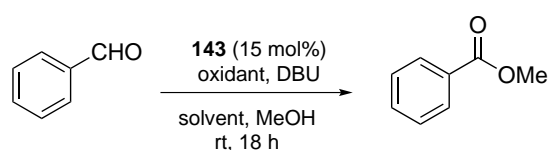
The oxidant/catalyst system **146** was then tested in the oxidative esterification of benzaldehyde with methanol; importantly, it could be easily separated from the products by exposure of the reaction vessel to an external magnet and decantation of the reaction solution. Using **146** in the standard conditions, the methyl ester was isolated in good yield, even if lower than that obtained with **145**.



Scheme 3-13 Evaluation of **146**. * 7 mol% catalyst loading, *ca.* 2 equivalents of MnO₂.

At this point, before attempting to optimize the reaction yield, attention turned to the question of recyclability: we needed the presence of a co-oxidant in the reaction environment, to regenerate the manganese (IV) oxide and enable the potential recycling of the functional nanoparticles.

In this regard we were intrigued by the opportunity of carrying out the oxidative esterification reaction in air to use atmospheric oxygen as the co-oxidant. To investigate this possibility, first we decided to perform the reaction in air in the presence of the homogeneous catalyst **143** under different reaction conditions. The results obtained are summarized in Table 3-1.



entry	MnO ₂ equiv.	reaction conditions	yield*(%)
1	5	THF, MeOH (5 equiv.), under Ar	98
2	2	THF, MeOH (5 equiv.), under Ar	66
3	2	THF, MeOH (5 equiv.), in air	69
4	0.5	THF, MeOH (5 equiv.), in air	67
5	-	THF, MeOH (5 equiv.), in air	40
6	-	THF/MeOH 1:1, in air	49
7	-	CH ₂ Cl ₂ /MeOH, 1:1, in air	91
8	-	CH ₂ Cl ₂ , MeOH (5 equiv.), in air	50

*determined by ¹H NMR spectroscopy using styrene as an internal standard

Table 3-1 Evaluation of the homogeneous catalyst **143** as a promoter of the oxidative esterification of benzaldehyde with methanol using air/MnO₂.

Using two equivalents of MnO₂ under argon, the yield was decreased to slightly less than 70% (entries 1, 2); the reaction yield was similar in the presence of air (entry 3), also with only 0.5 equivalents of MnO₂ (entry 4). To our surprise, performing the reaction in air in the absence of MnO₂, the methyl ester was produced in 40% yield (entry 5); the main side product was benzoic acid, while benzoin product was obtained in less than 10% yield. This unexpected result showed that the atmospheric oxygen dissolved in the reaction mixture plays an important role and prompted us to further investigate the reaction using air as the sole oxidant. Thus we have found

that the yield increased to 49% using THF/MeOH (1:1) solvent mixture (entry 6); more importantly, the methyl ester was obtained in very good yield carrying out the reaction in CH₂Cl₂/MeOH (1:1) solvent mixture (entry 7). Using five equivalents of methanol in CH₂Cl₂ the ester yield decreased (entry 8), in favor of benzoic acid.

These results seemed very interesting, showing that unexpectedly the simple triazolium salt **143** is able to promote the aerobic oxidative esterification of benzaldehyde with methanol.

Recently Yoshida *et al.* have reported the use of air as an oxidant in NHC-catalyzed oxidations of electron-deficient aldehydes to acids using a sulfoxylalkyl-substituted imidazolium catalyst.¹⁵⁸ Their mechanistic proposal invokes the formation of an acyl azolium, which then undergoes hydrolysis, consistently with the other reports on NHC-catalyzed oxidations of aldehydes. Reasonably, in our case the atmospheric O₂ is able to oxidate the Breslow intermediate to acyl azolium; then the acyl azolium transfers its acyl group to a nucleophile present in the reaction environment, *i.e.* methanol or water. Therefore, minimizing the presence of adventitious water, it could be possible to optimize the ester formation reaction.

At this point, our attention turned to the appealing NHC-catalyzed aerobic oxidative esterification of aldehydes. Because the MnO₂ oxidant seemed to be no longer necessary, we were now interested in supporting our triazolium precatalyst onto more convenient magnetite nanoparticles, instead of magnetic core-shell nanoparticles.

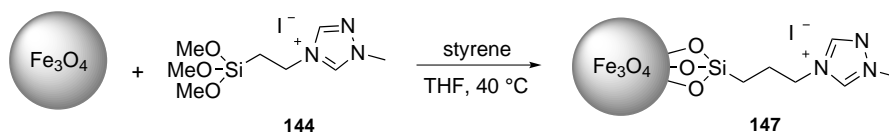
3.2.2 Magnetite nanoparticle-supported NHC catalysts

We decided to attach the triazolium salt to magnetite nanoparticles to take advantage of the easy catalyst recovery from the reaction mixture by magnetic separation. Furthermore, it was reasonable to expect a catalytic effect by the iron ions on nanoparticle surface. In fact, very recently, an example of NHC/iron cooperative catalysis in the aerobic oxidative esterification of aldehydes with phenols has been described by Gois and coworkers.¹⁵⁹ The authors reported a Fe (II) complex acting as a co-catalyst in the reaction, possibly through coordination of the oxidant (atmospheric O₂). Moreover, a study, carried out previously within Connon's group, had brought out that oxidation of thiols to disulfides in air was promoted in the presence of magnetite nanoparticles.

¹⁵⁸ Yoshida, M.; Katagiri, Y.; Zhu, W.-B.; Shishido, K. *Org. Biomol. Chem.* **2009**, *7*, 4062

¹⁵⁹ Reddy, R. S.; Rosa, J. N.; Veiros, L. F.; Caddick, S.; Gois, P. M. P. *Org. Biomol. Chem.*, **2011**, *9*, 3126.

In view of these considerations, Fe₃O₄ nanoparticles (around 7-9 nm in diameter) were prepared by the co-precipitation technique¹⁶⁰ and then treated with the trimethoxysilane derivative **144** in THF at 40 °C (Scheme 3-14). As before, the loading (0.53 mmol/g) was quantitatively monitored by ¹H NMR analysis using styrene as an internal standard. Also FTIR analysis showed that the catalyst has been successfully immobilized onto the magnetite nanoparticles.



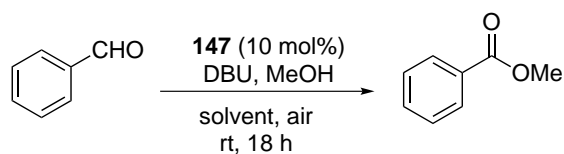
Scheme 3-14 Immobilization of the triazolium salt onto magnetite NPs.

The magnetite nanoparticle-supported triazolium precatalyst **147** was subsequently tested in the aerobic oxidative esterification of benzaldehyde with methanol to determine catalyst reactivity and recyclability. The results obtained under different conditions are summarized in Table 3-2.

147 proved to be capable of catalyzing the oxidative esterification of benzaldehyde with methanol in air, affording the methyl ester in good to excellent yields, depending on the solvent (entries 1, 2, 5, 6, 8). Excellent results were obtained using CH₂Cl₂ as solvent, also with a slight excess of methanol (entry 6, 8). It is noteworthy that the reaction yield decreased a lot (to 50%) when the homogeneous catalyst **143** was employed in the same conditions (Table 3-1, entry 8). Importantly, we observed no background reaction in the presence of unfunctionalized magnetite nanoparticles (entry 9).

The supported triazolium precatalyst **147** was easily separated from the products by exposure of the reaction vessel to an external magnet and following decantation of the reaction solution. The remaining catalyst was washed with THF to remove residual product and dried under high vacuum before reusing it. To our disappointment, catalyst reactivity decreased over cycles (entries 3, 4, 7).

¹⁶⁰ Massart, R.; *IEEE Trans. Magn.* **1981**, *17*, 1247; b) Qiu, X. P.; *Chin. J. Chem.* **2000**, *18*, 834.



entry	reaction conditions	cycle	yield* (%)
1	THF, MeOH (5 equiv)	1	66
2	THF/MeOH 1:1	1	82
3	THF/MeOH 1:1	2	72
4	THF/MeOH 1:1	3	45
5	CH ₂ Cl ₂ /MeOH, 1:1	1	93
6	CH ₂ Cl ₂ , MeOH (5 equiv.)	1	90
7	CH ₂ Cl ₂ , MeOH (5 equiv.)	2	60
8	CH ₂ Cl ₂ , MeOH (1.5 equiv.)	1	90
9**	CH ₂ Cl ₂ /MeOH, 1:1	1	no reaction

* determined by ¹H NMR spectroscopy using styrene as an internal standard;

** unfunctionalized magnetite nanoparticles tested as catalyst.

Table 3-2 Evaluation of **147** as a recyclable catalyst.

In an attempt to better understand the fate of **147** after its use, we characterized three batches of nanoparticles: one batch which had not been loaded with catalyst, one which had been loaded but then simply stored under argon and not used in any catalytic processes, and finally the batch which has been employed in our reaction (Table 3-2, entry 6, 7). After loading the nanoparticles with catalyst to prepare **147** and after using them, the TEM images showed no changes in either nanoparticle size or morphology, though they appear slightly more aggregated (Figure 3-3). FT-IR analysis also demonstrated that no catalyst leaching appeared to occur as a result of use.

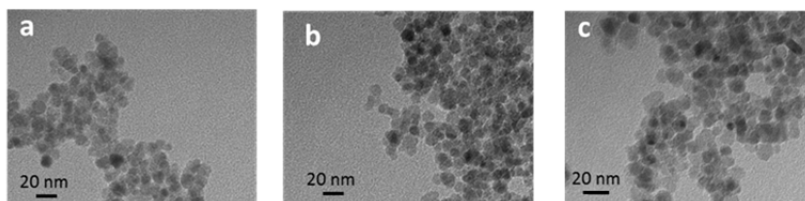
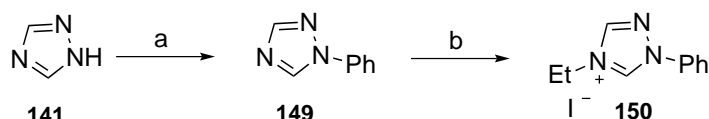


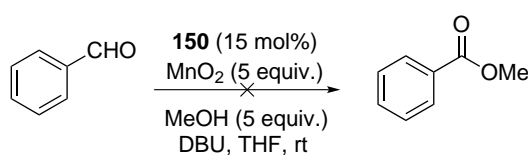
Figure 3-3: TEM images of (a) magnetite nanoparticles, (b) triazolium catalyst-loaded nanoparticles **147** and (c) triazolium-loaded nanoparticles **147** after recycling.

Probably, decreasing of catalytic activity over cycles was due to instability of the supported triazolium ion; as confirmation of this, we found that the corresponding homogeneous triazolium catalyst **143** became less efficient when several days elapsed since its preparation.

Therefore, efforts were needed to improve the catalyst stability, modifying the triazolium ring substituents and/or the counterion. A first attempt along this direction was made synthesizing the phenyl-substituted triazolium ion **150**. For this purpose, 1-phenyl-1H-1,2,4-triazole **149** was prepared by the well-established copper(I)-catalyzed coupling reaction of 1H-1,2,4-triazole and iodobenzene;¹⁶¹ **149** was then treated with an excess of iodoethane at 70 °C, giving the triazolium salt **150** in fairly good yield (Scheme 3-15). Unfortunately, when **150** was evaluated as a catalyst in our reaction test (Scheme 3-16), no catalytic activity has been observed (after 20 hours benzaldehyde was recovered completely unchanged). Further investigations along this line are currently underway.



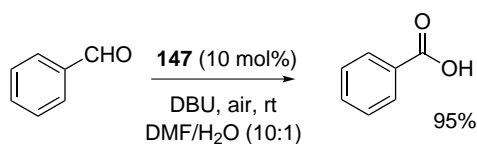
Scheme 3-15 Reagents and conditions: a) PhI, Cu₂O, 1,10-phenantroline, K₂CO₃, DMF, 110 °C, 64% b) EtI (neat), 70 °C, 60%.



Scheme 3-16 Evaluation of **150** as a promoter of the oxidative esterification of benzaldehyde with methanol.

Nanoparticle-supported triazolium catalyst **147** was also evaluated in the aerobic oxidative carboxylation of benzaldehyde in DMF/H₂O, affording the benzoic acid in excellent yield (Scheme 3-17).

¹⁶¹ Meyer, D.; Strassner, T.; *J. Org. Chem.* **2011**, 76, 305.



Scheme 3-17 Evaluation of **147** as a promoter of the aerobic oxidative carboxylation of benzaldehyde.

This preliminary result was very interesting, because Yoshida and coworkers¹⁶² had reported that only arylaldehydes having an electron-withdrawing group can be successfully converted to the corresponding carboxylic acids using an imidazolium catalyst in air; in particular, the authors reported that the carboxylic acid was obtained in <10% yield starting from benzaldehyde.

3.3 Conclusion

For the first time, a multifunctional “nanosystem” which combines a magnetic core (CoFe₂O₄), an oxidant shell (MnO₂) and an NHC catalyst precursor on its surface, has been designed and synthesized. Functionalized magnetic core-shell nanoparticles have been showed to be able to promote the oxidative esterification of benzaldehyde with methanol in THF, affording the methyl ester in good yield (79%).

Unexpectedly, it has been found that the simple triazolium precatalyst **143** is able to catalyze the oxidative esterification of benzaldehyde with methanol using air as the oxidant. The issue of reaction scope, with respect to the aldehyde substrate and the alcohol nucleophile, is currently addressed within Connon’s group.

The triazolium precatalyst was then successfully immobilized on magnetite nanoparticles. The supported catalyst **147** has proven to catalyze the aerobic oxidative esterification of benzaldehyde in higher yield than that obtained using the corresponding homogeneous catalyst, also employing nearly equimolar amount of methanol. **147** also showed to be capable of efficiently catalyzing the oxidative carboxylation of benzaldehyde in air. Magnetic nanoparticle-supported catalyst can be easily recovered from the reaction mixture by decantation after applying an external magnet. Therefore, both the reaction protocol and the work up are mighty practical and operationally

¹⁶² See ref. 158.

simple. Efforts to improve the stability of the NHC precursor are currently underway within Cannon's group, in order to make possible the catalyst recycling.

3.4 Experimental section

3.4.1 General information

Flash chromatography was carried out using silica gel (230–400 mesh). TLC analysis was performed on precoated 60F₂₅₄ slides, and visualized by either UV irradiation or KMnO₄ staining. THF were distilled from sodium. Methylene chloride and DMF were distilled from calcium hydride. Benzaldehyde was freshly distilled before use. Unless otherwise stated, all other chemicals were obtained from commercial sources and used as received. Unless otherwise specified, all reactions were carried out in oven-dried glassware under an atmosphere of argon. Mechanical agitation of reaction mixtures was carried out using an IKA, KS 130 basic, shaker.

¹H NMR spectra were recorded using a 400 MHz spectrometer. Residual solvent peaks were used as internal references for ¹H NMR spectra: chloroform (δ 7.26 ppm), DMSO (δ 2.05 ppm). Chemical shifts (δ) are reported in parts per million (ppm) and coupling constants (J) in Hz. Splitting patterns are designated as s, singlet; bs, broad singlet; d, doublet; bd, broad doublet; dd, doublet of doublets; ddd, doublet of doublet of doublets; t, triplet; dt, doublet of triplets; q, quartet; m, multiplet. ¹³C spectra were recorded using the same instrument (100 MHz) with total proton decoupling. Infrared spectra were obtained using neat samples on a diamond Perkin Elmer Spectrum 100 FT-IR spectrometer using a universal ATR sampling accessory. TEM images were obtained on a Jeol JEM-2100, 200 kV LaB₆ instrument, operated at 120 kV with a beam current of about 65 mA. Samples for TEM were prepared by deposition and drying of a drop of the powder dispersed in water onto a formvar-coated 300-mesh copper grid.

3.4.2 Synthesis of nanoparticles

CoFe₂O₄@MnO₂ nanoparticles were prepared and characterized within Y. Gun'ko's group.

MnO₂ nanoparticles. KMnO₄ (500 mg) was dissolved into deionized water (30 mL). To this solution, ethanol (10 mL) was added dropwise, leading to the formation of brownish precipitate of MnO₂. The precipitate was filtered and washed extensively with deionized water until the pH of the washed water is neutral. Then the precipitate was dried *in vacuo*.

Fe₃O₄ nanoparticles. FeCl₂·4H₂O (2.0 mmol) and FeCl₃·6H₂O (4.0 mmol) were dissolved into deoxygenated water (100 mL). The solution was allowed to stir for 15 min at room temperature to allow full dissolution. Nanoparticles were precipitated by the addition of ammonium hydroxide solution until the solution reached a pH of 11-12. This alkaline solution was then vigorously stirred at 80 °C for 1 h, yielding a black colloidal suspension of magnetite nanoparticles, which were washed several times with deionized water until pH neutral. The nanoparticles were then dried *in vacuo* for 24 h.

3.4.3 Synthesis of heteroazolium precatalysts

3-ethyl-4-methyl thiazolium iodide (140). A 5 mL round bottom flask, equipped with a reflux condenser, was charged with 4-methylthiazole (1.0 g, 10.1 mmol) and ethyl iodide (1.6 mL, 20.2 mmol) and the resulting mixture was heated to reflux and stirred for 20 h under an argon atmosphere. The resulting precipitate was washed with cold CH₂Cl₂ to obtain **140** as a white powder in 53% yield. ¹H NMR (400 MHz, DMSO-d₆) δ: 10.1 (s, 1H), 8.03 (s, 1H), 4.45 (q, 2H, J = 6.5, CH₃CH₂), 2.56 (s, 3H, CH₃), 1.46 (t, 3H, J = 7.0, CH₃CH₂); ¹³C NMR (100 MHz, DMSO-d₆) δ: 158.4, 145.6, 121.8, 47.85, 14.45, 12.65.

1-methyl-1,2,4-triazole (142). A 100 mL round bottom flask, equipped with a reflux condenser, was charged with methanol (30 mL) and (1H)-1,2,4-triazole (3.0 g, 43.44 mmol). With ice-bath cooling and under a gentle argon purge, sodium methoxide (2.35 g, 43.44 mmol) was added cautiously. Using an oil bath, the reaction mixture was heated to 56 °C for 2 hours under an argon atmosphere (balloon). The flask was then cooled with an external ice-bath and iodomethane (3.0 mL, 47.82 mmol) was added dropwise. The ice-bath was removed and was replaced with an oil bath. The reaction mixture was heated to gentle reflux for 20 h and then cooled to room temperature. The solvent was concentrated *in vacuo*. The residue was diluted with water and extracted several times with chloroform. Organic extracts were washed with brine and dried over dry MgSO₄. 1.10 g of **142** was obtained as a pale yellow oil. ¹H NMR (400 MHz, DMSO-d₆) δ: 8.45 (s, 1H), 7.94 (s, 1H), 3.86 (s, 3H, CH₃N); ¹³C NMR (100 MHz, DMSO-d₆) δ: 151.3, 144.4, 35.68.

1-methyl-4-ethyl-1,2,4-triazolium iodide (143). A 5 mL round bottom flask, wrapped with aluminium foil, was charged with 1-methyl-1,2,4-triazole (1.0 g, 12.05 mmol) and ethyl iodide (2.12 mL, 26.50 mmol) and the resulting mixture was stirred at 50 °C under an argon atmosphere for 48 h. The resulting orange precipitate was dissolved in warm CH₂Cl₂, then Et₂O was added to obtain **143** as a white powder in 35% yield. ¹H NMR (400 MHz, CDCl₃) δ: 1.70 (t, 3H, J = 7.0,

CH_3CH_2), 4.27 (s, 3H, CH_3N), 4.59 (q, 2H, $J = 7.0$, CH_3CH_2), 8.77 (s, 1H), 11.23 (s, 1H); ^{13}C NMR (100 MHz, CDCl_3) δ : 15.3, 39.9, 44.5, 142.9, 143.0.

1-phenyl-1,2,4-triazole (149). After standard cycles of evacuation and refilling with argon, an oven-dried Schlenk tube equipped with a magnetic stir bar was charged with Cu_2O (210 mg, 1.5 mmol), 1,10-phenanthroline (520 mg, 2.9 mmol), 1H-1,2,4-triazole (1.0 g, 14.5 mmol), and K_2CO_3 (6.01 g, 44 mmol). The tube was evacuated, filled with argon, and capped with a rubber septum. Iodobenzene (2.42 mL, 4.43 g, 22 mmol) was added via a syringe, followed by anhydrous and degassed DMF (10 mL). The reaction mixture was stirred for 48 h at 120°C under a positive pressure of argon. After cooling to room temperature, it was diluted with 20 mL of dichloromethane and filtered through a plug of Celite, the filter cake being further washed with dichloromethane. The resulting organic layer was washed with water and brine and then dried. The solvent was removed *in vacuo*. The crude product was purified by flash chromatography (gradient ethyl acetate/petroleum ether 2:8 to ethyl acetate) to provide **149** (1.36 g, 64%) as a pale-yellow solid. ^1H NMR (400 MHz, DMSO-d_6) δ : 7.41 (1 H, t, $J = 7.4$), 7.58 (2 H, t, $J = 7.4$), 7.87 (2 H, d, $J = 7.5$), 8.25 (1 H, s), 9.31 (1 H, s). ^{13}C NMR (100 MHz, DMSO-d_6) δ : (100 MHz, DMSO-d_6) 119.4, 127.8, 129.8, 136.7, 142.3, 152.4.

Synthesis of 1-phenyl-4-ethyl-1,2,4-triazole (150). A 5 mL round bottom flask, equipped with a reflux condenser, was charged with 1-phenyl-1,2,4-triazole (0.200 g, 1.37 mmol) and ethyl iodide (0.9 mL, 10.9 mmol) and the resulting mixture was heated to reflux and stirred for 24 h under an argon atmosphere. Hexane was added and the resulting precipitate was washed with THF/hexane (1:1) to obtain **150** as a white powder in 60% yield. ^1H NMR (400 MHz, DMSO-d_6) δ : 10.90 (s, 1H), 9.48 (s, 1H), 7.92 (d, $J=8.03$, 2H), 7.65-7.60 (m, 3H, Ph), 4.36 (q, 2H, $J = 7.0$, CH_3CH_2), 1.56 (t, 3H, $J = 7.5$, CH_3); ^{13}C NMR (100 MHz, DMSO-d_6) δ : 144.8, 141.3, 130.4, 130.1, 120.5, 43.47, 14.14.

1-methyl-4-(trimethoxysilylethyl)-1H-1,2,4-triazolium iodide (144). A 5 mL round bottom flask was charged with 1-methyl-1,2,4-triazole (500 mg, 6.02 mmol) and (3-iodopropyl)trimethoxysilane (1.8 mL, 9.04 mmol). The resulting mixture was heated to 70°C and stirred for 20 h under a positive pressure of argon. The resulting precipitate was washed several times with dry Et_2O under argon and dried *in vacuo*, affording **144** as a yellow solid in 50% yield. NMR spectra were registered using as solvent CDCl_3 pretreated with potassium carbonate to eliminate residual acidity, which could catalyze the trimethoxysilane hydrolysis. ^1H NMR (400 MHz, CDCl_3) δ : 0.68 (t, 2H, $J = 6.5$, CH_2Si), 2.08-2.18 (m, 2H), 3.43 (s, 9H, OCH_3 x3), 4.29 (s, 3H, CH_3N), 4.51 (t, 2H, $J = 5.5$, CH_2N), 8.43 (s, 1H), 11.55 (s, 1H); ^{13}C NMR (100 MHz, CDCl_3)

δ : 5.33, 23.24, 39.44, 49.90, 50.33, 142.11, 143.54. IR (neat/cm⁻¹) ν_{\max} : 3029, 2943, 2839, 1580, 1459, 1195, 1169, 1052, 1017, 982, 822, 775, 675. m/z (ESI⁺) 246.1281 (M⁺, C₉H₂₀N₃O₃Si requires 246.1274).

3.4.4 Catalyst loading

Manganese oxide nanoparticle-supported triazolium catalyst (145). A 50 mL reaction vessel was charged with the siloxane **144** (35.5 mg, 0.10 mmol) and styrene (internal standard, 11.4 μ l, 0.10 mmol). The reaction vessel was placed under an argon atmosphere and fitted with a septum and dry THF (10 mL) was added *via* syringe. At this point ¹H NMR spectroscopic analysis (t=0 min) was carried out. Nanoparticles (150 mg) were then added and the resulting suspension was sonicated for 5 min at room temperature. The resulting mixture was heated to 50 °C for 24 h under mechanical agitation. After stopping the agitation, the solution was decanted and catalyst loading (0.40 mmol/g) was determined by ¹H NMR spectroscopic analysis of the resulting solution. The remaining particles were subjected to five washing cycles with dry THF. IR (neat/cm⁻¹) ν_{\max} : 2945, 2869, 1744, 1653, 1532, 1411, 1368, 1220, 1164, 1041, 948.

CoFe₂O₄@MnO₂ nanoparticle-supported triazolium catalyst (146). A 50 mL reaction vessel was charged with the siloxane **144** (35.5 mg, 0.10 mmol) and styrene (internal standard, 11.4 μ l, 0.10 mmol). The reaction vessel was placed under an argon atmosphere and fitted with a septum and dry THF (10 mL) was added *via* syringe. Core-shell nanoparticles (100 mg) were then added and the resulting suspension was sonicated for 5 min at room temperature. The resulting mixture was heated to 50 °C for 24 h under mechanical agitation. The vessel was then placed in proximity of an external magnet and the solution was separated from the nanoparticles *via* a Pasteur pipette. Catalyst loading (0.22 mmol/g) was determined by ¹H NMR spectroscopic analysis of the resulting solution. The remaining particles were subjected to five washing cycles with dry THF using magnetic decantation. IR (neat/cm⁻¹) ν_{\max} : 2952, 2878, 1691, 1546, 1408, 1337, 1225, 1041, 948.

Magnetite nanoparticle-supported triazolium catalyst (147). A 50 ml reaction vessel was charged with the siloxane **144** (56 mg, 0.15 mmol) and styrene (internal standard, 11.4 μ l, 0.10 mmol). The reaction vessel was placed under an argon atmosphere and fitted with a septum and dry THF (6.0 mL) was added *via* syringe. At this point ¹H NMR spectroscopic analysis (t=0 min) was carried out. Magnetite nanoparticles (200 mg) were then added and the resulting suspension

was sonicated for 5 min at room temperature. The resulting mixture was heated to 40 °C for 24 h under mechanical agitation. The vessel was then placed in proximity of an external magnet and the solution was separated from the nanoparticles *via* a Pasteur pipette. Catalyst loading (0.53 mmol/g) was determined by ¹H NMR spectroscopic analysis of the resulting solution. The remaining particles were subjected to five washing cycles with dry THF using magnetic decantation. IR (neat/cm⁻¹) ν_{max} : 3029, 2935, 1584, 1450, 1337, 1225, 1165, 1017, 987, 822.

3.4.5 Evaluation of catalysts in the oxidative esterification of benzaldehyde with manganese oxide as the oxidant

Homogeneous catalyst. To a solution of benzaldehyde (1.0 mmol) and catalyst (0.15 mmol) in THF (5 mL), methanol (0.20 mL, 5.0 mmol), DBU (1.1 mmol) and MnO₂ were added. After mechanical stirring for 4-24 h at rt, the mixture was filtered through a thin pad of Celite. The Celite was washed with ethyl acetate and the filtrate was then concentrated *in vacuo*. The resulting residue was purified by flash chromatography using hexane/EtOAc (80:20).

NP-supported catalyst. A 5 mL reaction flask, containing **145** or **146**, was charged with THF (5 mL), benzaldehyde (1.0 mmol), methanol (5 mmol) and DBU (1.1 mmol). The reaction mixture was mechanical shaken for 16-24 h at rt. The solution was then separated from the nanoparticles (by magnetic decantation if nanoparticles were magnetic). The solvent was removed *in vacuo* and the resulting residue was purified by flash chromatography using hexane/EtOAc (80:20).

3.4.6 Evaluation of magnetite nanoparticle-supported catalyst in the aerobic oxidative esterification of benzaldehyde

A 5 mL reaction flask containing the supported catalyst **147** (96 mg, 10 mol%) was charged with styrene (57.5 μ L, 0.50 mmol, internal standard), solvent, MeOH, benzaldehyde (51 μ L, 0.50 mmol) and DBU (85.0 μ L, 0.55 mmol). The resulting suspension was shaken under mechanical agitation for 24 h at room temperature. The reaction was stopped by placing the reaction vessel over an external magnet. The reaction vessel was kept over the magnet until the reaction mixture became transparent. The solution was separated from the nanoparticles *via* a Pasteur pipette and the conversion was determined by ¹H NMR spectroscopy. Nanoparticles were washed several times with THF and dried *in vacuo*.

3.4.7 Aerobic oxidative carboxylation of benzaldehyde with magnetite nanoparticle-supported catalyst

A 5 mL reaction flask containing the supported catalyst **147** (96 mg, 10 mol%) was charged with DMF (1.0 mL), H₂O (0.1 mL), benzaldehyde (0.15 mL, 1.0 mmol) and DBU (0.112 mL, 0.76 mmol) at rt. After stirring at rt for 16 h, the reaction vessel was placed over an external magnet and the solution was separated from the nanoparticles. The solution was then added to 10% aq. NaOH and extracted with AcOEt. 10% aqueous HCl was added to the water phase and it was carefully extracted with AcOEt again. The separated organic layer was dried over anhydrous MgSO₄ and the solvent was removed *in vacuo* to provide benzoic acid in 90% yield. ¹H NMR (400 MHz, CDCl₃) δ: 7.45-7.62 (m, 3H), 8.12 (d, 2H), 12.09 (s, 1H). ¹³C NMR (100 MHz, CDCl₃) δ: 128.5, 129.5, 130.3, 133.8, 172.7.

4 Conclusions

During my three years of PhD, I have focused my research on the functionalization of magnetic nanoparticles with suitable molecules in order to obtain new, useful, magnetically recoverable “nanosystems” capable of catalyzing different organic reactions.

The main part of my work has concerned the synthesis of optically active β -amino alcohols able to functionalize magnetic nanoparticles for application in asymmetric catalysis.

One route followed was to modify the amino alcoholic structures **24** (Pericas-type ligands) and **40** (ephedrine derivatives), well-known in literature for their enantioselective catalytic properties, to support them on magnetite nanoparticles; unfortunately all attempts along this direction have proved unsuccessful.

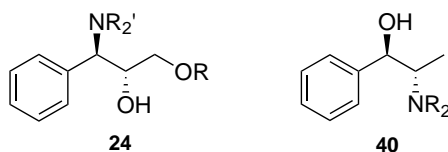


Figure 4-1 Pericas type ligands (**24**) and ephedrine derivative ligands (**40**).

In parallel, a study has been addressed with the aim to design and synthesize new β -amino alcohol ligands having a fine-tunable catalytic site and a functionality (an alkoxy silane group) allowing their covalent anchoring to the magnetite nanoparticle surface.

The approach used for the amino alcohol fragment synthesis was based on the regio- and stereocontrolled elaboration of optically active functionalized epoxides. The formation of an amide bond between the commercially available 3-aminopropyltriethoxysilane and a carboxylic group, suitably incorporated in the amino alcohol ligand structure, has been identified as the key step for the successful immobilization onto the nanoparticles.

A new, mild, regioselective method for the aminolysis of 2,3-epoxy amides has been developed; thus a family of optically active amino alcohols **97**, characterized by the presence of the amide

moiety (Figure 4-2), has been synthesized and tested as homogeneous ligands in the enantioselective addition of diethylzinc to benzaldehyde in order to optimize the catalytic behavior.

The amino alcohol **131**, where a double bond acts as spacer between the catalytic site and the amide moiety (Figure 4-2), was identified as the best enantioselective catalyst, affording the (*S*)-1-phenyl-1-propanol in nearly quantitative yield and excellent enantiomeric excess (Scheme 4-1).

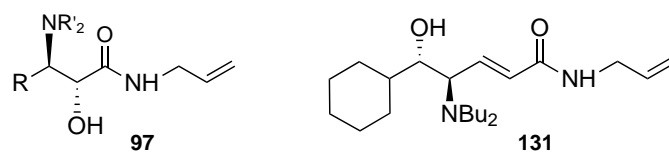
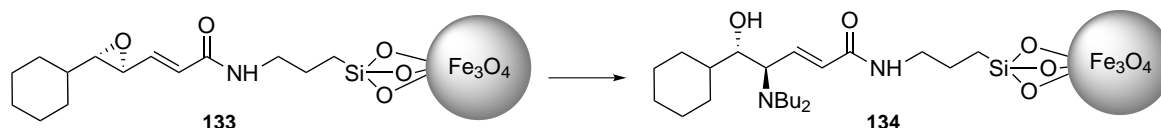


Figure 4-2 New amino alcohol ligands.

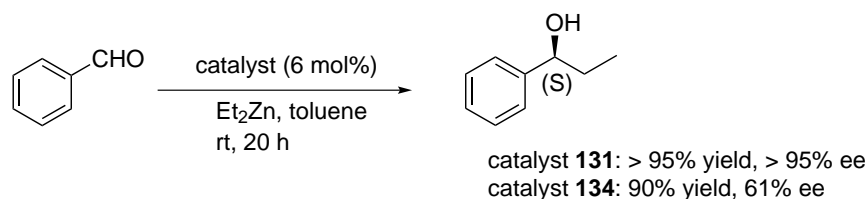
The corresponding supported catalyst **134** was prepared by immobilization of the precursor epoxide on the magnetite nanoparticles, followed by a regio- and stereocontrolled ring opening reaction (Scheme 4-1).



Scheme 4-1 MNP-supported amino alcohol ligand.

When **134** was evaluated in the enantioselective addition of diethylzinc to benzaldehyde, the reaction yield was comparable with that obtained using the corresponding free ligand, whereas the enantioselectivity was lower (Scheme 4-2).

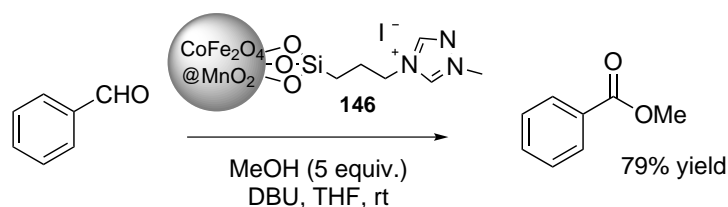
Efforts to improve the supported catalyst enantioselectivity, and investigations on the possibility of fully recycling the catalyst, are currently underway. However, this extensive study has allowed identifying the key structural features which open a straightforward route to the development of a new, recyclable, asymmetric amino alcohol-based “magnetic nanocatalyst”.



Scheme 4-2 Enantioselective addition of diethylzinc to benzaldehyde.

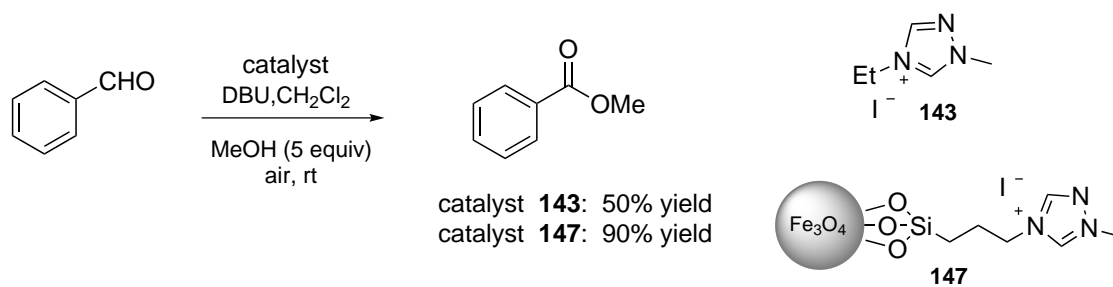
During the six months I spent at Trinity College of Dublin, Ireland, I had the opportunity of working under the supervision of Prof. Stephen Connon, focusing on the oxidative esterification of aldehydes catalyzed by nucleophilic N-heterocyclic carbenes, with the aim to design and synthesize a useful magnetic nanoparticle-supported catalyst for this reaction.

Initially, the novel multifunctional “nanosystem” **146** has been prepared, where both the NHC precursor (triazolium salt) and the oxidant (MnO_2 shell) can be easily, magnetically recovered from the reaction mixture thanks to the CoFe_2O_4 nanoparticle magnetic core. **146** proved to be capable of promoting the oxidative esterification of benzaldehyde with methanol, affording the methyl ester in good yield (Scheme 4-3).



Scheme 4-3 Oxidative esterification of benzaldehyde with MeOH.

Surprisingly, it has been found that the homogeneous triazolium precatalyst **143** is able to catalyze the oxidative esterification of benzaldehyde with methanol also using air as the oxidant (Scheme 4-4). Thus the triazolium precatalyst was immobilized onto magnetite nanoparticles. The supported catalyst **147** has proven to catalyze the reaction above in higher yield than that obtained using the corresponding homogeneous catalyst, also employing nearly equimolar amount of methanol (Scheme 4-4). The supported catalyst **147** also showed to be capable of efficiently catalyzing the oxidative carboxylation of benzaldehyde in air.



Scheme 4-4 Aerobic oxidative esterification of benzaldehyde with MeOH.

Efforts to improve the stability of the NHC precursor are currently underway within Connon's group in order to make possible the very useful recycling of the catalyst.